A THEORETICAL STUDY OF THE ELECTRONIC PROPERTIES OF METALLIC VO_2

by

Tacettin Altanhan

A dissertation submitted to the University of Warwick for admission to the degree of Doctor of Philosophy

August, 1977.

CONTENTS

	Page
CHAPTER 1. INTRODUCTION	1
CHAPTER 2. ELECTRONIC BAND STRUCTURE OF METALLIC VO_2	
2.1. Introduction	8
2.2. Ligand Field Theory and ESR Spectrum of V^{4+}	11
2.3. Bloch Functions and Band Structures	16
2.4. Properties of the Calculated Band Structures	
(a) Densities of States and Fermi Level E_F	28
(b) Occupancies of the d_{11} and Π^* Bands	31
(c) Bloch Effective Masses at E_F	31
2.5. Comparison with existing work	32
2.6. Discussion	34
CHAPTER 3. THE VALIDITY OF THE BAND MODEL FOR RUTILE VO_2	
3.1. Introduction	36
3.2. Dielectric Constants and Polarizabilities in rutile (TiO_2)	45
3.3. The Mott-Littleton Method	
(A) Polarization in a Rigid Lattice	54
(B) Polarization when the Ions are displaceable	59
3.4. Results	63
3.5. Conclusions	65

Page

CHAPTER 4. THE POLARON PROBLEM IN METALLIC VO_2

4.1. Introduction 68

4.2. Optical Mode Frequencies 70

4.3. Electron-Lattice Interactions in Metallic VO_2 73

4.4. Conclusions 79

CHAPTER 5. APPLICATIONS

5.1. Introduction 81

5.2. Electronic Specific Heat of Metallic VO_2

5.2.1. Introduction 82

5.2.2. Calculations 83

5.2.3. Conclusions 88

5.3. Plasma Oscillations in Metallic VO_2

5.3.1. Introduction 88

5.3.2. Plasma Oscillations 91

5.3.3. Results 96

5.4. The Low Field Hall Effect in Metallic VO_2

5.4.1. Introduction 98

5.4.2. The Calculation of Hall constant 99

5.4.3. Results 101

5.5. The Relaxation Time Approximation 102

CHAPTER 6. SUMMARY OF THE PRESENT INVESTIGATIONS 109

REFERENCES 113

APPENDIX I The Electrostatic and Repulsive Forces. 117

ACKNOWLEDGEMENTS

I wish to express my deep gratitude to Dr. G. J. Hyland, for his guidance and encouragement throughout the course of this work and in particular in the preparation of this thesis. I am also grateful to Dr. C. J. Hearn for his continued interest in this work and for many valuable discussions.

I wish to thank the Turkish Government for the award of a scholarship during the tenure of which this work was performed, and the British Council for an Overseas Fees Award (O.S.F.A.S.).

I would like to thank Ms. Terri Moss for her careful and rapid typing of the manuscript.

MEMORANDUM

This dissertation is submitted to the University of Warwick in support of my application for admission to the degree of Doctor of Philosophy. It contains an account of my own work performed at the School of Physics of the University of Warwick in the period October 1972 to October 1976, under the general supervision of Doctor G. J. Hyland. No part of this dissertation has been used previously in a degree thesis submitted to this or any other university. The work described in this thesis is a result of my own independent research except where specifically acknowledged in the text.

The main results of Chapters 2 and 3 have been published in collaboration with G. J. Hyland in

Phys. Lett. 61A, 426 (1977)

and a full account has been submitted for publication in *Philosophical Magazine*.

Tacettin Altanhan

August, 1977.

ABSTRACT

One-electron dispersion relations are obtained in the tight-binding approximation for the two bands d_{11} and π^* which are generally considered to be involved in the metallic conduction which characterizes high temperature rutile phase of VO_2. An upper limit on the Coulomb potential energy associated with on-site (intra-cationic) correlations between electrons of antiparallel spins is calculated. The dispersion relations are used to calculate the average energy associated with the delocalised band states; this energy is compared with that of the corresponding Mott-insulating state in which the d-electrons are localised, one per cation, and it is found that the metallic phase is stable against Mott-insulation.

In spite of the existence of strong electron-optical polar phonon interaction, the formation of a degenerate gas of *lattice* polarons is ruled out in metallic VO_2; the possibility of *electronic* polaron formation is examined, and is also found to be suppressed by screening effects.

As an application of the energy dispersion relations the electronic specific heat, the plasma frequency and the Hall coefficient are calculated, and found to be in fairly good agreement with experiment.

CHAPTER 1

INTRODUCTION.

It is now well established that Coulomb correlations play a decisive rôle in the determination of the electronic properties of materials in which the electrically "active" electrons are associated with orbitals of limited spatial extention and overlap; examples of such materials are oxides and sulphides of those transition metals lying between titanium and nickel in the periodic table. In NiO, for example, with 8 d-electrons on each cation, one would expect a metallic state, whereas it is a perfect insulator (de Boer and Verwey 1937); here the Coulomb correlations are so dominant that they completely suppress the itinerancy of the electrons and establish a Mott-insulating state (1949) in which these electrons remain localised. Compounds containing transition metals from the opposite end of the series, however, exhibit a variety of electrical behaviours; TiO for example is metallic and even becomes superconducting below $0.68^{o}K$ (Hulm et.al. 1965). On the other hand the lower oxides of vanadium, in particular V_2O_3 and VO_2 show thermally induced phase transitions from low temperature semiconducting phases to higher temperature metallic phases, (Morin 1959).

Unlike the situation in NiO, it is possible in the case of VO_2 to explain the low temperature insulating phase within the framework of the band model, independently of the particular mechanism by which the insulating phase evolves out of the metallic phase. Although a mechanism based on phonon

softening has much to recommend it (Hearn 1972, 1973), other mechanismsbased on Coulomb correlations have been intermittently proposed since 1968 (Hyland 1968, Rice et. al. 1970), whilst more recently, proposals which incorporate both effects simultaneously have been considered (Valiev et. al. 1975). Such proposals are, of course, of particular interest from the point of view of a more ambitious programme whose aim would be to afford a universal understanding of the multitude of semiconductor $\rightleftharpoons$ metal phase transitions which are now known to exist; the present, rather unsatisfactory situation, is by contrast, characterized by the existence of almost as many different models of semiconductor $\rightleftharpoons$ metal phase transitions as there are materials exhibiting them.

As already mentioned correlation effects may cause the electrons in a narrow band to become localised, so leading to a nonconducting state; this is known as Mott-insulator. In order to assess the relevance of Coulomb correlations in establishing the low temperature insulating phase it is useful to know quantitatively the stability of the metallic state against Mott insulation. VO_2 is one of the simplest transition metal compounds which can be hoped to be understood theoretically since after bonding, each cation has the electronic configuration $V^{4+}(3d)^1$ and each anion the configuration $O^{2-}(2p)^6$. It is to these single 3d-electrons per cation that the metallic properties of VO_2 are attributed. Thus each cation can be considered to be effectively a one-electron ion (the electron being the single

3d-electron) and possible complications associated with the existence of more than one electron do not arise. VO_2 can be therefore considered to be the closest experimental counterpart of the half-filled s-band often considered in theoretical many-body calculations, in which the orbitally non-degenerate s-band is simply replaced by an orbitally non-degenerate 3d-band, the so called d_{11}-band (which is, however partially overlapped by a hybridized π^*-band).

In consequence of Coulomb correlations the existence of the metallic state requires that it be stable against Mott-insulation. This can be ascertained quantitatively by comparing the energy of the metallic state, calculated within the band model, with that of the corresponding Mott-insulating state in which the 3d-electrons remain localised, one per cation. Accordingly, accepting the empirical fact that VO_2 *is* metallic for $T_t > 341^oK$, we first calculate in the following chapter its band structure. In particular, using Bloch's tight-binding approximation, one-electron energy dispersion relations are obtained for the two bands which considerations of quantum chemistry indicate are involved in the metallic conduction which characterizes the high temperature, rutile phase of VO_2, namely, an orbitally non-degenerate d-band, conventionally called d_{11} and a higher energy band, π^*. The d_{11}-band is quite anisotropic, being based on pure 3d-orbitals, the dominant overlap amongst which occurs parallel ($\|$) to the rutile c_r-axis; the π^*-band, on the other hand, is more isotropic, being the antibonding band

arising from covalent hybridization between another cation d-orbital and the six anions which octahedrally co-ordinate every cation.

Some of the quantities which occur as parameters in the tight-binding method used are assigned the values required by Hearn's phonon-softening model of the semiconductor $\rightleftharpoons$ metal phase transition (Hearn 1972), whilst the remainder are evaluated by reference to the spectrum of V^{4+} in the orthorhombic anion field, as obtained from E.S.R. measurements. In this way the maximum width of the d_{11}-band is found to be 2 eV and that of the overlapping π^*-band, 2.22 eV; at the zone centre their separation is 0.2 eV.

The joint of d_{11} - π^* density of states is obtained by a Monte Carlo procedure, from which the Fermi energy E_F is found to be 0.93 eV above the bottom of the d_{11}-band, in close agreement with existing estimates, whilst the density of states at E_F is 1.3 eV^{-1} per cation.

Chapter 3 is devoted to a calculation of the Coulomb correlation energy (U) based on a method originally proposed by Hyland (1969). The important part of our calculations is the evaluation of the polarization energies in rutile VO_2. Since doubly occupied cations occur in the band picture, our purpose is to calculate the polarization which one of the two electrons on such a doubly occupied cation induces in its ionic environment. The other electron then interacts attractively with this polarization and hence effectively reduces its Coulomb repulsion

with the first electron. To calculate these polarization effects we adapt a method developed originally by Mott and Littleton in 1938 to study polarizations induced by defects in alkali halides. Our elaboration is conceptually straightforward but technically rather complicated in consequence of the rutile crystal structure over which certain lattice sums have to be evaluated numerically. The value for U turns out to be 1.74 eV; this, however is to be regarded as an upper limit for the reasons mentioned in Chapter 3.

The total average one-electron energy of the metallic state is calculated using our parametrized one-electron dispersion relations and the above value of U, and found to be lower than that of the corresponding Mott-insulating state by 0.46 eV; it is further found that this stability of the metallic state is not contingent upon the d_{11}-band being overlapped by the π^*-band.

The existence of strong electron-optical phonon interaction in the metallic VO_2 is supported experimentally by the Raman scattering study of Srivastava and Chase (1971) and on the theoretical side its effect on the phonons manifests itself in softening their modes (Hearn 1972). This interaction will also affect the electrons in the form of polaron formation. On several occasions it was suggested (Mott 1969, Mott and Zinamon 1970) that the electrons in the metallic phase of VO_2 form a degenerate gas of polarons. In view of the high velocities ($\sim 5 \times 10^7$ cm-sec^{-1}) of the electrons at the Fermi level, it is not possible, however, for an electron to polarize (ionic

polarization) the surrounding ions, since the residence time of an electron on an ion is too short to allow the lattice displacements to get established; accordingly, conventional (ionic) polarons are not formed. Whilst this is not the case for the *electronic* polarization, however, whose frequency *is* comparable to that of a typical electron, momentarily resident at a cation, the formation of the associated "electronic" polaron is, however, suppressed by another effect which is absent in the case of a single electron - namely, screening of the electron-phonon interaction by the degenerate gas of conduction electrons. We conclude therefore that the charge carriers in metallic VO_2 are electrons.

In Chapter 5, we turn to some applications of the one-electron dispersion relations to the interpretation of various electronic properties of metallic VO_2. In particular we compute the electronic specific heat and use our results to explain the anomolously high value of the specific heat found experimentally at high temperatures.

Starting from the dielectric response function of the conduction electron gas in metallic VO_2 we next calculate the plasma frequency and deduce qualitatively the contribution arising from interband transitions ($d_{11} \rightarrow \pi^*$); in addition we calculate the optical effective mass in metallic VO_2.

Finally we make a preliminary attempt to calculate the low field Hall constant based on the assumption of a *constant* relaxation time, whose existence is discussed towards the end of Chapter 5; the result obtained differs from the experimental value

by a factor of about 4 which is perhaps rather better than might have been anticipated in view of our assumption about the relaxation time.

Finally in Chapter 6 we review the results of our investigations and highlight some areas where further research would seem necessary and worthwhile.

CHAPTER 2

ELECTRONIC BAND STRUCTURE OF METALLIC VO_2

2.1. Introduction

Despite the existence of detailed band structure calculations for the metallic (rutile) phase of VO_2 (Mitra et. al. 1971, Chatterjee et.al. 1972, Mitra et.al. 1973, Caruthers et.al. 1973) their connection with the more intuitive approach of Goodenough (1965, 1971) based on considerations of quantum chemistry remains obscure; indeed there even exists a case of qualitative disagreement in which the existence of Goodenough's semi-metallic rutile phase is not endorsed by the results of certain A.P.W. calculations (Caruthers et. al. 1973). In assessing the relative reliabilities of these two approaches it is important to remember in the case of materials such as rutile VO_2 with its non-symmorphic space group D_{4h}^{14} ($P4_2/mnm$), and containing two such dissimilar atoms as V and O that the seemingly more sophisticated A.P.W. method is not devoid of certain intrinsic difficulties associated both with the use of the usual Muffin Tin artifice and with the choice of atomic potentials - a point which has been stressed by Honig et.al.(1969) and recognized in the work of Chatterjee et. al. (1972).

On the other hand, the quantum chemistry approach has the obvious attraction, even in materials with highly complex crystal structures, that it can separate out from the totality of cation and anion states those most likely to be involved in bonding from those available for participation in

conduction band formation; for the purposes of interpreting and correlating various transport phenomena only the latter minority subset of states are, of course, relevant. Whilst existing approaches recognize this they either confine themselves to simply identifying these various states and postulating the existence of corresponding bands, which are then depicted in terms of broadened energy level diagrams e.g. Goodenough (1971) - or, they include, *ab initio*, <u>all</u> the orbitals involved in the quantum chemistry considerations and proceed with a complete band structure calculation.

The Slater-Koster L.C.O.A.O. method used by Mitra et. al. (1973) belongs to this second category; unfortunately its utility turns out to be purely formal in consequence of the impossibility obtaining from experiment the values of the vast number of tunnel integrals which occur as (unknown) parameters in the 34 × 34 secular determinant resulting from including vanadium 3d, 4s and 4p orbitals and oxygen 2s and 2p orbitals.

In this chapter we attempt to achieve a compromise between these two extremes by calculating the structures of just those bands which the quantum chemistry of VO_2 indicates are most likely to be involved in electronic conduction, namely a pure orbitally non-degenerate d_{11}-band and a higher energy π^*-band containing admixtures of oxygen orbitals (Goodenough 1965, 1971). The method used is essentially Bloch's tight-binding approximation employing those vanadium 3d-orbitals indicated as relevant from a ligand field-theoretic interpretation (Shimizu 1967) of available

E.S.R. data; these orbitals are then superposed in accordance with the space group of VO_2. A most suggestive way of doing this is to form linear combinations, over the structure's simple tetragonal Bravais lattice, of appropriate admixtures of the bonding and anti-bonding orbitals which exist in the rutile unit cell of VO_2 in consequence of the non-equivalence of the two cations contained therein. The resulting band structures are parametrized by a total of six quantities whose values will not, in view of our earlier remarks, be determined by comparison with the results of other existing (A.P.W.) calculations as is sometimes advocated but instead by reference to what is probably the most satisfactory model yet proposed for the semi-conductor $\rightleftharpoons$ metal phase transition found in VO_2 at $341^{o}K$ ($= T_t$) and which, in addition, affords an understanding of certain anomalous properties of the high temperature metallic phase (Hearn 1972, 1973). In this model, due to Hearn (1972), the transition to the semi-conducting state is attributed to phonon softening which causes a splitting and uncrossing of the *same* two bands whose structure is here characterized by the six unknown parameters. Accordingly, by complementing the separation of the (localized) parent $d_{x^2-y^2}$ and d_{Π^*} levels as found by E.S.R. with the values which the parameters of Hearn's model must take in order that the correct transition temperature and conductivity discontinuity be obtained, the values of *our* six unknown parameters can, with the aid of Goodenough's assumption that the Π^*-band is isotropic, be uniquely determined.

Strictly speaking this procedure is, of course, inconsistent since the adopted values of Hearn's parameters are relevant to *his* assumed band structures and not ours which turn out to be quite different. However, the agreement subsequently found (see Chapter 5) between experimental measurements of various electronic transport properties such as plasma frequency, Hall constant and specific heat and the values of these quantities as calculated using our band structures does inspire some degree of confidence in the quantitative details of the associated one-electron dispersion relations whose (qualitative) $\underset{\sim}{k}$-dependences are, of course, *exact* to next-nearest neighbours. The degree of agreement could perhaps be considered surprising in view of the neglect of electron-phonon and electron-electron interactions which, it is known, can assume a dominating significance in other transition-metal oxides.

We now begin with a discussion of those aspects of the quantum chemistry of VO_2 relevant to our calculations.

2.2. Ligand Field Theory and E.S.R. Spectrum of V^{4+}

The vanadium ions (cations) in the rutile phase of VO_2 have orthorhombic point symmetry D_{2h} being co-ordinated by slightly distorted anion octahedra, each oxygen ion of which e.g. E, has 3 coplanar cation nearest neighbours labelled P, Q and R in Fig. 2.1. The anion sub-lattice can be anticipated to have important repercussions of the nature of the cation d-bands both through the effect of its electric field on the orbital degeneracy of the cation d-orbitals and through the interaction of anion orbitals with those of the octahedrally

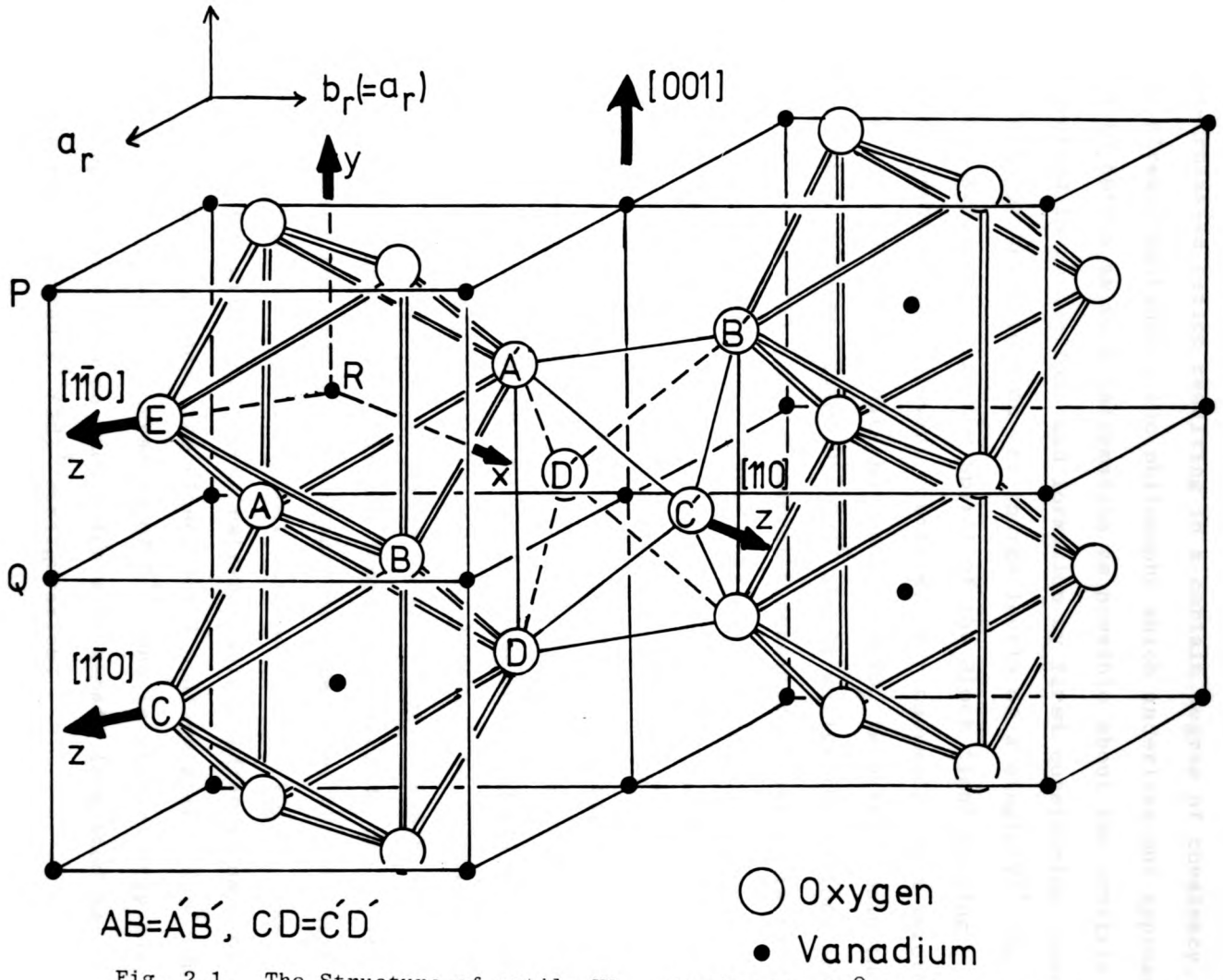

Fig. 2.1. The Structure of rutile VO_2, showing the 90° difference in orientation of the anion octahedra between successive (100) planes, separated by $+\frac{1}{2}|c|$.

co-ordinated cation resulting in a certain degree of covalency. As already mentioned, the philosophy which underlies our approach is to obtain as much information as possible about the orbitals involved in conduction band formation by first considering these effects of the anions on the energy levels of a single V^{4+} ion *before* superposing, in the spirit of the Bloch tight-binding approximation, the relevant orbitals. For assuming, as a zeroth order approximation, that the bonding in VO_2 is purely ionic then the anions acquire closed $O^{2-}(2p)^6$ shells whilst the cations are reduced to $V^{4+}(3d)^1$; it is generally considered that it is to these single d-electrons/cation that the electronic transport properties of rutile VO_2 are due. Experimental information on the structure of the energy spectrum of a single V^{4+} ion cannot, of course, be obtained from studies on VO_2 itself since the d-electrons do not remain localized (one per cation) but are instead itinerant, VO_2 in its rutile phase being metallic. Some idea of the effects of the anions can, however, be obtained from a ligand field-theoretic analysis of the observed E.S.R. spectrum of V^{4+} ions substituted into the isostructural oxide TiO_2. It may be noted that the V - O distance averaged over the six near neighbour anions of the TiO_2 host exceeds that in VO_2 by less than 2%. For within the above extreme ionic bonding assumption the titanium ions adopt the closed shell configuration $(3p)^6$ $(3d)^o$ and, provided the concentration of V^{4+} ions is sufficiently low, the single d-electron on each V ion will remain localized so giving the required $V^{4+}(3d)^1$ configuration.

co-ordinated cation resulting in a certain degree of covalency. As already mentioned, the philosophy which underlies our approach is to obtain as much information as possible about the orbitals involved in conduction band formation by first considering these effects of the anions on the energy levels of a single V^{4+} ion *before* superposing, in the spirit of the Bloch tight-binding approximation, the relevant orbitals. For assuming, as a zeroth order approximation, that the bonding in VO_2 is purely ionic then the anions acquire closed $O^{2-}(2p)^6$ shells whilst the cations are reduced to $V^{4+}(3d)^1$; it is generally considered that it is to these single d-electrons/cation that the electronic transport properties of rutile VO_2 are due. Experimental information on the structure of the energy spectrum of a single V^{4+} ion cannot, of course, be obtained from studies on VO_2 itself since the d-electrons do not remain localized (one per cation) but are instead itinerant, VO_2 in its rutile phase being metallic. Some idea of the effects of the anions can, however, be obtained from a ligand field-theoretic analysis of the observed E.S.R. spectrum of V^{4+} ions substituted into the isostructural oxide TiO_2. It may be noted that the V - O distance averaged over the six near neighbour anions of the TiO_2 host exceeds that in VO_2 by less than 2%. For within the above extreme ionic bonding assumption the titanium ions adopt the closed shell configuration $(3p)^6$ $(3d)^o$ and, provided the concentration of V^{4+} ions is sufficiently low, the single d-electron on each V ion will remain localized so giving the required $V^{4+}(3d)^1$ configuration.

The most complete analysis of the E.S.R. spectrum of V^{4+} ions in TiO_2 is due to Shimizu (1967) and incorporates not only cation-anion interactions but also admixtures, arising from the orthorhombic component of the anion field, of the d_{z^2} orbital of the e_g-manifold into the $d_{x^2-y^2}$ ground state, the inclusion of which is essential if consistent agreement between g-factors and the hfs constants is to be obtained.

Only the former effect was included in the earlier work of Hyland (1968), through the use of an effective spin-orbit coupling constant (1.86×10^{-2} eV) in place of that relevant to a free V^{4+} ion (3.0×10^{-2} eV). For the present work, it will, however, be necessary to be more explicit about the possible V-O interactions in order to be able to identify those orbitals available for conduction band formation.

The simplest approach is to note that the two 3d (e_g), 4s and 4p orbitals of a given cation homo-hybridize to form an orbital with six lobes directed at the six surrounding near-neighbour anions. In turn, two of the three 2p orbitals of a given anion ($2p_y$ and $2p_z$ in the co-ordinate system shown in Fig. 2.2) homohybridize with its 2s-orbital to form a trigonal orbital whose lobes are directed towards the three coplanar cation near neighbours (each one of which is, of course, surrounded by a different anion octahedron) and σ-bonding results; the bonding σ-orbital is predominantly anion-like whilst the anti-bonding σ^*-orbital is cation-like. The remaining oxygen

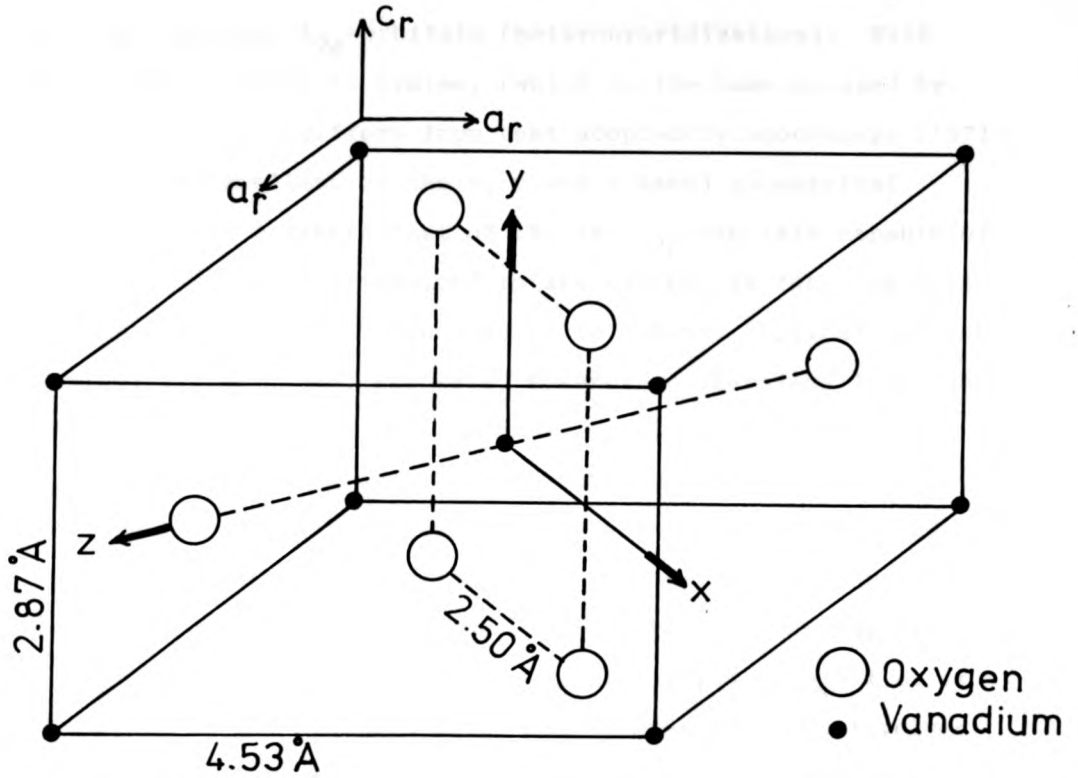

Fig. 2.2. The Unit cell of rutile VO_2.

$2p_x$ orbital, on the other hand is available for Π-bonding with the cationic t_{2g}-orbitals (heterohybridization). With the chosen co-ordinate system, (which is the same as used by Shimizu and which differs from that adopted by Goodenough (1971) only by a relabelling of the x, y and z axes) geometrical considerations indicate that of the two t_{2g}-orbitals capable of Π-bonding only d_{zx} is involved to any extent; in fact, in what follows *only* d_{zx} will be considered to Π-bond. Optical reflectivity (Verleur et. al. 1968, Fan 1972, Mokerov and Saraiken 1976) and photo-emission (Powell et. al. 1969) measurements on *metallic* VO_2 indicate that the associated Π-bonding bands (which are slightly less stabilized than the σ-bonding bands) lie at least 2.5 eV below the Fermi surface which, following Goodenough, we assume to be located within the band complex originating from the $d_{x^2-y^2}$ level and anti-bonding d_{Π^*}-level, $(3d_{zx}:2p_x)$ i.e. it is just these *two* orbitals which are considered to be involved in conduction band formation, to be partially occupied by the *single* 3d-electron per cation; the fate of the remaining d_{yz} orbital will be discussed in Chapter 2.3.

These results for the energy levels of a single VO_6 octahedron *within* TiO_2 are shown in Fig. 2.3 in which the values shown for the $d_{x^2-y^2}$-d_{yz} and $d_{x^2-y^2}$-d_{Π^*} energy gaps are taken from Shimizu's work. It should be noted that whilst the ordering of the d_{zx} and d_{yz} levels are reversed from that shown in Fig.3 of Hyland (1968) the separation of the d_{Π^*}-level from the ground-state differs only by 0.01 eV from that calculated by Hyland

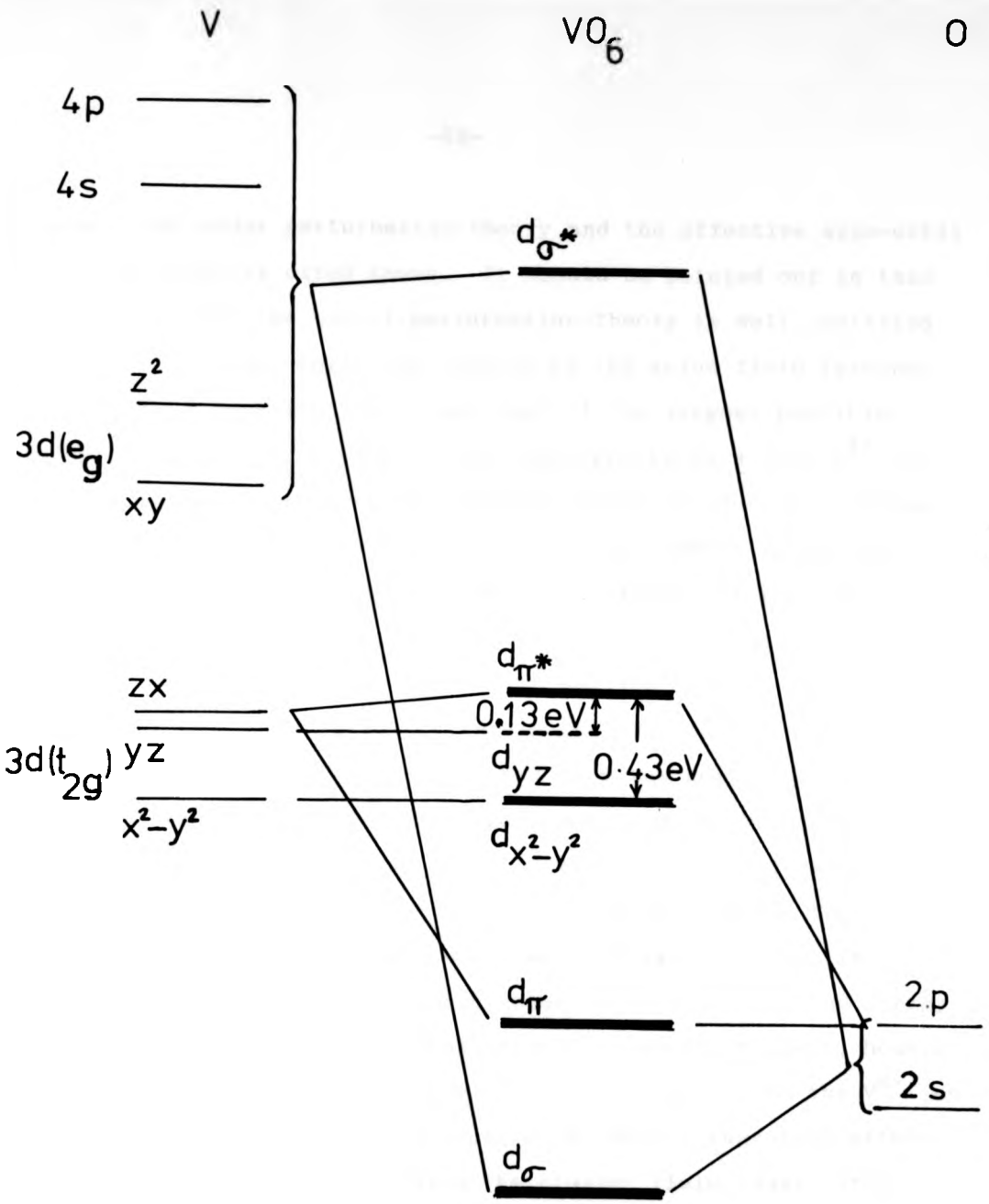

Fig. 2.3. The energy spectrum of a single VO_6 - complex in TiO_2.

using first-order perturbation theory and the effective spin-orbit coupling constant cited above. It should be pointed out in this connection that the use of perturbation theory is well justified since the smallest splitting induced by the anion field (ground-state - d_{yz}) is almost ten times that of the largest possible spin-orbit coupling constant (that appropriate to a free V^{4+} ion); the criticism of Lazukova and Gubanov (1976) is thus only relevant to the results of their own *calculated* orthorhombic splittings within an *isolated* VO_6-cluster, which are indeed of the same order of magnitude as the spin-orbit coupling constant. In addition to obtaining these very much smaller orthorhombic splittings the ordering of the levels is also found to be different with d_{zx} lying lowest being separated from the next ($d_{x^2-y^2}$) by 0.03 eV-c.f. the corresponding separation of 0.43 eV inferred from the E.S.R. data; it may be noted that these small calculated values of the splittings are in good agreement with the VO_6-cluster calculation performed by Sommers et. al. (1975). In adjudging the relevance of such cluster calculations to the energy spectrum of V^{4+} in an octahedral crystal anion environment, however, it must be remembered that the electric field acting on the V^{4+} ion within an isolated cluster is necessarily weaker than that within a crystal, with respect to which the cluster field constitutes only the nearest neighbour contribution. Accordingly, the much larger V^{4+} splittings found experimentally from measurements in the crystal are at least qualitatively understandable.

A second important difference on going from a VO_6-complex *within* the rutile host crystal to an isolated one is that the three coplanar cation near neighbours of an octahedrally co-ordinated cation are absent with a consequent *increase* in the number of anion orbitals available for Π-bonding. It is, therefore, perhaps surprising to note that there is almost exact agreement between Shimizu and Sommers et. al. concerning the degree of covalency present; both groups find that only about 70% of the d-electron in the nominal V^{4+} ion actually resides on the cation, the remainder being covalently distributed over the six near neighbour oxygen ions.

Finally, it should be noted that within the adopted VO_6 energy level spectrum covalency can obtain only in the excited states of the V^{4+} ion since only d_{zx} is assumed to Π-bond with the anions. Of course, once Bloch functions are formed from these levels a certain degree of covalency even in the ground state of metallic VO_2 will be possible provided the Π^*-band overlaps the lower $d_{x^2-y^2}$ *band* to a sufficient extent; experimentally, this would appear to be most likely the case.

2.3. Bloch Functions and Band Structures

The first step towards the construction of the Bloch functions associated with each of the three cation orbitals $d_{x^2-y^2}$, d_{yz} and d_{Π^*}, which the foregoing considerations suggest as those most likely involved in conduction band formation, is

the recognition that the two cations contained in the apparently body-centred tetragonal unit cell of rutile VO_2 (Fig. 2.2) are, in fact, non-equivalent in consequence of the 90^o rotation about the c_r-axis of the respective co-ordinating anion octahedra (see Fig. 2.1). Accordingly, two equivalent procedures are possible at this point:

1. Treat the cation sub-lattice as two interpenetrating, non-equivalent simple tetragonal lattices, and construct Bloch functions for each, finally superposing them to form the Bloch function for the actual crystal.
2. Treat the cation sub-lattice in terms of a simple tetragonal Bravais lattice with a basis of two cations and construct the crystal Bloch functions from linear superpositions of the bonding and anti-bonding unit cell orbitals associated with the two-cation basis per unit cell.

We shall adopt the latter in view of its more natural connection with the ideas and concepts (e.g. bonding and anti-bonding) familiar within the quantum chemistry approach.

Consideration based on the relative orientations of the lobes of the two d_{yz} orbitals within a given two-cation basis then suggest that these orbitals do not participate in the formation of cell orbitals and should be considered to remain

localized. This will be assumed in what follows,* whence there are only two bands whose structures have to be calculated: a band deriving from the $d_{x^2-y^2}$ ground-state orbitals which is conventionally denoted (Goodenough 1971) by d_{11} (in consequence of the predominant overlap of the $d_{x^2-y^2}$ being parallel to the c_r-axis) and a higher lying band deriving from the hybridized $d_{\Pi*}$ orbitals and conventionally donated as Π^*. The actual location of the assumed localized d_{yz}-level within this two-band complex will be considered later in Chapter 2.4. once the Fermi energy has been calculated

Let $^{(1)}d_{11}$ ($^{(1)}d_{\Pi*}$) and $^{(2)}d_{11}$ ($^{(2)}d_{\Pi*}$) denote, respectively, the normalized orbitals associated with the two cations within a given basis. In what follows the location of $^{(2)}d$ within a given two-cation basis will be referred to $^{(1)}d$ as origin; thus $^{(1)}d$ is to be understood as shorthand for $^{(1)}d(\underset{\sim}{r})$ and $^{(2)}d$ for $^{(2)}d\ (\underset{\sim}{r} + \underset{\sim}{\mu})$, where $\underset{\sim}{\mu}$ is the vector joining the two cations of the basis. Distinguishing superscript numbers (1 and 2) are, however, still necessary to respect the 90° difference in rotation between the orbitals of the two cations. Then the corresponding normalized bonding and anti-bonding cell orbitals are given, respectively, by

---

* A more exact treatment would, of course, consider the possibility of formation, upon superposition of unit cells, of a d_{yz}-energy band based on the associated cellularly *localized* orbitals.

$$\psi_b = \frac{^{(1)}d_{11} + {}^{(2)}d_{11}}{\sqrt{2 + 2\,S_{11}}} \quad , \qquad \psi_a = \frac{^{(1)}d_{11} - {}^{(2)}d_{11}}{\sqrt{2 - 2\,S_{11}}} \qquad 2.3.1.$$

$$\phi_b = \frac{^{(1)}d_{\Pi}^{*} + {}^{(2)}d_{\Pi}^{*}}{\sqrt{2 + 2\,S_{\Pi^*}}} \quad , \qquad \phi_a = \frac{^{(1)}d_{\Pi}^{*} - {}^{(2)}d_{\Pi}^{*}}{\sqrt{2 - 2\,S_{\Pi^*}}} \qquad 2.3.2.$$

wherein the S's denote the relevant overlap integrals. The crystal Bloch functions are now constructed from superpositions of these cell orbitals in accordance with the simple tetragonal Bravais lattice of the rutile structure; thus

$$\Psi_{\underset{\sim}{k}}(\underset{\sim}{r};\eta) = \frac{1}{\sqrt{N(1+|\eta|^2)}} \sum_{l} e^{i\underset{\sim}{k}\cdot\underset{\sim}{R}_l} \{\psi_a(\underset{\sim}{r}-\underset{\sim}{R}_l) + \eta\,\psi_b(\underset{\sim}{r}-\underset{\sim}{R}_l)\} \qquad 2.3.3.$$

$$\Phi_{\underset{\sim}{k}}(\underset{\sim}{r};\eta) = \frac{1}{\sqrt{N(1+|\eta|^2)}} \sum_{l} e^{i\underset{\sim}{k}\cdot\underset{\sim}{R}_l} \{\phi_a(\underset{\sim}{r}-\underset{\sim}{R}_l) + \eta\,\phi_b(\underset{\sim}{r}-\underset{\sim}{R}_l)\} \qquad 2.3.4.$$

where N is the number of unit cells (= ½ the number of cations, since each cell contains one two-cation basis), $\underset{\sim}{R}_l$ locates the two-cation bases in the simple tetragonal Bravais lattice, and η is a complex admixture parameter, the introduction of which is necessary in consequence of the loss of the identity of the bonding and anti-bonding levels away from $\underset{\sim}{k} = 0$. It should be noted that in equations (2.3.3) and (2.3.4) and in what follows, the components of $\underset{\sim}{k}$ are assumed to be based on an axes system

related to that shown in Fig. 2.2 by a rotation of the x and z axes through 45^{o} followed by an interchange in the labelling of the y and z axes. In the new co-ordinate system the x and y axes are parallel to the rutile a_r-axes whilst z is parallel to rutile c_r-axis and the associated Brillouin zone is shown in Fig. 2.4.

Provided all intra and intermotif atomic overlaps are neglected, then

$$\int \Psi^*_{\underline{k}} \Psi_{\underline{k}} \, d^3 \underline{r} = 1 = \int \Phi_{\underline{k}}^* \Phi_{\underline{k}} \, d^3 \underline{r}, \text{ as} \qquad 2.3.5.$$

is readily deduced from equation (2.3.4).

The required band structures are now obtained in the standard way by computing the expectation values, E, of the one-electron Hamiltonian, H, for both Bloch states $\Psi_{\underline{k}}(\underline{r};\eta)$ and $\Phi_{\underline{k}}(\underline{r};\eta)$ and finally, in respect of the existence of two non-equivalent cations per unit cell, minimizing the resulting energies with respect to η. If $V(\underline{r})$ denotes the periodic crystal potential of the cation sublattice, then H is given by

$$H = \frac{-\hbar^2}{2m} \nabla^2 + V(\underline{r}) \qquad 2.3.6.$$

Further, if $U(\underline{r} - \underline{R}_l)$ denotes the potential of an isolated two-cation basis ("motif" for short) centred on $\underline{R}_l$, then H can be rewritten in the usual way thus:

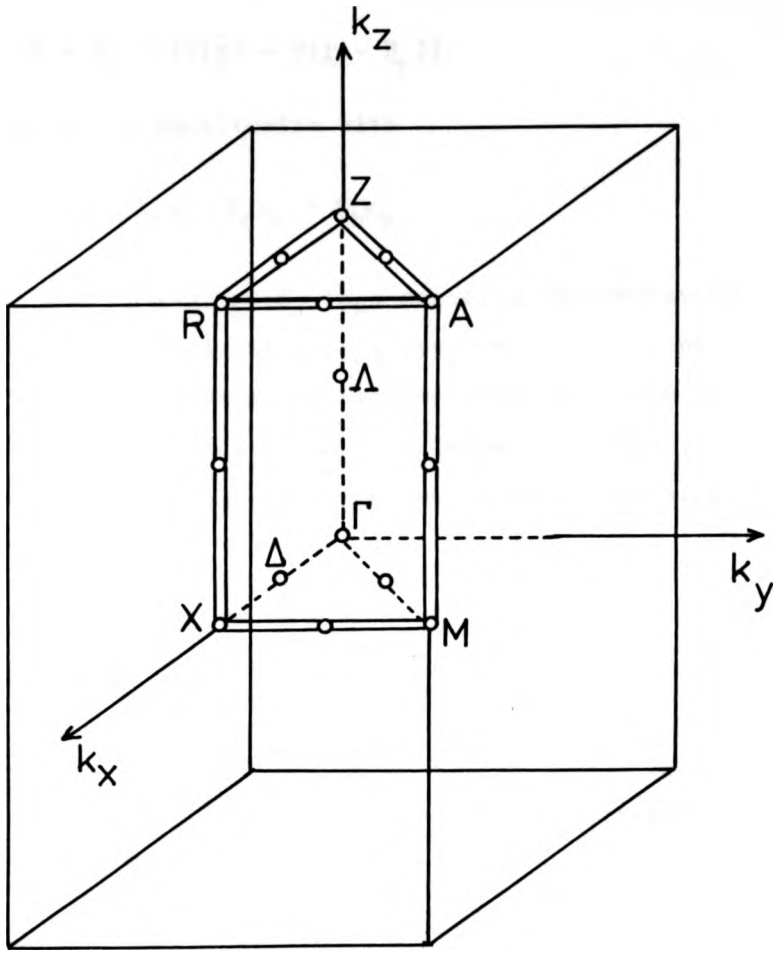

Fig. 2.4. The Brillouin zone of the simple tetragonal Bravais lattice of rutile VO_2.

$$H = H_o + [V(\underset{\sim}{r}) - U(\underset{\sim}{r} - \underset{\sim}{R}_l)] \qquad 2.3.7.$$

where H_o is the motif Hamiltonian with

$$H_o\psi_a = E_a\psi_a, \; H_o\psi_b = E_b\psi_b \qquad 2.3.8.$$

(and similarly for ϕ_a and ϕ_b) E_a (E_b) denoting the energy of the anti-bonding (bonding) state of a given motif. In the spirit of the Bloch tight-binding approach the last term in equation (2.3.7) is now treated as a perturbation. Thus, with equation (2.3.5), the required eigenvalues are given by

$$E(\underset{\sim}{k};\eta) \equiv \int \Psi_{\underset{\sim}{k}}^{*}(\underset{\sim}{r};\eta)\, H\, \Psi_{\underset{\sim}{k}}(\underset{\sim}{r};\eta)\, d^3\underset{\sim}{r} \qquad 2.3.9.$$

which using equations (2.3.3), (2.3.7) and (2.3.8) can be rewritten,

$$E(\underset{\sim}{k};\eta) = \frac{E_a + |\eta|^2 E_b}{1+|\eta|^2} + \sum_{m,n} \int e^{i\underset{\sim}{k}\cdot(\underset{\sim}{R}_m - \underset{\sim}{R}_n)} \psi_k^{*}(\underset{\sim}{r}-\underset{\sim}{R}_n)[V(\underset{\sim}{r}) - U(\underset{\sim}{r}-\underset{\sim}{R}_l)]\psi_k(\underset{\sim}{r}-\underset{\sim}{R}_m)\, d^3\underset{\sim}{r} \qquad 2.3.10.$$

Neglecting, as usual, the 3-centre integrals in (2.3.10) (equivalent to replacing $\underset{\sim}{R}_l$ in $U(\underset{\sim}{r}-\underset{\sim}{R}_l)$ by $\underset{\sim}{R}_m$), setting

$$-\underset{\sim}{R}_j = \underset{\sim}{R}_m - \underset{\sim}{R}_n \qquad 2.3.11.$$

and taking $\underset{\sim}{R}_m = 0$, the sum over m can be performed to give a factor N which cancels that contained in the definition (2.3.3) and $\Psi_{\underset{\sim}{k}}$ (and $\Psi_{\underset{\sim}{k}}^{*}$); equation-(2.3.10) can then be written,

$$E(\underset{\sim}{k};\eta) = \frac{E_a+|\eta|^2 E_b}{1+|\eta|^2} + \frac{1}{1+|\eta|^2}\,[S_1 + \eta S_2 + \eta^* S_3 + |\eta|^2 S_4] \qquad 2.3.12.$$

where, e.g.

$$S_2 = S_2\,(a,b) \equiv \sum_j e^{-i\underset{\sim}{k}\cdot\underset{\sim}{R}_j} \int \psi_a^*\,(\underset{\sim}{r}-\underset{\sim}{R}_j)\; v(\underset{\sim}{r})\psi_b(\underset{\sim}{r})d^3\underset{\sim}{r} \qquad 2.3.13.$$

and within the same convention,

$$S_1 = S_1\,(a,a),\quad S_3 = S_3\,(b,a),\; S_4 = S_4\,(b,b) \qquad 2.3.14.$$

where $v(\underset{\sim}{r}) \equiv V(\underset{\sim}{r}) - U(\underset{\sim}{r})$. 2.3.15.

Minimization of equation (2.3.12) w.r.t. η yields,

$$\eta = \frac{(S_4 - S_1 - \delta) \mp \sqrt{(S_4 - S_1 - \delta)^2 + 4\,S_2\,S_3}}{2\,S_2} \qquad 2.3.16.$$

where $\delta \equiv (E_a - E_b)$ is, assuming $U(\underset{\sim}{r}) = {}^{(1)}U(\underset{\sim}{r}) + {}^{(2)}U(\underset{\sim}{r})$, given by

$$\delta = -\,2 \int {}^{(1)}d_{11}^*(\underset{\sim}{r})\;\; {}^{(1)}U(\underset{\sim}{r})\;\; {}^{(2)}d_{11}(\underset{\sim}{r})\; d^3\underset{\sim}{r} \qquad 2.3.17.$$

Equation (2.3.12) then takes the form,

$$E(\underset{\sim}{k}) = \frac{E_a+E_b}{2} + \frac{S_1+S_4}{2} \pm \sqrt{\left(\frac{S_4-S_1-\delta}{2}\right)^2 + S_2\,S_3} \qquad 2.3.18.$$

Consistent with the neglect of intra-motif overlap integrals the first term on R.H.S. of equation (2.3.18) is the energy of a single electron within either cation of the motif and equal to E_o, say, whilst expressing S_1 and S_4 in terms of cation orbitals via equation (2.3.1) it is readily shown that the first term in the square-root on the R.H.S. of equation (2.3.18) is independent of δ. Then correct to next-nearest neighbours, equation (2.3.18) assumes the final form:

$$E(\underline{k}) = E_o - \alpha - 2\beta \cos k_z c \pm 8\gamma \left| \cos \frac{k_x a}{2} \cdot \cos \frac{k_y a}{2} \cdot \cos \frac{k_z c}{2} \right| \quad 2.3.19.$$

where the positive quantities α, β and γ are defined by

$$\alpha \equiv - \int {}^{(1)}d_{11}^{*}(r) \, [V(\underline{r}) - {}^{(1)}U(\underline{r})] \, {}^{(1)}d_{11}(\underline{r}) \, d^3\underline{r} \quad 2.3.20$$

$$\beta \equiv - \int {}^{(1)}d_{11}^{*}(\underline{r} - \underline{R}_j) \, [V(\underline{r}) - {}^{(1)}U(\underline{r})] \, {}^{(1)}d_{11}(\underline{r}) \, d^3\underline{r} \quad 2.3.21.$$

$$\gamma \equiv + \int {}^{(1)}d_{11}^{*}(\underline{r} - \underline{R}_j) \, [V(\underline{r}) - {}^{(2)}U(\underline{r})] \, {}^{(2)}d_{11}(\underline{r}) \, d^3\underline{r} \quad 2.3.22.$$

and have the following interpretation.

α renormalizes the total energy, E_o, of the localized $d_{x^2-y^2}$ state of a isolated cation to a value appropriate to the stronger binding which occurs when the same cation is a member of the cation sub-lattice of the crystal, whilst the "tunnel" integrals β and γ control the decrease in kinetic energy

achieved through delocalization; in particular, β incorporates the delocalization associated with electron tunnelling between nearest neighbour cations belonging to the same cation sublattice and, accordingly, located along the rutile c_r-axis at $\pm |\underline{c}|$, whilst γ incorporates the tunnelling to the eight next-nearest neighbours of a given cation which are equidistantly located on the "other" cation sublattice at a distance of $|\underline{\mu}|$. It should be noted that the sign difference between equations (2.3.21) and (2.3.22) is a direct consequence of the respective intra and inter cation sublattice natures of β and γ and the associated identity in sign, in the latter case, of the orbitals connected by $[V(\underline{r}) - {}^{(2)}U(\underline{r})]$.

Finally the modulus sign associated with the last term in the one-electron energy dispersion relation (2.3.14) (arising from the square root in equation (2.3.18) automatically guarantees the correct periodicity of the energy, whilst the associated positive and negative signs correspond, respectively, to the anti-bonding and bonding branches arising from the existence of two non-equivalent cations per unit cell; it is to be stressed, however, that these bonding and anti-bonding bands are not in a 1-1 correspondence with the corresponding motif levels but individually receive contributions from both bonding and anti-bonding motif orbitals.

The Π^*-band has the same structure as that of the d_{11}-band (2.3.19) but with E_o now interpreted as the total energy of the localized $d_{\Pi*}$-orbital of an isolated cation and d_{11} replaced by $d_{\Pi*}$ in the definitions of β and γ.

Thus there are altogether eight parameters characterizing the structures of the two bands considered, four of which are, however, related through the evident identification

$$(E_o - \alpha)_{\Pi^*} - (E_o - \alpha)_{11} = 0.43 \text{ eV} \qquad 2.3.23$$

where 0.43 eV is, it will be recalled, the energy separation of the d_{11} and d_{Π^*} levels of a cation in the crystal, as infered from Shimizu's E.S.R. analysis discussed in Chapter 2.2. A further reduction in the number of independent parameters can be achieved by relating the β's and γ's to the widths of the d_{11} and Π^*-bands appropriately defined. To this end if $W_{11}^{(\Lambda)}$ denotes the width of the d-band in the Γ - Z direction ($\underset{\sim}{k} = 0, 0, k_z$) (Fig. 2.4), and defined as the difference between the maximum and minimum values of equation (2.3.19), located, respectively, at

$$k_z^o = \frac{2}{c} \cos^{-1} \left(\frac{-\gamma}{\beta}\right) \qquad 2.3.24.$$

on the anti-bonding branch and at $k_z^o = 0$ on the bonding branch, then

$$W_{11}^{(\Lambda)} = \frac{4\gamma^2}{\beta} + 4\beta + 8\gamma \qquad 2.3.25.$$

On the other hand, the width $W_{11}^{(\Delta)}$ along the Γ - X direction in the basal plane is given by

$$W_{11}^{(\Delta)} = 16\gamma$$

Now to ensure the stability of the crystal through the phase transition the ratio $W_{11}^{(\Delta)}/W_{11}^{(\Lambda)}$ cannot be arbitrarily small; indeed a minimum value of about 33% emerges from Hearn's analysis, (in this connection it might be pointed out that the slightly larger value of 35% used later by Hearn (1972) leads to a latent heat in good agreement with experiment) of the phase transition (Hearn 1971). In what follows, it will be assumed that

$$W_{11}^{(\Delta)} = \frac{1}{3} W_{11}^{(\Lambda)} \qquad 2.3.27.$$

Equation (2.3.25) then yields, via (2.3.26) and (2.3.27) a quadratic equation in β, the acceptable (in the sense that it ensures that the evident inequality $\beta > \gamma$ is satisfied and hence, via equation (2.3.24), the reality of k_z^o) solution of which is

$$2\beta = 0.41\ W_{11}^{(\Lambda)} \qquad 2.3.28.$$

Finally equation (2.3.19) can for the case of the d_{11}-band be written, for

$$|k_x|,\ |k_y| \leq \frac{\pi}{a},\ |k_z| \leq \frac{\pi}{c}$$

$$E_{11}(\underset{\sim}{k}) = (E_o - \alpha)_{11} + \frac{W_{11}^{(\Lambda)}}{6}\left[-2.48 \cos k_z c \pm \cos\frac{k_x a}{2} \cdot \cos\frac{k_y a}{2} \cdot \cos\frac{k_z c}{2}\right] \qquad 2.3.29.$$

The Π^*-band can be treated in a similar way, with the exception that equation (2.3.27) is to be replaced by

$$W_{\Pi^*}^{(\Delta)} = W_{\Pi^*}^{(\Lambda)} \qquad 2.3.30.$$

in respect of the approximate isotropy in various transport properties (Goodenough 1965, 1971). Equation (2.3.30) in turn imposes

$$\beta = \gamma \qquad 2.3.31.$$

whence the maximum on the anti-bonding branch in the Γ - Z direction is changed into an inflexion point located at $k_z = \frac{2\pi}{c}$, in the Jones zone (k_z = O in the reduced Brillouin zone).

Thus for the case of the Π^*-band, equation (2.3.19) takes the final form, for

$$|k_x|, |k_y| \leq \pi/a, \; |k_z| \leq \pi/c$$

$$E_{\Pi^*}(\underset{\sim}{k}) = (E_o - \alpha)_{\Pi^*} + \frac{W_{\Pi^*}^{(\Lambda)}}{2} \left[- 0.25 \cos k_z c \pm \cos \frac{k_x a}{2} \cdot \cos \frac{k_y a}{2} \cdot \cos \frac{k_z c}{2} \right] \qquad 2.3.32.$$

Now from Hearn's theory of the phase transition (Hearn 1972) $W_{11}^{(\Lambda)}$ = 2 eV and for the case in which the Π^*-band was assumed to be 3-dimensional, with an associated free-electron dispersion relation (as indeed equation (2.3.32) has for $\underset{\sim}{k} \simeq$ O)

$$E_{\Pi^*}(O) - E_{11}(O) = 0.2 \text{ eV} \qquad 2.3.33.$$

Equations (2.3.29), (2.3.32) together with (2.3.23) then imply $W_{\Pi*}^{(\Lambda)} = 2.22$ eV. Taking the zero of energy to coincide with the bottom of the d_{11}-band (at $\underset{\sim}{k} = 0$), equations (2.3.29) and (2.3.32) then assume, using (2.3.23) the following quantitative forms

$$E_{11}(\underset{\sim}{k}) = 1.16 - 0.83 \cos k_z c \pm 0.33 \cos \frac{k_x a}{2} \cdot \cos \frac{k_y a}{2} \cdot \cos \frac{k_z c}{2},$$

$$|k_x|, |k_y| \leq \pi/a, |k_z| \leq \pi/c. \qquad 2.3.34.$$

$$E_{\Pi*}(\underset{\sim}{k}) = 1.59 - 0.28 \cos k_z c \pm 1.11 \cos \frac{k_x a}{2} \cdot \cos \frac{k_y a}{2} \cdot \cos \frac{k_z c}{2},$$

$$|k_x|, |k_y| \leq \pi/a, |k_z| \leq \pi/c. \qquad 2.3.35..$$

which are displayed in Figs. 2.5a, and 2.5b for the Γ - Z and Γ - X directions, respectively.

2.4. Properties of the Calculated Band Structures

(a) Density of states and Fermi level E_F

The densities of states (including spin) $N_{11}(E)$ and $N_{\Pi*}(E)$ associated independently with equations (2.3.34) and (2.3.35) were obtained by Monte Carlo calculation as follows. Consider the Brillouin zone of rutile VO_2. For constant $\underset{\sim}{k}$, the dispersion relation $E(\underset{\sim}{k})$ defines a constant energy surface. Let us divide E into a finite number of equal partitions, each of which is ΔE. Let us create a random number set of (k_x, k_y, k_z) values and calculate the corresponding energy E. If the energy lies between the interval E and $E + \Delta E$, this is to be counted as 1.

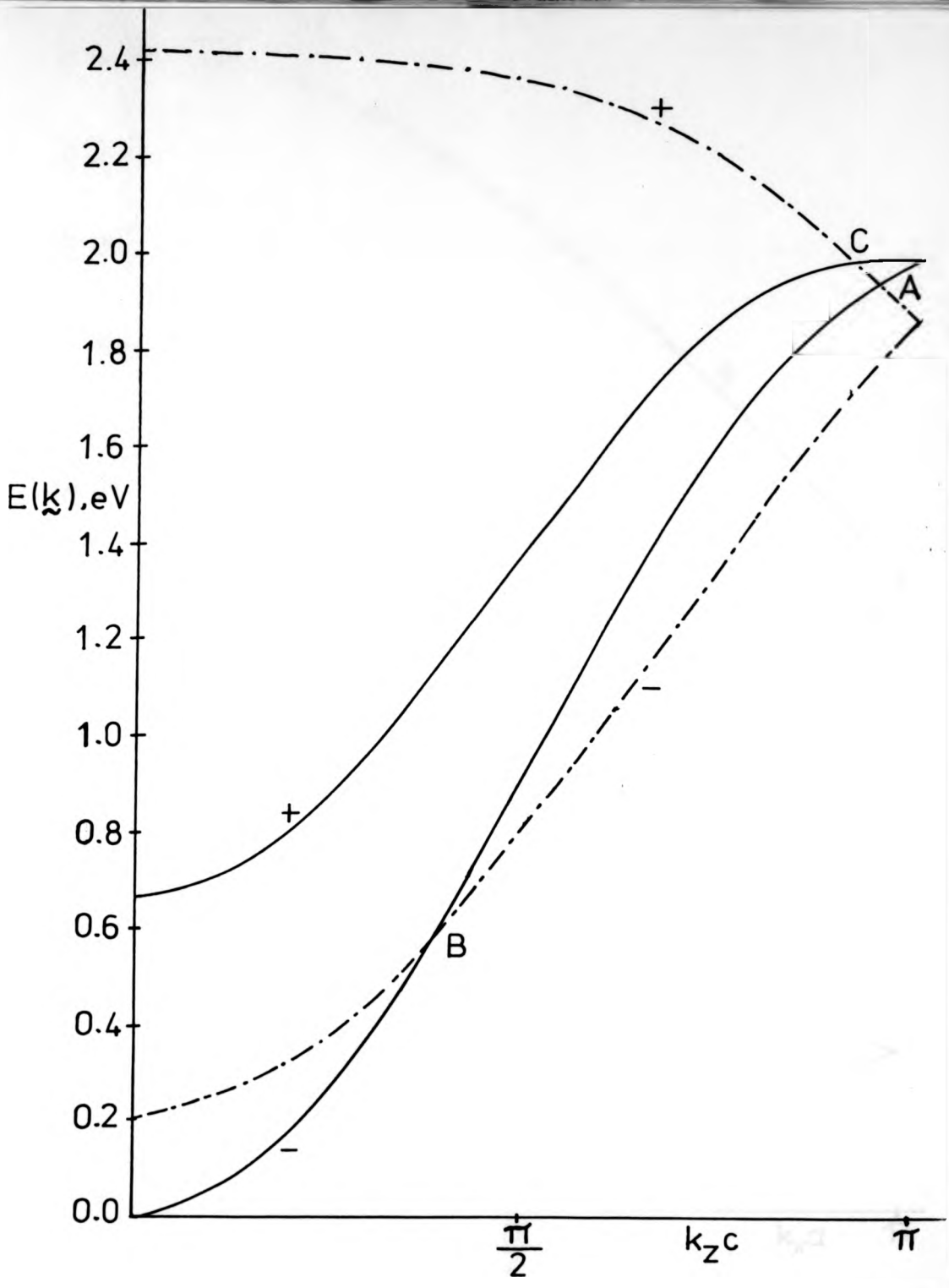

Fig. 2.5a. The energy dispersion of the d_{11}(———) and Π^*(-·-·-·-·) bands along the Γ-Z direction of the Brillouin zone.

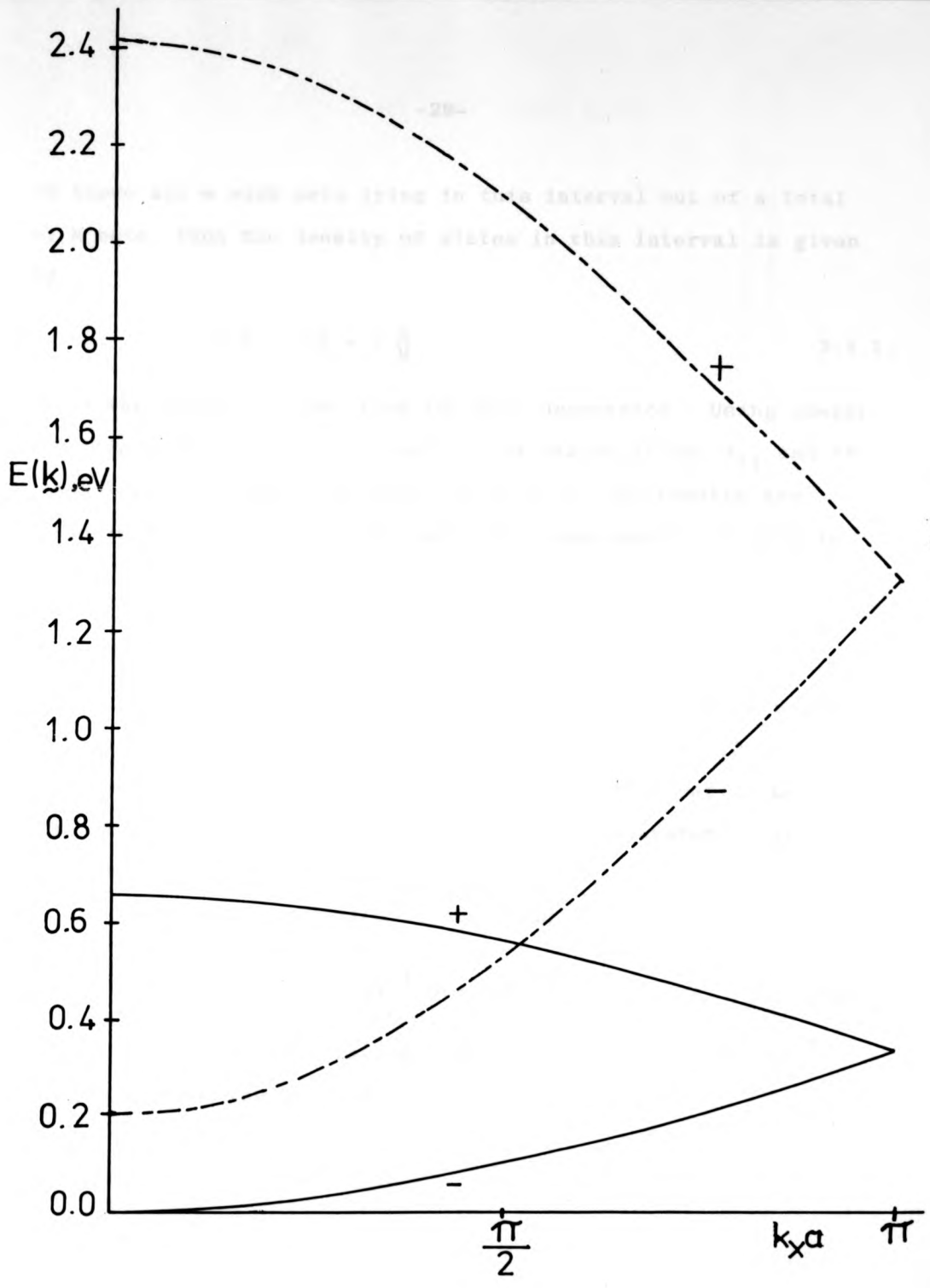

Fig. 2.5b. The energy dispersion of the d_{11} (———) and Π^* (—•—•—•)bands along the Γ-X direction of the Brillouin zone.

If there are m such sets lying in this interval out of a total of M sets, then the density of states in this interval is given by

$$N(E) \quad \Delta E = 2 \frac{m}{M} \qquad 2.4.1.$$

where the factor 2 comes from the spin degeneracy. Using energy partitions of 0.1 eV, the densities of states of the d_{11} and Π^* bands are determined from equation (2.4.1); the results are shown in Figs. 2.6a and 2.6b, and their superpositions N(E) in Fig. 2.7, which is not to the same scale.

Normalizing N(E) to eV^{-1} *per cation* and recalling that each cation contributes one d-electron, the approximate location of the Fermi level, E_F, was obtained by summing the area under N(E) to unity. Leaving the calculations to Chapter 5.2 here we only give the result. The Fermi level, E_F, turns out to be 0.93 eV and constant within the considered temperature range (340-900^{o}K).

The density of states at the Fermi level is

$$N(E_F) = 1.3 \text{ eV}^{-1} \text{ per cation} \qquad 2.4.2.$$

made up of 0.8 eV^{-1} per cation from the d_{11}-band and 0.5 eV^{-1} per cation from the Π^*-band.

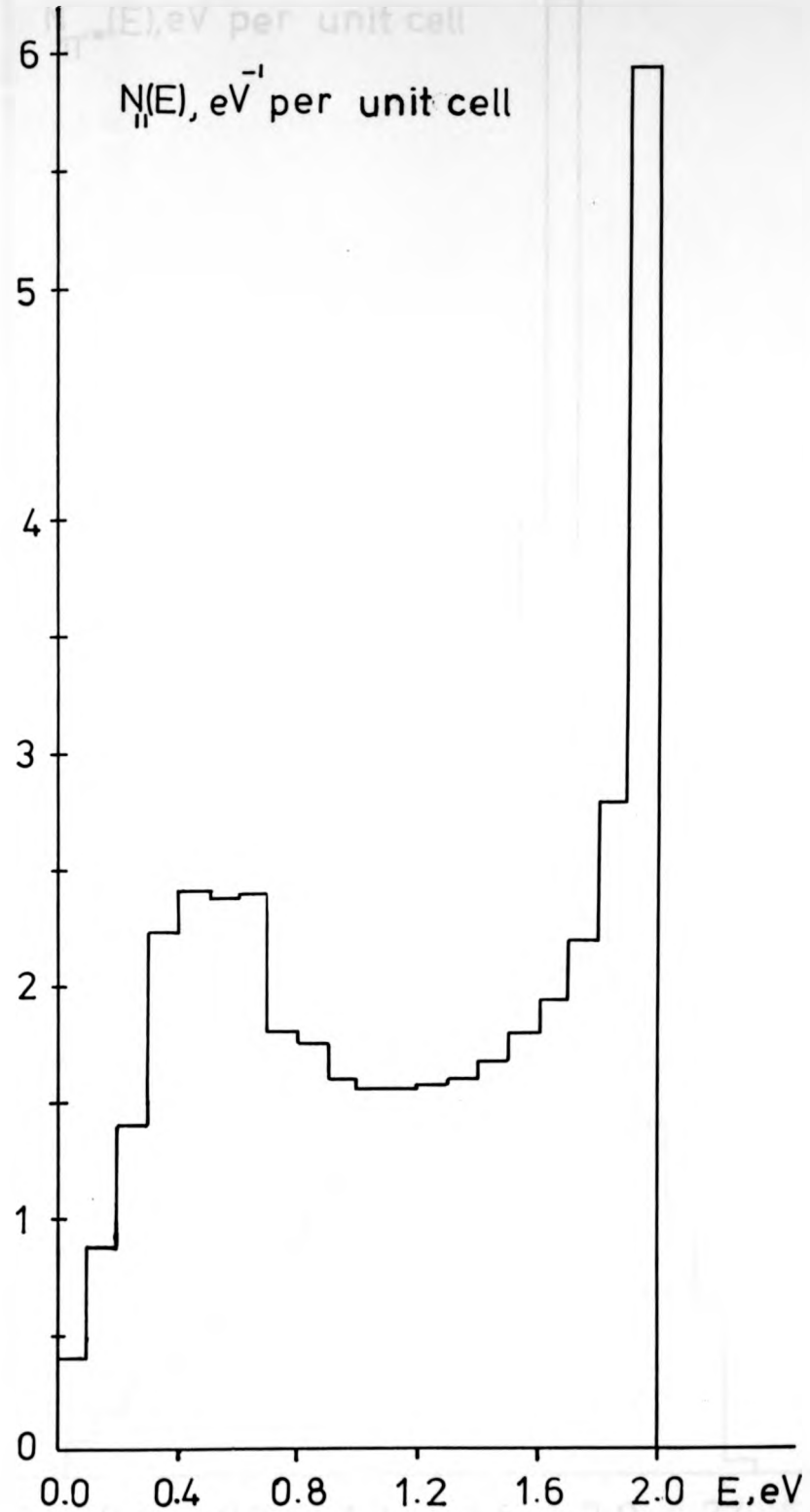

Fig.2.6a. The density of states in the d_{11}-band

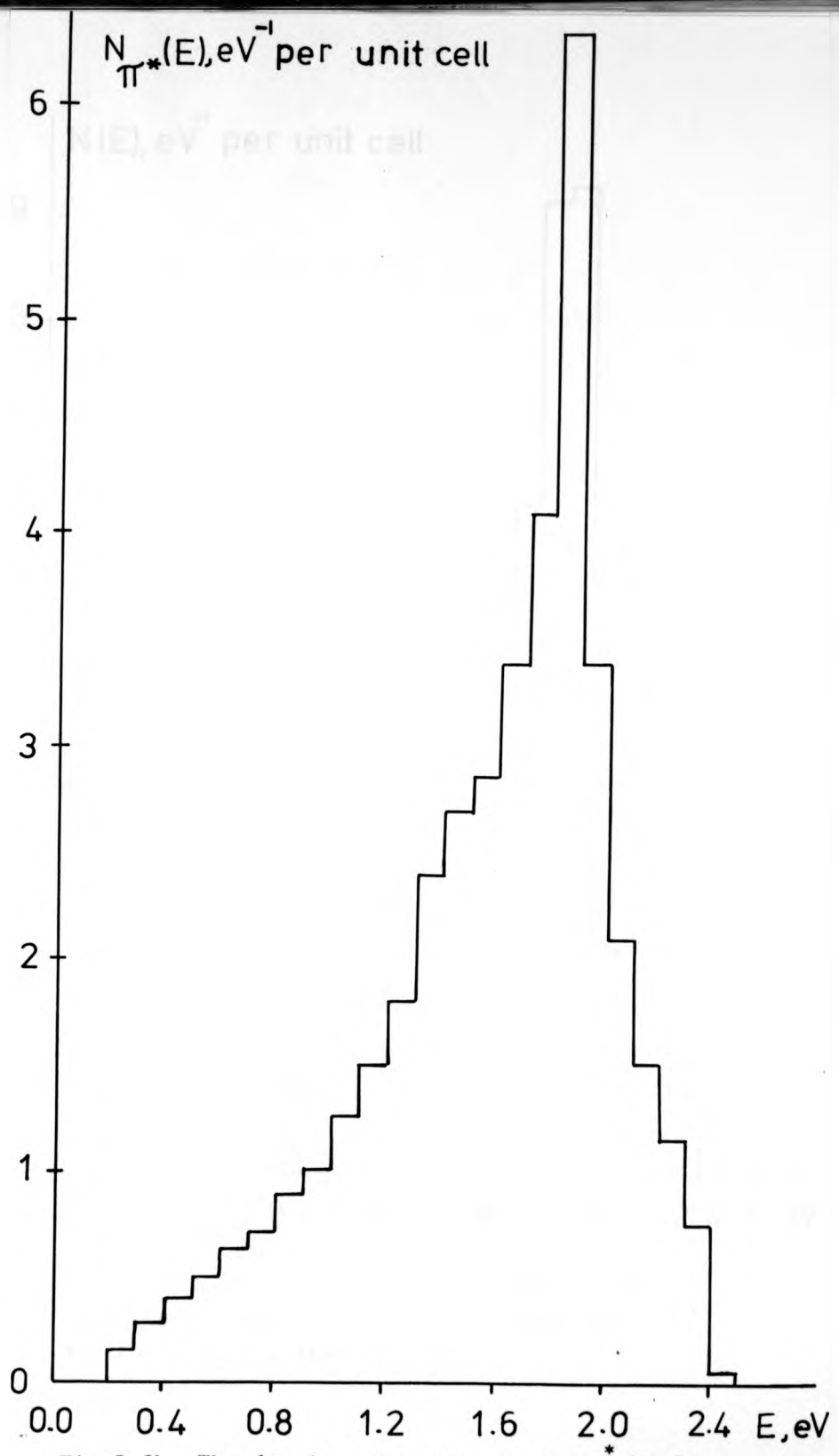

Fig.2.6b. The density of states in the Π^*-band

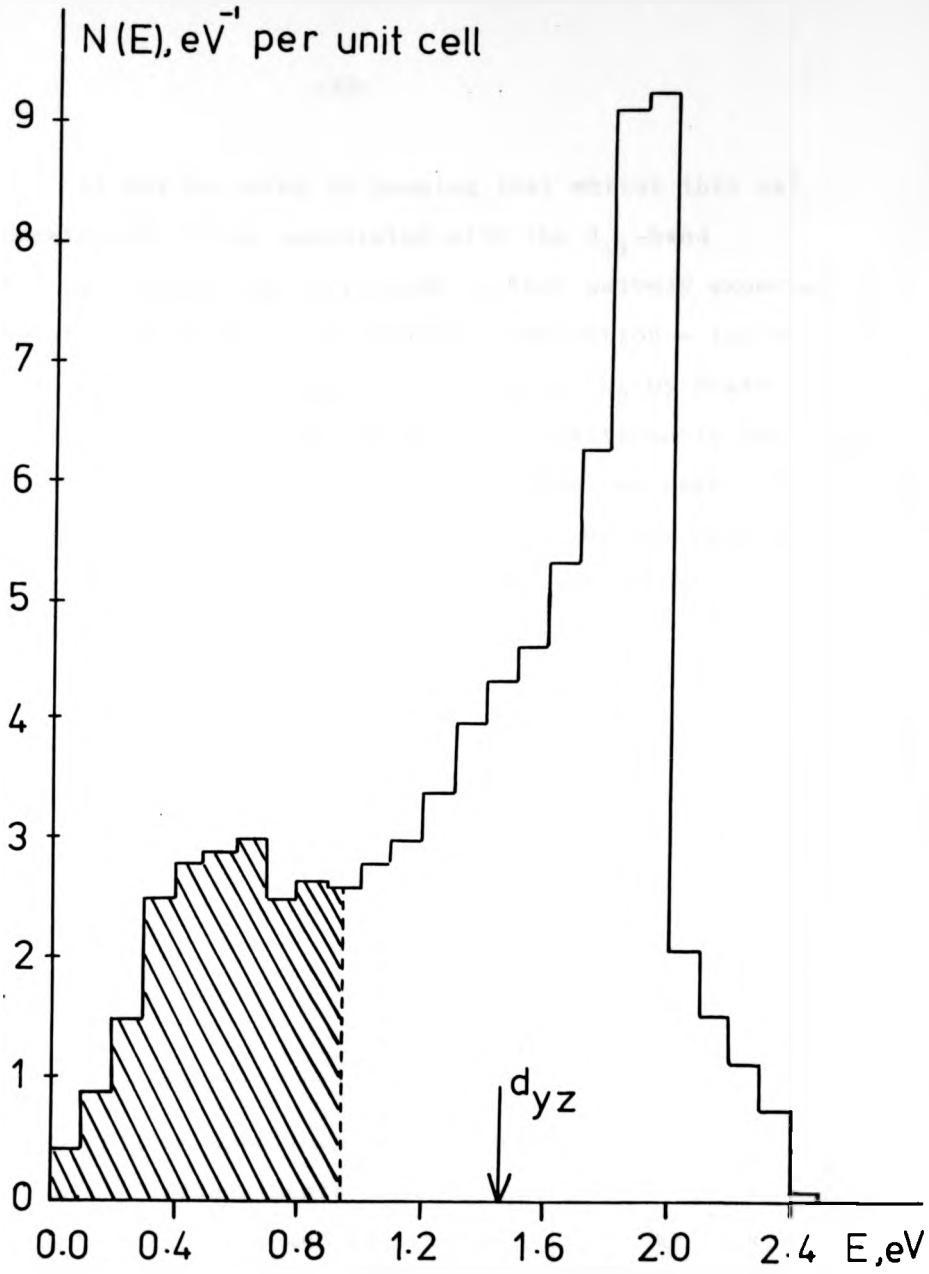

Fig.2.7. The joint density of states of the combined d_{11} and Π^* bands; the shaded area denotes occupied states.

It may be noted in passing that whilst this calculated density of *levels* associated with the d_{11}-band ($\simeq$ 0.4 eV^{-1} per cation) is very close to that naively expected for a band of width 2 eV - i.e. 0.5 eV^{-1} per cation - and used in a discussion of the Coulomb interaction in VO_2 by Hearn and Hyland (1973), it is still, nevertheless, significantly less than the figure of 10 eV^{-1} per cation inferred from the magnitude of the d-spin magnetic susceptibility indicating the persistence of an exchange enhancement of the same order as calculated by Hearn and Hyland.

In Fig. 2.7 is also shown the location of the d_{yz} level whose orbital, it will be recalled, was assumed to remain localized and not participate in conduction band formation; lying as it does some 0.5 eV above * E_F its effect on transport properties can be safely ignored over the range of temperature normally considered.

---

* This value follows upon identifying the energy of an isolated $d_{x^2-y^2}$ ground-state with the energetic "centre of gravity" of the d_{11}-band (defined by $\int E_{11}\, d^3\underset{\sim}{k} / \int d^3\underset{\sim}{k}$, wherein the $\underset{\sim}{k}$-integrations are taken over the whole extended (Jones) zone) and using the values of energy separations inferred from the E.S.R. data displayed in Fig. 2.3.

(b) Occupancies of the d_{11} and Π^* bands

Next, it is of interest to ascertain the fractional electron occupancies of the two bands implied by the separate densities of states and the *joint* E_F value (2.4.3). By calculating the area under $N_{11}(E)$ from 0 to E_F the d_{11}-band is found to contain 0.8 electron per cation whence the Π^*-band must contain 0.2 electron per cation (= n, in Hearn 1972). It is gratifying that this value of n implied from our calculated band-structure falls in the range of possible values cited by Hearn (1972) - $0.1 < n < 0.3$ - since it implies a certain internal consistency between the use of some of his parameters (namely W = 2 eV and equation (2.3.32) to quantify our qualitative band-structure (2.3.19) and our subsequent prediction of another of his parameters, namely n.

(c) Bloch effective masses at E_F

Finally we report the values of the Bloch effective masses m* *at the Fermi level*, for the d_{11} and Π^* bands. Defining m* through

$$\left(\frac{m}{m^*}\right) = \frac{2}{3}\left(\frac{m}{m^*_{\perp}}\right) + \frac{1}{3}\left(\frac{m}{m^*_{11}}\right) \qquad 2.4.3.$$

where

$$\left(\frac{1}{m^*_{\perp}}\right) \equiv \frac{1}{\hbar^2}\left(\frac{\partial^2 E}{\partial k_x^2}\right)_{k_x=k_x^F} \quad \text{and}$$

$$\left(\frac{1}{m^*_{11}}\right) \equiv \frac{1}{\hbar^2}\left(\frac{\partial^2 E}{\partial k_z^2}\right)_{k_z=k_z^F} \qquad 2.4.4.$$

and solving equations (2.3.34) and (2.3.35) for the x and z components of the Fermi wave-fector k^F(k_z^F = 0.50 π/c and k_z^F = 0.27 π/c for the bonding and antibonding branches of the d_{11}-band respectively and k_x^F = 0.78 π/a, k_z^F = 0.56 π/c for the Π*-band), equation (2.4.7) together with (2.4.4) and (2.3.34) and (2.3.35) yields,

$$m^*_{d_{11}} = 13.4m \text{ and } m^*_{d_{11}} = 1.95m$$

for the bonding and antibonding branches and

$$m^*_{\Pi^*} = 4.64m$$

for the Π*-band. We note that whilst the latter value is averaged from equation (2.4.3) the former are along the c_r-axis, on account of the complete filling of the band in the basal plane.

2.5. Comparison with Existing Work

The value obtained above for the Fermi energy (E_F = 0.93 eV) is different from that found in the A.P.W. calculation of Chatterjee et. al. (1972) using neutral vanadium and oxygen atomic potentials and is 0.35 eV above that

obtained subsequently by Caruthers et. al. (1973) using a modified A.P.W. method with a semi-empirical potential chosen to give agreement with the energy difference between the top of the oxygen bonding bands and the Fermi surface as inferred from optical reflectivity (Verleur et. al. 1968, Mokerov and Rakov 1969, Fan 1972) and photoemission (Powell et. al. 1969) measurements.

This same optical work points to the existence of a much smaller gap of order 0.7 - 0.9 eV which is usually interpreted as a (vertical) inter d-band gap; however as first emphasized by Powell et. al (1969) and Paul (1970) the occurrence of optical transitions within the d-band complex is contingent upon the existence of final states which are not purely d-like. Now the states within the π^*-band satisfy this criterion since they contain a significant admixture of oxygen 2p states, resulting in an overall covalency of about 30% (Shimizu 1967); it is of particular interest, therefore, to note that the vertical gap implied by our band structure between the bonding π^* and anti-bonding d_{11} bands is of the same order of magnitude as this optical gap, being 0.6 eV and 0.48 eV at the Fermi level in the Γ- Z and Γ-X direction respectively.

Finally it should be pointed out that the semi-metallic nature of the rutile phase of VO_2 which has been assumed *ab initio* in our semi-empirical work is supported by the A.P.W. calculation of Chatterjee et. al (1972) but *not* by that of Caruthers et. al. (1973). It will be recalled that the existence of two partially

overlapping conduction bands followed originally from Goodenough's quantum chemical considerations and was later to prove instrumental in ensuring, within Hearn's phonon softening model, the occurrence of two metastable phases with very similar crystal structures connected by the observed first order semiconductor → metal phase transition.

2.6. Discussion

Finally, attention must be drawn to the accidental degeneracy shown in Fig. 2.5a, which occurs below the Fermi-level. The lifting of this degeneracy is most readily demonstrated within the first possible approach alluded to in Chapter 2.3, upon admitting admixtures of both $d_{x^2 - y^2}$ and d_{Π^*} orbitals into the Bloch sum relevant to each cation sub-lattice. First-order degenerate perturbation theory then yields the results qualitatively depicted in Fig. 2.8 which should be contrasted with the situation shown in Fig. 2.5a; the persistence of degeneracy at the point A is a consequence in the difference in symmetry of the bonding and anti-bonding orbitals involved. The magnitude of the separation, θ, which now exists at the point of the original degeneracy(B in Fig. 2.5a) is given formally by $2 \int d^*_{11} (U - V) d_{\Pi^*} d^3\underline{r}$, the magnitude of which is difficult to estimate, although a consistent interpretation within this new band structure of the optical gap discussed in Chapter 2.5 would suggest a value of at least 0.5 eV. It is tempting, however, to suppose that it is rather small; for then a mechanism for the

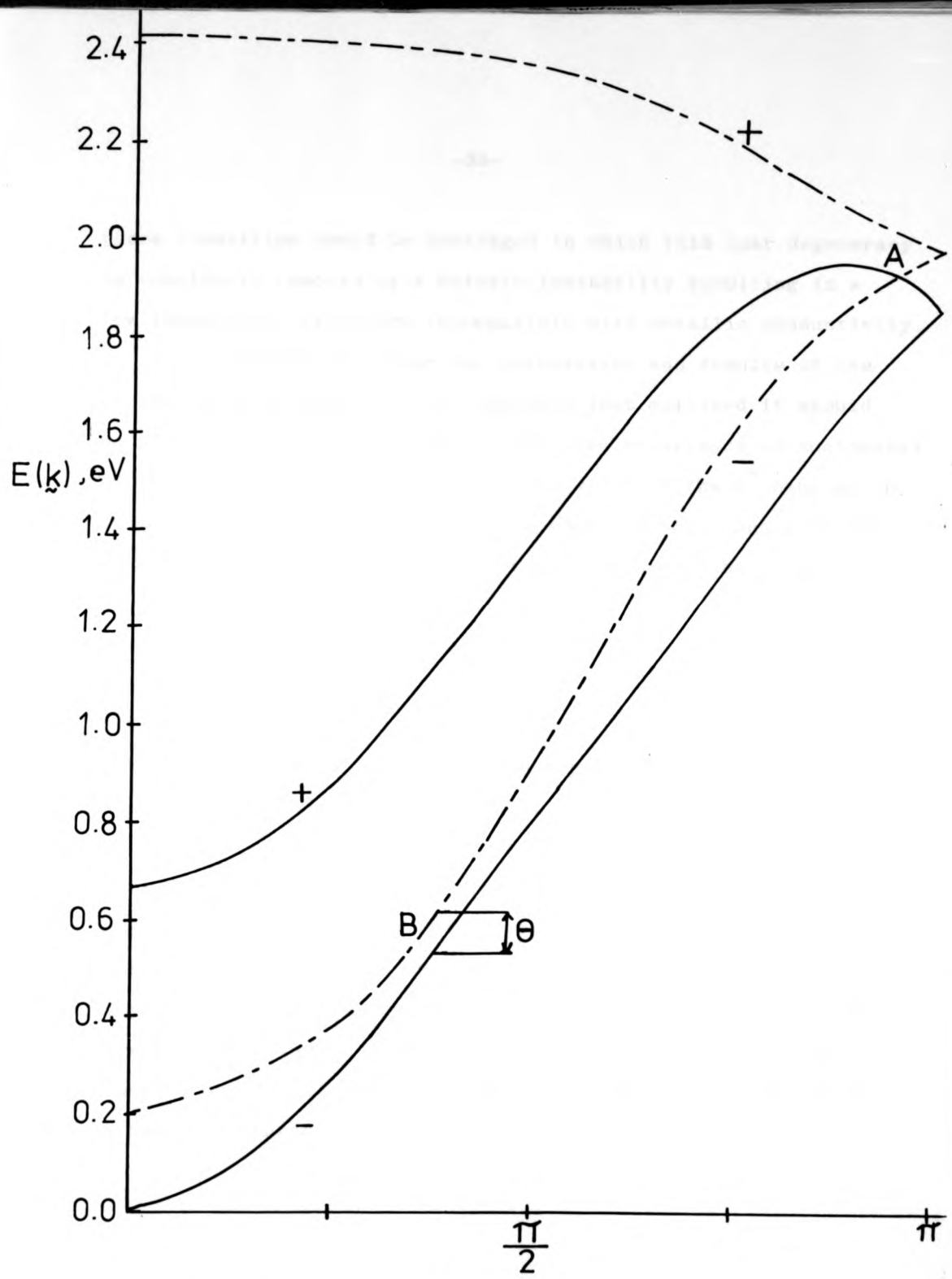

Fig.2.8. The removal of the accidental degeneracies B and C of Fig. 2.5a in degenerate perturbation theory.

phase transition could be envisaged in which this near degeneracy is completely removed by a Peierls instability resulting in a low temperature structure incompatible with metallic conductivity.

Before rejecting the calculation and results of the present work in favour of the approach just outlined it should be pointed out that the location and even occurrence of accidental degeneracy is highly sensitive to the width of the Π^*-band which, as discussed in Chapter 2.3, is dependent on equations (2.3.23), (2.3.24) and the width assumed for the d_{11}-band; the values adopted in the above for the last two quantities in particular are, however, subject to a non-negligible uncertainty at the present time. Accordingly, it is difficult to adjudge the necessity of such a recalculation, which, although straightforward in principle, leads to a more parameters than can be evaluated with existing experimental data.

A more pertinent criticism which could be directed against the present work (even in the event of no accidental degeneracy occurring), is the use of first-order perturbation at all, considering that the values of the bandwidths eventually adopted ($\simeq$ 2eV) exceed by far the energy separation between the parent $d_{x^2-y^2}$ and d_{Π^*}-levels ($\simeq$ 0.4 eV); the same criticism is, however, surely relevant to existing calculations of the 3d and 4s band structures in transition metals.

CHAPTER 3

THE VALIDITY OF THE BAND MODEL FOR RUTILE VO_2

3.1. Introduction

Having obtained the one-electron band structure of rutile VO_2 it is, of course, necessary to check whether the itinerancy implied by the band model in this case (partially filled overlapping d_{11} and π^* bands) and which is found experimentally is, in fact, consistent with the interactions neglected in the model - in particular, the Coulomb interaction between the conduction d-electrons. The validity of the band model requires that the increase in Coulomb potential energy, $\mathcal{V}$, consequent upon delocalization be small in comparison with the associated itinerant kinetic energy, T, the magnitude of which is reflected in the one-electron bandwidths. It is possible, however, for the band model to retain a certain qualitative validity even when $\mathcal{V} \lesssim T$ in the sense that itinerancy still obtains; quantitatively, however, a realistic description of such an itinerant state cannot be expected in consequence of the importance therein of electron correlations (induced by $\mathcal{V}$) which the band model neglects.

The band theory is based on the Hartree-Fock approximation in which the Coulomb interaction between electrons is treated in an approximate way. For simplicity let us consider a simple cubic array of N s-centres (with lattice constant "a") and assume that each centre has only one electron. In the band

theory it is assumed that every electron moves independently in the potential of the crystal lattice and that of the remaining electrons. This latter potential is calculated self-consistently and the correlation between electrons with anti-parallel spin is lost in the averaging process involved. The only correlation then considered is a statistical one between electrons with parallel spin, which is embodied in the totally anti-symmetric N-electron wave functions of the system, the ground state of which can be written as a *single* Slater determinant built up from the N/2 single electron tight-binding Bloch functions corresponding to the lower occupied half of the s-band considered. This wave function allows two electrons with anti-parallel spin on one centre with a probability equal to that for finding a single electron of given spin at one centre; these "polar fluctuations" (double occupancies and an equal number of vacancies) are essential for the metallic conductivity allowed by the band model. However, it is not possible to treat the interaction between two electrons by perturbation theory because of the divergence of the long range part of Coulomb interaction. As pointed out by Bohm and Pines (1951) this long range part can be treated in a collective electron description (plasma oscillations); the remaining *short* range interaction, decisive for the individual motion of electrons, is now non-divergent and can be treated perturbatively. Using the single Slater determinantal wavefunction introduced above and assuming the residual short range Coulomb interaction to be so *short* as to be operative only when two electrons occupy the

same centre, the total energy per electron for the case of the simple centre lattice under consideration is:

$$E(\underset{\sim}{k}) = E_o - \alpha - \frac{W}{6}(\cos k_x a + \cos k_y a + \cos k_z a) + \frac{U}{4} \qquad 3.1.1.$$

in the nearest neighbour approximation, where $(E_o - \alpha)$ is the energy of a single electron localized at a centre in the crystal and W is the one-electron bandwidth. U is the intra-atomic (on-site) potential energy due to the short range part of the Coulomb interaction, whilst the 1/4 factor reflects the fact that the single Slater determinant used to compute E contains a 25% probability for the occurence of double occupancies.*

Clearly the existence of a metallic state requires that the one-electron energy averaged over the occupied lower half of the band E_B is less than the energy, $(E_o - \alpha)$, that the electron would have if it remained localized, and thereby not exposing itself to the Coulomb energy U i.e. the existence of a metallic state requires

$$E_B < (E_o - \alpha) \qquad 3.1.2.$$

Evaluating E_B using (3.1.1), from

$$E_B = \int_{-\pi/2a}^{\frac{\pi}{2a}} E(\underset{\sim}{k})\, d^3\underset{\sim}{k} \;/\; \int_{-\pi/2a}^{\frac{\pi}{2a}} d^3\underset{\sim}{k}$$

(3.1.2) requires

$$W > \frac{\pi U}{4} \qquad 3.1.3.$$

---

* At any instant, 50% of the centres will be neutral (containing one electron), 25% doubly occupied and 25% empty.

Which situation obtains in rutile VO_2 can be ascertained by noting that the dominant contribution, U, to $\mathcal{V}$ arises from double occupancies of the same $d_{x^2-y^2}$ cation orbital which the band model, through its neglect of positional correlations between electrons of antiparallel spin, allows to occur with a probability, P_2 given by the binomial distribution (Hubbard 1964):

$$P_2 = {}^{\nu}C_2\left(\frac{r}{\nu}\right)^2 \left(1 - \frac{r}{\nu}\right)^{\nu-2} \qquad 3.1.4.$$

where r is the mean number of electrons per cation and ν is the number of one-electron states per cation contained in the band. For the d_{11}-band with $\nu = 2$ and $r = 0.8$ $(= 1 - n)$,

$$P_2 = 0.16 \qquad 3.1.5.$$

whilst for the Π^*-band,

$$P_2 = 0.01 \qquad 3.1.6.$$

The total one-electron energy E_B averaged over the occupied portion of the d_{11}-band is thus given by

$$E_B = \langle E_{11} \rangle + 0.16\ U \qquad 3.1.7.$$

where

$$\langle E_{11} \rangle \equiv \int_0^2 N(E)\ E\ f_o(E)\ dE \qquad 3.1.8.$$

where $f_o(E)$ is the Fermi-Dirac distribution function

On the other hand, the total energy E_L of an electron localized in the $d_{x^2-y^2}$ orbital is simply given through equation (2.3.29)

$$E_L = (E_o - \alpha)_{11} \qquad 3.1.9.$$

Thus for the itinerant d_{11}-band motion to obtain, rather than a Mott-insulating state, requires

$$E_B < E_L \qquad 3.1.10.$$

Evaluating equation (3.1.8) using the numerical values of N(E) and integrating over the d_{11}-band gives $\langle E_{11} \rangle$ = 0.42 eV and, noting that relative to the bottom of the d_{11}-band (the adopted zero of energy), E_L = 1.16 eV, it is seen that for (3.1.10) to be satisfied requires U < 4.63 eV; accordingly we now consider the calculation of the magnitude of U for electrons in rutile VO_2.

Following Hyland (1969) we identify U with the energy required to create a well-separated $V^{3+}(3d)^2$ and $V^{5+}(3d)^o$ ion out of a hypothetical Mott-insulating VO_2, (in which owing to an assumed predominance of U over T each cation, in rutile VO_2 has the electronic configuration $V^{4+}(3d)^1$), due account being taken of contributions to this energy arising from lattice polarizability and from the effect of the electric field of the O^{2-} - anions on the energy spectrum of the V^{4+} and V^{3+} cations. In this way U was found to be given by

$$U = [I(4) - I(3)] - [\Delta(3) - \Delta(4)] - [P(5) + P(3)] \quad 3.1.11.$$

where the I's are experimental ionization energies of *free* V^{4+} and V^{3+} ions, and the P's, the lattice polarization energies induced by the "anomolously" charged final states V^{3+} and V^{5+} ions. Physically the decrease in U due to P can be understood as follows: one of the two electrons of V^{3+} interacts *attractively* with polarization field induced in its lattice environment by the "other" electron, thereby effectively reducing their Coulomb repulsion. The Δ's are the crystal field stabilization energies which have their origin in the removal of the orbital degeneracy of the 3d-orbitals of the V^{4+} and V^{3+} ions by the electric field of the O^{2-} anions which octahedrally coordinate a given cation in such a way that the cation has orthorhombic point symmetry D_{2h}.

The expression for U given by equations (3.1.11) requires, however, some modification in respect of the following considerations.

(a) Even for the case of *free* vanadium ions (when the second and third brackets on the R.H.S. of equation (3.1.11) vanish) U is not given by the first bracket since the difference between the ionization energies of V^{3+} and V^{4+} is not due solely to the potential energy of inter-electronic Coulomb repulsion which exists in the case of V^{3+} (not in the case of V^{4+}) but also to the reduction δ_1 in the binding energy of one of the two electrons in V^{3+} due to the screening of the nuclear Coulomb field by the other electron; thus [I(4) - I(3)] should be

replaced by $[I(4) - I(3)] - \delta_1$, where $\delta_1 > 0$. The value of U obtained by Hyland must thus be taken as an upper limit only; in the absence of the wave-functions necessary to calculate δ_1, however, we shall be forced to continue to neglect it.

(b) As already mentioned above we are interested in the Coulomb potential energy associated with cations which are doubly occupied by electrons of anti-parallel spin; I(3), however, is the experimental ionization energy of $V^{3+}(3d)^2$ which naturally exists in the *high* spin configuration ^3F, in accordance with Hund's rule. Thus I(3) must be replaced by $I(3) - \delta_2$, where δ_2 (> 0) denotes the energy separation between the high spin ^3F ground state and the lowest lying *low* spin state of the V^{3+} ion, which is known to be the term ^1D; δ_2 = 1.36 eV (Moore 1949).

(c) Owing to the impossibility of incorporating V^{3+} ions substitutionally in TiO_2, the value of $\Delta(3)$ cannot be obtained from experiment and an approximate value of 1.86 eV appropriate to the *cubic* field stabilization energy of V^{3+} ions in Al_2O_3 was used by Hyland; this value together with that of the *cubic* stabilization energy of V^{4+} in TiO_2 (which *can* be obtained from experiment, (Shimizu 1967)) resulted in a value of 0.62 eV for the second term on R.H.S. of equation (3.1.11).

However, from the empirical observation that the term splittings in $V^{3+}(3d)^2$ are very much larger than those induced by the anion electric field, it turns out to be possible to

calculate the actual *orthorhombic* stabilization of the relevant ^1D term; for the angular momentum of ^1D is the same as that of the ^2D ground state of the $V^{4+}(3d)^1$ ion. The results of this calculation, taking into account the Madelung energies at the V^{4+} and V^{3+} sites, (Dixon and Hyland, to be published) reveal that Hyland's original value of 0.62 eV is to be replaced by 3.58 eV.

(d) The value of the last term on the R.H.S. of equation (3.1.11) was estimated by Hyland to have the value of 14.06 eV, in an approximation in which only the six nearest-neighbour oxygen anions of the anomolously charged cation were treated as discrete and non-displaceable whilst the remainder of the crystal was treated as a dielectric continuum. Accordingly, the only contribution to the polarization energy from the six discretely treated anions arises from the deformation of their electron shells.

It is the main purpose of this chapter to present a more sophisticated calculation of the polarization energy associated with a V^{3+} (or V^{5+}) ion in a hypothetical Mott-insulating VO_2. Our calculation will be based on the method originally developed by Mott and Littleton (1938) to study lattice defects in alkali-halide crystals with cubic symmetry, it is based on the Born theory of ionic crystals. In view of the different crystal structure of VO_2 and the nature of our problem a modification of their calculation is required; in

particular the defect is to be replaced by an excess electric charge (corresponding to one of the doubly occupied cations) and the cubic crystal structure replaced by the rutile one relevant to VO_2 for $T > T_t$. In performing the calculation we assume that the excess charge has a residence time long compared to the period of the lattice vibrations so that polarization of the medium to its full static value is possible. The field of the excess electron induces dipoles on all the vanadium and oxygen ions and in turn these induced dipoles produce an electrostatic potential back at the location of the excess charge.

The polarization field on any ion,whose value decreases with the distance from the excess charge, is due not only to the excess charge but also contains the effects of the dipoles induced on the other ions. Obviously it is difficult to make an exact calculation taking into account all the effects and we therefore consider only those dipole-dipole interactions within the nearest neighbour ions of the cation on which the excess charge is located.

In the first instance our treatment will assume a rigid lattice which only subsequently is allowed to move. In the first case then only the electronic polarizabilities of the anions and cations are active, whilst in the second case additional contributions to the polarization arising from ionic displacements

are included. Hence the difference between these two calculations of the polarization energy gives the "binding energy" or "self energy" of the excess electron; this quantity is of great importance in connection with the polaron problem in metallic VO_2 and will be discussed in the next Chapter.

It should be mentioned that a similar adaptation of the Mott and Littleton method to calculate the binding energy of a self-trapped electron in NaCl was made a long time ago by Markham and Seitz (1948). In this problem the wave function of the self-trapped 3s-electron spreads out over several ions. Accordingly the field causing the polarization of the ions will depend on the form of the wave function, which is itself determined by solution of the Schrödinger equation containing a potential due to induced dipoles; a self-consistent solution is thus required. In VO_2, however, the electron occupies a 3d-orbital and is, accordingly, fairly well localized around the ion; it would then appear that our semiclassical approach is a reasonable assumption.

3.2. Dielectric Constants and Polarizabilities in Rutile (TiO_2)

In the following sections we shall need the static and high frequency dielectric constants ε_s and ε_∞, respectively, and polarizabilities of oxygen and vanadium ions in an hypothetical Mott insulating VO_2. Since real VO_2 is metallic the required dielectric constants cannot be found experimentally. Accordingly we shall be compelled to use those of the isostructral oxide TiO_2 ;

unlike Mott-insulating VO_2 (in which each cation has one resident 3d-electron), however the cations in TiO_2 have *empty* 3d-shells ($Ti^{4+}(3d)^0$)so that the use of TiO_2's ε_∞ value for our problem is likely (in consequence of the greater electronic polarizability of V^{4+} over Ti^{4+}) to result in an underestimate. In TiO_2 the high frequency dielectric constant ε_∞ is determined from the indices of refraction, according to $\varepsilon_\infty = n^2$, (Traylor et.al. 1971), whilst the static dielectric constant ε_s is obtained from the capacitance measurements (Parker 1961).

The high frequency dielectric constant can be related to the electronic polarizabilities of the ions. If $\underset{\sim}{E}$ is the average field in the dielectric medium then the effective field polarizing an ion (i) is given by

$$\underset{\sim}{E} + L_i \underset{\sim}{P} \qquad 3.2.1.$$

where $\underset{\sim}{P}$ denotes the polarization of the medium and L_i is the Lorentz correction, which for cubic lattices is equal to the familiar $4\pi/3$ factor; for rutile structures its value is, however, different. Equation (3.2.1) treats the ions as point charges and point dipoles. If one considers the overlap between anions and cations this can be modified as follows. The effective field polarizing the cations is now given by

$$\underset{\sim}{E} + L_i (\underset{\sim}{P}_c + \gamma \underset{\sim}{P}_a) \qquad 3.2.2.$$

where γ is a constant and, $\underset{\sim}{P}_c$ and $\underset{\sim}{P}_a$ are polarizations due to

cations and anions, respectively. A similar expression to this can be written for the anions. Equation (3.2.2) reduces to (3.2.1) for $\gamma = 1$, which corresponds to the case of no overlap between the ions.

If α_c and α_a are the electronic polarizabilities of the cations and the anions, respectively, then $\underset{\sim}{P}_c$ can be expressed as

$$\underset{\sim}{P}_c = \frac{2\alpha_c}{a^2c} \left[\underset{\sim}{E} + L_c \left(\underset{\sim}{P}_c + \gamma \underset{\sim}{P}_a\right)\right] \qquad 3.2.3.$$

where a^2c is the volume of the rutile unit cell, with a similar expression for $\underset{\sim}{P}_a$. Considering the total polarization

$$\underset{\sim}{P} = \underset{\sim}{P}_c + \underset{\sim}{P}_a$$

and using the relation,

$$\varepsilon_\infty - 1 = 4\pi \; P/E \qquad 3.2.4.$$

we obtain, following Mott and Littleton,

$$\frac{\varepsilon_\infty - 1}{4\pi} = \frac{\dfrac{\alpha_c + \alpha_a}{a^2c} + (L_c + L_a)\dfrac{\alpha_c \alpha_a}{(a^2c)^2}(\gamma - 1)}{1 - \dfrac{L_c\alpha_c + L_a\alpha_a}{a^2c} + \dfrac{L_c L_a \alpha_c \alpha_a (1-\gamma^2)}{(a^2c)^2}} \qquad 2.2.5.$$

In order to calculate the Lorentz field corrections and electronic polarizabilities, together with ionic polarizabilities Parker (1961) derived the local field equations for the rutile structure. Solution to these equations requires some assumption regarding the relative motion of ions. Taking into consideration that the anions form a h.c.p. structure in the crystal it was assumed that cations are displaced with respect to anions, the latter, in consequence of their mutual contact, being held fixed. It should be mentioned that the dielectric constants and the polarizabilities must reflect the anisotropy of the crystal symmetry; therefore the results are given in Table 3.1 for two directions, one along the c_r-axis and the other in the basal plane.

In addition to the directional differences in the values of Lorentz corrections, it should be noted that there will in general be a different Lorentz correction for each of the ions in a unit cell which contains two different types of cations and two different types of anions. Their values are obtained along the c_r-axis and in the [110] direction of the basal plane for two cases considered: the rigid lattice and the displaceable case in which the cations are free to move (Parker 1961). Although the results along the c_r-axis for both type of oxygens are equal, they are quite different in the [110] direction; the same can be said for Ti^{4+} as well. Making use of these values, together with values of the dielectric constant ε_∞, electronic polarizabilities of Ti^{4+} and O^{2-}, and the lattice constants of TiO_2 the value of γ calculated from equation (3.2.5) in the c_r-direction turns out to be 0.93 for the first case.

In order to calculate the Lorentz field corrections and electronic polarizabilities, together with ionic polarizabilities Parker (1961) derived the local field equations for the rutile structure. Solution to these equations requires some assumption regarding the relative motion of ions. Taking into consideration that the anions form a h.c.p. structure in the crystal it was assumed that cations are displaced with respect to anions, the latter, in consequence of their mutual contact, being held fixed. It should be mentioned that the dielectric constants and the polarizabilities must reflect the anisotropy of the crystal symmetry; therefore the results are given in Table 3.1 for two directions, one along the c_r-axis and the other in the basal plane.

In addition to the directional differences in the values of Lorentz corrections, it should be noted that there will in general be a different Lorentz correction for each of the ions in a unit cell which contains two different types of cations and two different types of anions. Their values are obtained along the c_r-axis and in the [110] direction of the basal plane for two cases considered: the rigid lattice and the displaceable case in which the cations are free to move (Parker 1961). Although the results along the c_r-axis for both type of oxygens are equal, they are quite different in the [110] direction; the same can be said for Ti^{4+} as well. Making use of these values, together with values of the dielectric constant ε_∞, electronic polarizabilities of Ti^{4+} and O^{2-}, and the lattice constants of TiO_2 the value of γ calculated from equation (3.2.5) in the c_r-direction turns out to be 0.93 for the first case.

TABLE 3.1.

	c_r	a_r
Electronic Polarizabilities *		
Titanium	0.19	0.19
Oxygen	2.6	2.29
Dielectric Constants †		
ε_∞	8.427	6.843
ε_s	170	86

	Lorentz correction *	
	Rigid lattice	Displaceable lattice
	c_r-direction	
Titanium (corner and centre)	6.546	6.548
Oxygen (type I and II)	4.042	4.530
	[110] direction	
Titanium (corner)	5.378	11.307
(centre)	3.713	5.954
Oxygen (type I)	3.500	8.347
(type II)	3.310	0.362

* Parker (1961)

† Traylor et. al. (1971)

If now the ions are allowed to move there will be an additional contribution to the polarizability; the local field on a cation is now given by

$$\underset{\sim}{E} + L_c' (\underset{\sim}{P}_c + \gamma \underset{\sim}{P}_a + \gamma \underset{\sim}{P}_c')$$

where P_c' is the polarization due to the cation displacements and L_c' is the new Lorentz correction. It is possible to give an expression similar to equation (3.2.5) for the static dielectric constant ε_s. The calculated value of γ, as before in the c_r-direction, in this new case is 0.86. The calculation of γ in the basal plane was not possible, however, because the values of the dielectric constant and polarizabilities are given along the a_r-axis, whilst the Lorentz corrections are available only in the [110] direction.

The result that γ is near unity implies that there is small overlap along the c_r-direction in TiO_2. As an approximation we shall take γ to be 1 in this direction, as well as in the basal plane. In VO_2 we use this value (γ=1), which considerably simplifies our calculations throughout the next section, thereby neglecting ionic overlap except to the extent to which it causes a modification of the ionic charge (see below).

In the next section we introduce an excess charge into the lattice and calculate the displacements of vanadiums and oxygens. We therefore need the displacive ionic polarizability of vanadiums as well as that of oxygens. In view of the difficulty in obtaining both values with the local field equations we

calculated them from the formula

$$\alpha' = \frac{(Ze^*)^2}{p} \qquad 3.2.6.$$

where p is the force constant of the crystal lattice, Z the valence i.e. 2 for oxygen and 4 for vanadium and e^* is the effective charge, first introduced by Szigeti (1949), and incorporates the effects of ionic distortion due to the overlap of neighbouring ions. For rutile e^* can be calculated from the Szigeti relation and is found to be 0.64e (Samara and Peercy, 1973). The force constant p can be estimated as follows. Let us apply an external electric field along the c_r-axis and consider the relative displacements of the vanadium and oxygen ions. Owing to the different environment, the displacement of two of the oxygen ions will not be equal to that of the other two (see Figure (3.1)). However, if we remain in the nearest neighbour approximation a simplification results if we assume that all the oxygens move by the same amount; this will be assumed in what follows. Then, considering the anion octahedron around any vanadium ion, let the oxygens be displaced a distance x in the direction of c_r-axis and the vanadium in the opposite direction (alternatively, we can equally well assume the vanadium ions will move a distance 2x relative to the oxygens). The change in the energy per cation-anion pair is

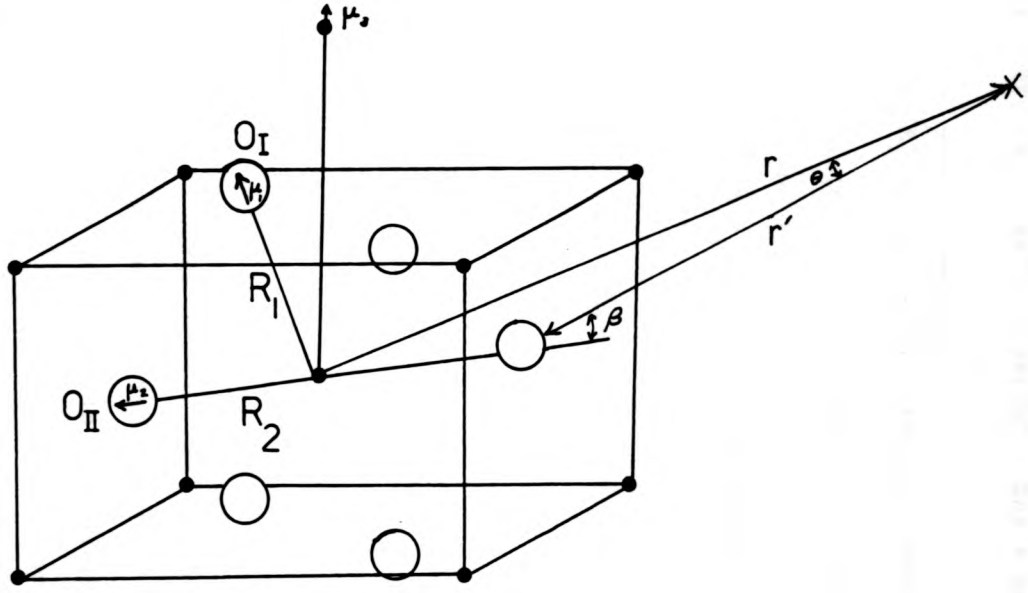

Fig. 3.1. The dipoles and the angle of equation (3.3.6) in the unit cell of rutile VO_2.

$$\Delta W = 2W(\sqrt{R_2^2 + 4x^2}) + 2W(\sqrt{R_1^2 - 2cx + 4x^2})$$

$$+ 2W(\sqrt{R_1^2 + 2cx + 4x^2}) - 4W(R_1) - 2W(R_2) \qquad 3.2.7.$$

where R_1 and R_2 are anion-cation distances for the two types of oxygens (Figure 3.1) and W(r) is the repulsive energy. Since x is small compared with R_1 and R_2 we can expand the square roots on the RHS of equation (3.2.7) to obtain:

$$\Delta W = \frac{4x^2}{R_2} W'(R_2) + \left(\frac{8x^2}{R_1} - \frac{2c^2x^2}{R_1^3}\right) W'(R_1)$$

$$+ \frac{2c^2x^2}{R_1^2} W''(R_1) \qquad 3.2.8.$$

p is then given by

$$px = \frac{1}{2} \frac{\partial \Delta W}{\partial x} \qquad 3.2.9.$$

The repulsive force between two ions decreases very rapidly as the distance increases. Two different formulations of the repulsive force are available in the literature, one due to Born and one to Pauling. The exponential form due to Born and Göppert-Mayer (1933) is A exp(-r/ρ), where r is the ion separation and A and ρ are two parameters to be determined. So long as only the anion-cation contacts are involved this form can be easily used since A_{+-} and ρ_{+-} can be determined from the first and second derivatives of the repulsive force. The inclusion, however, of anion-anion contacts into problem,

which is necessary in our problem as will be seen in the next section, introduces two extra parameters (A_{--} and ρ_{--}) and results in an undetermined problem. Accordingly, we use the alternative inverse power form of the repulsive force due to Pauling (1928).

Following Pauling the repulsive potential W(r) between two ions A and B at a distance r is given by

$$W(r) = B_o \beta_{AB} \, e^2 \frac{(r_A + r_B)^{n-1}}{r^n} \qquad 3.2.10.$$

where r_A (and r_B) is the radius of the ion A (and B). β_{AB} is defined as

$$\beta_{AB} = 1 + \frac{Z_A}{N_A} + \frac{Z_B}{N_B} \qquad 3.2.11.$$

where Z_A and N_A are the valence and the number of the outer electrons of the ion A, respectively. n is usually given the value 9. B_o is a characteristic constant which can be calculated as follows. The ionic crystal energy per vanadium ion (Pauling) is

$$E(r) = -\frac{4e^2 A_m}{r} + \frac{B_o \, r_-^{n-1} \, (1+k)^{n-1}}{r^n} \, e^2 x$$

$$[6 \, \beta_{+-} + \beta_{--} \left(\frac{2}{1+k}\right)^{n-1} \times \{ \frac{8}{2^{n/2}} + \left(\frac{2+\ell^2}{2(2-\ell^2)}\right)^n \}] \qquad 3.2.12.$$

where ℓ is the c/a ratio and k is ionic radius ratio r_+/r_-.

We take ℓ = 0.643 (Hearn, 1973) and k = 0.50 (Pauling, 1960). The first term in equation (3.2.12) denotes the electrostatic energy with a Madelung constant A_m = 4.77 (Johnson and Templeton, 1961).

In equilibrium

$$\left(\frac{\partial E}{\partial r}\right)_{r=R} = 0 \qquad 3.2.13.$$

where R is the nearest-neighbour cation-anion separation which is 1.92 ^{o}A, averaging from the two separations 1.90 and 1.95 ^{o}A. Equations (3.2.12) and (3.2.13) thus give B_o = 0.0669. Using these values in equations (3.2.8), (3.2.9) and (3.2.10) we obtain p and thus the ionic (displacive) polarizability α' via equation (3.2.6).

Hence α_v' = 0.83 $^{o}A^3$ and α_o' = 0.21 $^{o}A^3$.

3.3. The Mott-Littleton Method

(A) Polarization in a rigid lattice.

We consider a rigid lattice of Mott-insulating rutile VO_2 in which the ions are not allowed to move. An excess charge Q on a given cation induces dipoles on the other cations (V^{4+}) and anions (O^{2-}). The polarization of the medium at a large distance r from Q is

$$P = \frac{Q}{r^2} \frac{1}{4\pi} \left(1 - \frac{1}{\varepsilon_\infty}\right) \qquad 3.3.1.$$

where ε_∞ is the high frequency dielectric constant averaged over the two crystal directions according to $3/\varepsilon_\infty = (2/\varepsilon_\infty^{\perp} + 1/\varepsilon_\infty^{\shortparallel})$

where $\varepsilon_\infty^{\perp}$ and $\varepsilon_\infty^{\parallel}$ are the high frequency dielectric constants of rutile in the basal plane and along the c_r-axis, respectively. The polarization due to cations in terms of the local electric field is given by equation (3.2.3) as

$$\underset{\sim}{P}_V = \frac{2\alpha_V}{a^2 c} \quad [\underset{\sim}{E} + L_V(\underset{\sim}{P}_V + \gamma \underset{\sim}{P}_O)]$$

where the subscriptions V and O denote vanadium and oxygen respectively, and all the quantities which are defined in the previous section are directionally averaged values here e.g.

$$\alpha_V = \frac{2\alpha_V^{\perp} + \alpha_V^{\parallel}}{3} \quad \text{and} \quad L_V = \frac{2L_V^{\perp} + L_V^{\parallel}}{3} ,$$

and similar expressions for oxygens.

Taking $\gamma = 1$ and letting $\underset{\sim}{P} = \underset{\sim}{P}_O + \underset{\sim}{P}_V$, one gets

$$\underset{\sim}{P}_V = \frac{2\alpha_V}{a^2 c} \quad [\underset{\sim}{E} + L_V \underset{\sim}{P}] \qquad 3.3.2.$$

with a similar expression for anions. From equations (3.3.1) and (3.3.2) the induced dipole on one of the vanadium ions can be written as

$$\mu = a^2 c \frac{Q}{r^2} M_V \qquad 3.3.3a.$$

where $$M_V = \frac{\alpha_V}{2(\alpha_V + 2\alpha_O)} \quad \frac{1}{4\pi}\left(1 - \frac{1}{\varepsilon_\infty}\right)\left[1 + \frac{4\alpha_O}{a^2 c}(L_V - L_O)\right] \qquad 3.3.3b.$$

A similar equation to (3.3.3) can be written for the dipoles induced on the oxygen ions.

As a zeroth order approximation we assume that equation (3.3.3) holds for all the ions. The potential at the location of Q due to these dipoles is then

$$V = -Q\, a^2 c \left[M_V \sum_V \frac{1}{r^4} + M_O \sum_O \frac{1}{r^4}\right] \qquad 3.3.4a.$$

where the lattice sums* have been performed on a computer and found to be:

$$\sum_O \frac{1}{r^4} = 0.7239 \text{ and } \sum_V \frac{1}{r^4} = 0.1767 \qquad 3.3.4b.$$

For convergence it was found sufficient to take into account 20 unit cells on each side of the excess charge in three directions.

As a first order approximation the dipoles of the six nearest neighbour oxygens and two nearest neighbour vanadium ions (along the c_r-axis) of the vanadium ion occupied by the excess charge Q are treated as discrete, whilst it is assumed that equation (3.3.3) continues to hold for all other more distant ions treated as continuum. The field $\underset{\sim}{E}_{cont}$ at *one* of these discrete ions due to the outside *continuum* is calculated from

$$\underset{\sim}{E} = \frac{3(\underset{\sim}{\mu}.\underset{\sim}{r}) - r^2\underset{\sim}{\mu}}{r^5} \qquad 3.3.5.$$

---

* The lattice distances of VO_2 (as opposed to those of TiO_2) were used.

and found

$$E_{cont} = Q\, a^2 c\, (M_o\, x_o + M_v\, x_v) \qquad 3.3.6a.$$

where

$$x_v = \sum_v \frac{1}{r^2 (r')^3} \quad (\sin\theta \sin\beta - 2\cos\theta\cos\beta) \qquad 3.3.6b.$$

where the distances and angles are shown in figure (3.1). It should be pointed out that the field E_{cont} and the other fields hereafter are radial components of the vectoral quantity taken along the line joining the field point to the excess charge.

In the discrete set of ions considered there are two distinct types of oxygens, each being distinguished by their environment and by their distances to the cation on which the excess charge is placed. These distances are $R_1 = 1.9\ ^oA$ and $R_2 = 1.95\ ^oA$ (Westman 1961)and the corresponding oxygens will be represented by type I and type II respectively, see figure (3.1). The x_v and x_o in equation (3.3.6) have been calculated for the vanadium and each type of oxygens of the discrete set with the use of a computer, whence their values are given in the relevant field equations,

$$E^{O_I}_{cont.} = -Q\, a^2 c\, (0.01204\, M_o + 0.00156\, M_v) \qquad 3.3.7a.$$

$$E^{O_{II}}_{cont.} = -Q\, a^2 c\, (0.01022\, M_o - 0.01092\, M_v) \qquad 3.3.7b.$$

on the type I and II oxygens respectively and

$$E^{V}_{cont} = Q\, a^2 c\, (0.02384\, M_o + 0.0137\, M_v) \qquad 3.3.7c.$$

at the vanadium. The (-) sign in equation (3.3.7b) is entirely due to the crystal structure.

The contribution to the dipole fields arising from the other members of the *discrete* set can be easily calculated from equation (3.3.5); the fields are

$$E^{O_I}_{dis.} = -\frac{1.34\,\mu_1}{R_1^3} - \frac{6\,R_1R_2\,\mu_2}{(R_1^2 + R_2^2)^{5/2}} - (A^+ - A^-)\mu_3 \qquad 3.3.8a$$

$$E^{O_{II}}_{dis.} = -\frac{12\,R_1R_2\,\mu_1}{(R_1^2 + R_2^2)^{5/2}} - \frac{0.25\mu_2}{R_1^3} - \frac{6c\,R_2}{(c^2+R_2^2)^{5/2}}\,\mu_3 \qquad 3.3.8b.$$

on the two oxygens type I and II with induced dipoles μ_1 and μ_2, respectively, and

$$E^{V}_{dis.} = -\frac{6c\,R_2\,\mu_2}{(R_2^2 + c^2)^{5/2}} - \frac{0.25\mu_3}{c^3} - 2(A^+ - A^-)\mu_1 \qquad 3.3.8c.$$

on the vanadium with an induced dipole μ_3, where A is

$$A^{+}_{-} = 1.51\,\frac{c^2 + R_1^2 \pm 2.36\,cR_1}{(R_1^2 + c^2 \pm 1.51\,cR_1)^{5/2}}\,.$$

The unknown dipoles μ_1, μ_2 and μ_3 can now be calculated from the relations

$$\mu_1 = \alpha_o \left(\frac{Q}{R_1^2} + E^{o_I}_{cont.} + E^{o_I}_{dis}\right) \qquad 3.3.9a.$$

$$\mu_2 = \alpha_o \left(\frac{Q}{R_2^2} + E^{o_{II}}_{cont.} + E^{o_{II}}_{dis.}\right) \qquad 3.3.9b.$$

$$\mu_3 = \alpha_v \left(\frac{Q}{c^2} + E^{v}_{cont} + E^{v}_{dis}\right) \qquad 3.3.9c.$$

The first term in equation (3.3.9) is the field of Q itself.

The potential in the first order approximation is then written as

$$V = - Q\, a^2 c \left[M_o \sum_o{}' \frac{1}{r^4} + M_v \sum_v{}' \frac{1}{r^4}\right] - \frac{4\mu_1}{R_1^2} - \frac{2\mu_2}{R_2^2} - \frac{2\mu_3}{c^2} \qquad 3.3.10.$$

where all the ions treated as discrete are excluded from the summations; thus $(4/R_1^4 + 2/R_2^4)$ and $2/c^4$ must be subtracted respectively from equation (3.3.4b).

(B) Polarization when the ions are displaceable.

Let us now consider the situation, when the ions are allowed to move. Due to the excess charge Q the ions will be displaced into new positions and settle down in equilibrium.

The induced dipoles on the ions can be found as before; for example, the polarization of the medium is now

$$p = \frac{Q}{4\pi r^2} \left(1 - \frac{1}{\varepsilon_s}\right) \qquad 3.3.11.$$

where ϵ_s is the directionally averaged *static* dielectric constant. In addition to equation (3.3.2) there will be some contribution to the cation polarization due to the *displacement* of vanadiums, which is given by

$$P'_v = \frac{2\alpha'_v}{a^2 c} [E + L'_v P] \qquad 3.3.12.$$

where α'_v is the displacive ionic polarizability of vanadium. From equations (3.3.2), (3.3.11), (3.3.12) and $P=P_v+P'_v+P_o+P'_o$ one gets the induced dipole μ'_v on a vanadium to be given by

$$\mu'_v = M'_v \frac{a^2 c}{r^2} Q \qquad 3.3.13a.$$

where

$$M'_v = \frac{\alpha_v + \alpha'_v}{2(\alpha_v + \alpha'_v + 2\alpha_o + 2\alpha'_o)} \frac{1}{4\pi} (1 - \frac{1}{\epsilon_s}) \times$$

$$\{1 + \frac{4\alpha_o + 4\alpha'_o}{a^2 c} (L'_v - L'_o)\} \qquad 3.3.13b.$$

with a similar expression for oxygens.

The displacement ξ of an ion in continuum, for example a vanadium, can be obtained from

$$(4e^*)\ \xi = \frac{M' a^2 c Q}{r^2} \qquad 3.3.14a.$$

where

$$M' = \frac{\alpha_v'}{2(\alpha_v + \alpha_v' + 2\alpha_o + 2\alpha_o')} \quad \frac{1}{4\pi}\left(1 - \frac{1}{\varepsilon_s}\right) \times$$

$$\{1 + \frac{4\alpha_o + 4\alpha_o'}{a^2 c} \quad (L_v' - L_o')\}. \qquad 3.3.14b.$$

A similar expression can be written for an oxygen ion.

The potential in the zeroth order approximation can be easily found as before. In the first order approximation we take the displacements x_i and the electronic dipoles of nearest neighbour ions to Q as unknowns. In so doing it is assumed that the dipoles of nearest neighbour ions, which are treated discretely, are separable into their electronic and displacive parts. For all the ions in continuum we assume that equations (3.3.13) and (3.3.14) hold. The discrete set contains the same eight ions as before: six oxygens and two vanadiums. There are, therefore, in total six unknowns, three displacements and three electronic dipoles to be determined (one cationic and two anionic, in each case).

The electronic dipole on an ion is written as

$$\mu_i = \alpha_i \underset{\sim}{E}(i) \qquad i = 1,2,3 \qquad 3.3.15.$$

where $\underset{\sim}{E}(i)$ is the local field at the considered ion and α_i is its electronic polarizability. $\underset{\sim}{E}(i)$ consists of the fields arising from the excess charge and the lattice dipoles. The

latter contains the dipole-dipole interactions between eight nearest neighbour ions and the field due to the ions in continuum as in the rigid lattice.

The local field $\underset{\sim}{E}(i)$ at the considered ion exercises a force on it and this force should be balanced by the repulsive forces. In reality, we have considered only the electrostatic force F_e resulting from dipoles (except for the excess charge) and neglected the Coulomb forces. Therefore we have to consider the change in the repulsive forces instead of the total force. This can be expressed as follows:

$$\Delta F_r(i) = x_i \frac{\partial F_r(i)}{\partial x_i} \qquad 3.3.16.$$

where x_i is the unknown displacement, and then the equilibrium condition of the i'th ion is

$$\Delta F_r(i) + F_e(i) = 0 \qquad i = 1,2,3 \qquad 3.3.17.$$

All the repulsive forces mentioned above are directed radially with respect to the excess charge, the displacements of oxygens and vanadiums being in opposite direction, with the vanadiums approaching and the oxygens receding from the excess charge.

The forces $F_r(i)$ can be obtained by differentiating equation (3.2.10) with respect to x_i. Equations (3.3.15) and (3.3.17) require length calculations, therefore we relegate the results to Appendix I. These six non-linear equations (3.3.15) and (3.3.17) have been solved for μ_i's and x_i's by a

computer programme, the results are given in Table (3.2).

Thus the potential is

$$V = -Qa^2c(M'_o \sum_o{}' \frac{1}{r^4} + M'_v \sum_v{}' \frac{1}{r^4}) - \frac{4(\mu_1 - 2e^*x_1)}{(R_1 + x_1)^2}$$

$$- \frac{2(\mu_2 - 2e^*x_2)}{(R_2 + x_2)^2} - \frac{2(\mu_3 - 4e^*x_3)}{(c - x_3)^2} \qquad 3.3.18.$$

where as before the sums exclude the contribution from the ions treated discretely.

3.4. Results

Taking $Q = -|e|$ as the excess charge in equations (3.3.10) and (3.3.18) we can calculate the potential V at the location of the excess charge. The polarization energy can then be obtained from $P = \frac{1}{2}$ eV. The results are given in the Table (3.2).

We note that the induced dipole on the vanadium ion becomes larger in the displacive case, whereas those on the oxygen ions are decreased. This is not unexpected since the vanadium ion moves towards the excess charge, contrary to the displacements of the oxygen ions.

TABLE 3.2.

		μ_1	μ_2	μ_3	x_1	x_2	x_3	P(eV)
		(^{o}A × electronic charge)			(10^{-3} A^{o})			
Rigid	Zeroth	-	-	-	-	-	-	5.14
Lattice	First	0.3522	0.3303	0.0030	-	-	-	6.11
Displace-able	Zeroth	-	-	-	-	-	-	5.23
Lattice	First	0.2934	0.3104	0.0064	57.0	51.3	28.8	6.62

The value of the last term on RHS of equation (3.1.11) is thus 12.22 eV when ion displacements are neglected (assuming P(5) = P(3)), indicating that the approximation used by Hyland (resulting in a value of 14.06 eV) lead to an overestimate of the polarization energy. Including now the ion displacements, to total polarization energy is increased to 13.24 eV, which, assuming * a separability between electronic and displacive polarizations, implies a purely displacive contribution of about 1 eV, as found by Hyland.

* Strictly speaking this is not possible since the very displacement of an ion itself results in some electronic distortion (Fröhlich, 1949).

3.5. Conclusions

Bringing together our results for the polarization energy with these mentioned in Chapter (3.1) we find

$$U < 1.74 \text{ eV}$$

the inequality resulting from our neglect of the positive quantity δ_1 (see Chapter 3.1(a)).

Recalling that the stability of the metallic state in rutile VO_2 required $U < 4.63$ eV, our calculations show that this is in fact the case, with the metallic state being stable against Mott-insulation by 0.46 eV.

A similar analysis for the π^*-band using equation (3.4.6) and N(E) given by equation (2.4.6) reveals that equation (3.1.10) is again satisfied.

Whilst for both bands the reduction in kinetic energy achieved through delocalization (from the Mott-insulating state having one electron localized in each cation $d_{x^2-y^2}$ orbital) outweighs the increase in Coulomb potential energy, consistent, of course, with the actual existence of a metallic state in rutile VO_2, the description of this state afforded by the band model cannot be anticipated to be quantitively realistic, especially for the case of the d_{11}-band, in consequence of the high degree of correlation which must therein exist in view of the close proximity of T to ν; the above calculation shows that average itinerant kinetic energy in the d_{11}-band exceeds to the

Coulomb potential energy by only 0.46 eV; thus despite existing assertions to the contrary (Friedman and Mott, 1974, Zylbersztejn and Mott, 1975) the electron gas in "metallic" VO_2 would appear to contain a significant degree of correlation and as such to be more appropriately described e.g. by the theory of Brinkman and Rice (1973).

It is of interest to note that a calculation similar to that performed above indicates that the validity of equation (3.1.10)is not contingent upon the d_{11}-band being overlapped by the π^*-band resulting in the d_{11}-band being *less* than half filled. For in the case of an *isolated* d_{11}-band E_F is increased to 1.19 eV and P_2 to 0.25, whence E_L still *exceeds* E_B (by 0.09 eV, now). The importance of hybridization between cation and anion orbitals was first stressed by Mott in 1969 and has more recently been considered by Valiev et. al. (1975) and Mokerov and Saraiken (1976) in connection with a possible model of the semiconductor → metal phase transition which incorporates both phonon softening *and* Mott-insulation. Their investigations of the absorption spectra of VO_2 above and below the semiconductor → metal phase transition temperature, T_t imply a large increase* in the degree of covalency as VO_2 is heated up towards T_t which they attribute to phonon-softening; in this way a Mott-insulating ground-state+ could become unstable once the covalency is sufficient for the π^*-band

---

* It should be pointed out, however, that this conclusion is at variance with that reached by Blaauw et.al. (1975) from XPS measurements.

\+ For a discussion of the low temperature phase of VO_2 in terms of a Mott-insulator see Hyland (1968).

to have a width sufficient to engulf the localized states.

In addition to the reduction in the Coulomb energy in the d_{11}-band arising from the overlapping by the Π^*-band a further reduction can be anticipated through the screening effects of the more highly itinerant Π^*-electrons which could thus be considered to play a rôle similar to the 4s electrons in transition metals (Mott 1967; Hearn and Hyland 1973; Zylbersztejn and Mott 1975).

CHAPTER 4

THE POLARON PROBLEM IN METALLIC VO_2

4.1. Introduction.

The polaron concept as usually understood arises from the consideration of the interaction of a single electron, moving slowly in the conduction band of an otherwise insulating material, with the longitudinal optical phonon field of the associated ionic lattice. The electron distorts and displaces its surrounding ions, establishing a polarization field in the crystal which acts back on the electron, whose properties are then modified; in particular, the electron acquires a (finite) self-energy and an enhancement of its Bloch effective mass. In the language of field theory these effects arise from the emission and reabsorption of *virtual* quanta of the longitudinal optical phonon field of the material.

Of the four underlined conditions which characterize the conventional polaron only the last is satisfied to any significant* extent in metallic VO_2. For in the first place metallic VO_2 contains not a *single* electron but rather 3.4×10^{22} per cm^3 which constitute a rather degenerate Fermi gas ($E_F/kT \sim 31$) with a well defined Fermi surface. Thus the question immediately arises as to whether polarons are still in fact formed since in the presence of *many* electrons a significant screening of the

---

* Recall that the analysis of Shimizu (1967) implies that Mott-insulating VO_2 would not be completely ionic, but contain a 30% degree of covalency.

electron-optical phonon interaction, which in the case of a single electron is responsible for polaron formation, can be anticipated; intuitively, the presence of many electrons reduces the effective range of the Coulomb field of an individual electron to lie within its Debye (or rather Thomas-Fermi) sphere, with the consequence that an electron can polarize its lattice environment only within this sphere (Mott 1969); the majority of the polaron's inertia, which in the conventional case comes from the long range part of its field, is thus lost (or at least very much reduced). As an associated consequence of this screening one would also expect a reduction in the frequency of the longitudinal optical modes.

On the other hand, despite the existence of 3.4×10^{22} electrons per cm^3 in metallic VO_2 only those in the vicinity of the Fermi surface are of interest from the point of view of potential polaron formation by the emission and reabsorption of virtual* optical phonons. In consequence of the relatively high velocity v of these electrons, however, (of order the Fermi velocity, $v_F \simeq 4.8 \times 10^7$ cm sec^{-1}) they cannot succeed in polarizing the crystal to the same extent as can the *slowly* moving

---

* The possibility of *real* phonon *emission* by these electrons requires that $kT >> \hbar\omega_{scr.}$ in order to ensure that after emission there is a vacant state which the electron can occupy; we shall see in the next section, however, that this condition is hardly satisfied in metallic VO_2.

electron usually considered, whose velocity is thermal $\sim \sqrt{\frac{3kT}{m}}$; for simple calculation shows that the time taken by an electron moving with $v \simeq v_F$ to cross a unit cell of rutile VO_2 is two order of magnitude shorter than the period of a typical longitudinal optical mode.

As a first step towards attempting to quantify the above considerations we shall now consider, in more detail, the optical phonon field in rutile VO_2 and the effect on its frequencies of the degenerate conduction electron gas.

4.2. Optical Mode Frequencies

We start by identifying the polar optical modes which are relevant to our calculations, from the analysis of Eagles (1964) for TiO_2. Polar optical modes are created by contrary displacement of the anions and cations in a crystal unit cell. The electric dipole moments associated with these displacements can be conveniently described in terms of the associated macroscopic polarization field $\underset{\sim}{P}$. Considering the anisotropy of rutile structure, the polarization $\underset{\sim}{P}$ may be perpendicular or parallel to the c_r-axis. In the former case there are three longitudinal and three transverse polar modes, which belong to the symmetry E_u. Along the c_r-axis, there is only one polar mode with symmetry A_{2u}, which consists of one longitudinal and one transverse mode.

From infrared reflection data on TiO_2, Eagles obtained the frequencies of the polar modes which we quote in Table 4.1.

TABLE 4.1.

	$\hbar\omega$ (eV)	$\hbar\omega$ (eV)	Screened $\hbar\omega$ (eV)
	LO	TO	LO
E_u	0.046	0.023	0.023
	0.057	0.048	0.048
	0.100	0.062	0.063
A_{2u}	0.100	0.021	0.022

It should be mentioned that the mode analysis of Eagles corresponds to zero wave vector; we shall use these values also at non-zero wave vector, assuming, as usual, that the optical mode frequencies are constant.

As already mentioned the frequencies of the longitudinal phonon modes in metallic VO_2 will be different from the values given in Table 4.1. for insulating TiO_2 in consequence of the existence in VO_2 of free electrons (the metallic conduction electrons). Following Cowley and Dolling (1965) the longitudinal mode frequency, $\omega(\underset{\sim}{q})$, is given by

$$\omega^2(\underset{\sim}{q}) = \omega_{TO}^2 + \frac{\omega_{LO}^2 - \omega_{TO}^2}{\epsilon(\underset{\sim}{q},0)} \qquad 4.2.1.$$

where ω_{LO} and ω_{TO} are, respectively, the unscreened longitudinal and transverse mode frequencies and $\epsilon(\underset{\sim}{q},0)$ is the wave vector dependent dielectric function. Since the optical frequencies concerned are appreciably smaller (by a factor of about 10) than the plasmon energy (see Chapter 5), the frequency dependence of $\epsilon(\underset{\sim}{q},\omega)$ can be safely neglected. In the Thomas-Fermi approximation $\epsilon(\underset{\sim}{q})$ is given, for small $\underset{\sim}{q}$, by

$$\epsilon_\gamma(\underset{\sim}{q}) = \varepsilon_{s,\gamma}\left(1 + \sum_l \frac{\lambda_{\gamma l}^2}{q^2}\right). \qquad 4.2.2.$$

$\lambda_{\gamma l}^{-1}$ is the Thomas-Fermi screening length, defined (Ziman 1964) by

$$\lambda_{\gamma l}^2 = \frac{4\pi e^2 N_l(E_F)}{V \varepsilon_{s,\gamma}} \qquad 4.2.3.$$

where V is the volume of the unit cell, $N(E_F)$ is the density of states at the Fermi level, γ refers to either the a_r or c_r direction and l refers to the d_{11} and Π^*-bands. Equation (4.2.3) is to be evaluated for the d_{11} and Π^*-bands by making use of their respective density of states, given in Chapter 2.4.

We note that as $q \to 0$, $\omega^2(\underset{\sim}{q})$ decreases to ω_{TO}^2, while as $q \to \infty$, $\omega^2(\underset{\sim}{q}) \to \omega_{LO}^2$; thus $\omega_{TO}^2 < \omega^2(\underset{\sim}{q}) < \omega_{LO}^2$. Physically this behaviour can be understood as follows:

the energy difference between the longitudinal and transverse modes is caused by long-range Coulomb effects. The screening is ineffective at large wave vector, and therefore the frequency is almost equal to ω_{LO}. At low wave vector, however, the long-ranged Coulomb effects are screened out by the electron plasma, whence the frequency approaches ω_{TO}.

Setting q equal to the relevant Fermi wave vector, equation (4.2.3) gives for the screening length in the $d_{11}(\Pi^*)$ band for directions parallel to the c_r-axis and in the basal plane the values 8.3 ^{o}A(10.51 ^{o}A) and 5.91 ^{o}A (7.48 ^{o}A), respectively. Equations (4.2.2) and (4.2.1) then yield the values of the longitudinal optical phonon frequencies shown in the third column of Table 4.1.*

4.3. Electron-Lattice Interactions in Metallic VO_2

Having investigated the effect of the degenerate conduction electron gas on the frequencies of the polar optical phonon modes in metallic VO_2 we now return to consider in more detail the interaction of these modes with an individual conduction electron. As already mentioned in Chapter 4.1, the only electrons which need to be considered are those within about kT of the Fermi surface whose velocity v is appreciable ($v \simeq 4.8 \times 10^7$ cm sec^{-1}).

---

* In connection with the footnote on page 69 it should be noted that these frequencies are comparable with $kT/\hbar$ for typical temperatures encountered above ($T_t \simeq 68^{o}C$).

Before proceeding, our discussion will be greatly facilitated by the introduction of (single) appropriately averaged values of certain parameters of relevance. These are given in the following Table 4.2.

TABLE 4.2.

Quantity	Value
Lattice spacing a	4.0 ^{o}A
Screened Optical Polar frequency ν	0.04 eV
Associated period $1/\nu$	1×10^{-13} secs.
Fermi velocity	4.8×10^{7} cm sec^{-1}
Screening length λ^{-1}	5 ^{o}A

The interaction of such a relatively "fast" electron with the optical phonon field of an ionic crystal has, in fact, been considered from a semiclassical point of view by Fröhlich et.al. (1950) in their introduction to conventional slow polaron theory and it is their treatment that we now adapt for our discussion of the situation in metallic VO_2. Let v be the

velocity of a typical electron in the vicinity of the Fermi surface and $\nu_{ir}^{(s)}$ the frequency of a typical (infrared) optical mode, after screening has been taken into account,with which the electron is considered to interact. Ions at very large distances from the electron will be displaced as they would be if the electron were stationary. At short distances, however, they will not have sufficient time to complete their full static displacement before the electron has moved elsewhere. Since it takes a time $1/\nu_{ir}^{(s)}$ to fully displace an ion, only those ions at a distance greater than $r_o \equiv v/\nu_{ir}^{(s)}$ will be so displaced; for distances $r < r_o$, on the other hand, the passage of the electron will be felt as a shock wave. Accordingly the electron carries with it a polarization whose potential can be approximated to that of a static charge for $r > r_o$, and which for $r < r_o$ can be taken as constant; r_o is the appropriate replacement for the case of fast electrons of the conventional (slow electron) polaron radius, r_p. Calculation of r_o, using the averaged values given in Table 4.2 yield $r_o = 480\ ^{o}A$ implying an extremely large polaron or equivalently to an extremely weak electron-polar optical phonon coupling. This is, of course, quite consistent with the fact that time τ_t taken for an electron moving with v_F to cross a distance "a" is 0.8×10^{-15} secs, almost two orders of magnitude small than period of the screened infrared optical polar mode ($\simeq 1 \times 10^{-13}$ secs).

On the other hand the transit time τ_t *is comparable* with the period of the ultraviolet (u.v.) polarization associated with the deformation of the electronic shells of the cation and, in particular, of the much more highly polarizable anions, O^{2-}. This follows from use of the lower limit on the frequency of this u.v. polarization field obtained from the magnitude of the energy gap between the filled bonding Π-band (primarily oxygenic) and the d_{11}-Π^* conduction band complex (see Fig. 2.3). As mentioned in Chapter 2 this gap is about 2.5 eV, corresponding to a u.v. frequency with an associated period of 1.7×10^{-15} secs, very close to τ_t ($= 0.8 \times 10^{-15}$ secs). Conditions favourable for the establishment of an "electronic" polaron thus obtain.* Since, however, $\tau_t \lesssim \tau_{uv}$ a modification of the Toyozawa theory (Toyozawa 1954), is required, analogous to that considered for the case of the lattice polaron when $\tau \lesssim \tau_{ir}$. Replacing τ_{ir} by τ_{uv} gives $r_{uv} =$ 8 ^{o}A, indicating that the electronic polaron is to be regarded as a "small" one, (r_{uv} is close to the value of the average lattice constant, a); this conclusion is of course in keeping with the use, in Chapter 2, of the tight-binding approximation. The width of the associated small polaron band is known to be smaller than that of the rigid lattice Bloch band by a factor $e^{-\gamma}$, where γ is given by (Chaiken et.al. 1972, 1973)

$$\gamma \equiv \frac{E_b}{\hbar\omega_o} \qquad 4.3.1.$$

---

* It's interesting to note that the ratio $E_F/\hbar\omega_{uv}$ is comparable to that appropriate to slow (i.e. thermal) electron interacting with the *infrared* mode $E_T/\hbar\omega_{ir}$ where $E_T \sim kT$.

where E_b is the self-energy of the small "electronic" polaron and $\hbar\omega_o$ the energy of the relevant uv. polarization quanta. In the case of small "lattice" polarons it is common practice to continue to treat the electron-optical phonon (ir.) interaction within the framework of a continuum polarization model - see e.g. Tyablikov 1952, Eagles 1966, Austin and Mott 1969. Adoption of this procedure in the case of our electronic polaron, enables us to use Toyozawa's expression for the polaron self-energy, E_b is modified, however, by the replacement of Toyozawa's polaron radius $(\frac{\hbar}{2m^* \omega_{uv}})^{1/2}$ by $r_{uv} = \frac{v_F}{\nu_{uv}}$ in accordance with the above considerations. E_b is then given by

$$E_b = -\frac{e^2}{2}\left(1 - \frac{1}{\varepsilon_\infty}\right)\frac{1}{r_{uv}} \qquad 4.3.2.$$

$$= -0.78 \text{ eV}$$

using the average values listed in Table 4.2; equation (4.3.1) then gives, with $\hbar\omega_{uv} = 2.5$ eV, $\gamma = 0.31$ such that

$$\frac{W_{el\text{-}pol.}}{W_{Bloch}} = 0.73 \qquad 4.3.3.$$

No account has been taken so far of the screening effect of the degenerate conduction electron gas on the interaction of an individual electron with the uv.electronic polarization field of the ion cores.

The results of Chapter 2 yield an average value of 5 ^{o}A for the screening length, λ^{-1}, beyond which the Coulomb field of an individual electron is exponentially small. Accordingly, since $\lambda^{-1} < r_{uv}$, the majority of the polarization previously associated with the electronic polaron is lost. Following Mott and Friedman (1974) this screening effect of the degenerate conduction electron gas can be quantified by supposing that the electron interacts with the uv polarization field through a screened Coulomb potential $\propto \frac{1}{r} \exp(-\lambda r)$. Noting that r_p of Mott and Friedman is for us to be replaced by r_{uv}, their result for the polaron self energy in the presence of screening, E_b^s takes the form

$$E_b^s = E_b \; e^{-2\lambda r_{uv}} \left(1 + \frac{\lambda r_{uv}}{2}\right) \qquad 4.3.4.$$

$$= E_b \times 0.07 = 0.06 \text{ eV}$$

using the E_b value found above together with $\lambda^{-1} = 5$ ^{o}A and $r_{uv} = 8$ ^{o}A. The screening thus seems to be highly significant, resulting in reduction of the electron self-energy by 93%.

Introducing now a corresponding $\gamma^{(s)}$ through (Ehrenreich 1959)

$$\gamma^{(s)} = \frac{E_b^s}{\hbar\omega_{uv}}.$$

we find $\gamma^s \simeq 0.02$, whence $\frac{W_{el\text{-}pol}}{W_{Bloch}}$ increased from 0.73(equation (4.3.3)) to 0.98 .

Before concluding it should be mentioned that instead of $r_{uv} = \frac{v_F}{\nu_{uv}}$ if we use in equation (4.3.2) Toyozawa's polaron radius, corresponding to a slow electron, then we obtain a value of 7.3 eV for E_b, which is quite close to that obtained in the Mott-Littleton calculations of Chapter 3, for the case in which the lattice is treated as rigid (6.11 eV). From the same calculations, the difference between the polarization energies of the rigid and displaceable lattice yields for the binding energy of the lattice polaron corresponding to the *first* free electron excited out of the Mott-insulating ground-state, the value 0.5 eV; in real *metallic* VO_2, however, this binding energy will be much reduced, due to the existence of many conduction electrons. In fact, re-evaluation of the appropriate modifications of equations (4.3.2) and (4.3.4) yields a vanishingly small value for the binding energy ($\sim 10^{-9}$ eV) which can be completely neglected.

4.4. Conclusions

The conclusion of this preliminary investigation is that due to the screening effect of the 3.4×10^{22} electrons per cm^3 which exist in metallic VO_2, polaron formation may, *as a first approximation,* be neglected and the charge carriers treated as electrons. It is to be noted that this conclusion is in accord with intuitive considerations of Mott (1969) that

the existence of a degenerate gas of polarons requires that the number of carriers be less than the number of sites since the lattice can't be distorted in more than one direction at a time; in rutile VO_2, it will be recalled from Chapter 2, each anion has 3 coplanar cation nearest-neighbours each of which is associated with a different anion octahedron. To what extent this is a valid point is, however, debatable since in the context of the Bloch tight-binding approximation the "charge carriers" are really to be identified with the doubly occupied cations whose number is certainly less than the total number of cations - see Chapter 2.

It is to be hoped that the results of the above semi-classical approach would be endorsed in the framework of a proper microscopic formulation of the problem of many electrons in interaction both with the infrared and ultraviolet polarization field in rutile VO_2, in which the restrictions imposed by the Pauli principle on the virtual transitions induced by electron-infrared and - ultraviolet lattice interactions are built in from the start; for the case of (i.r) lattice polarons this has been considered by Mahan (1972) for case of weak coupling.

CHAPTER 5

APPLICATIONS

5.1. Introduction

In this Chapter our purpose is to apply the one-electron dispersion relations obtained in Chapter 2 to the interpretation of some existing electronic properties of metallic VO_2, such as the electronic specific heat, the electron plasma frequency and the Hall effect.

First we compute the electronic contributions to the specific heat of metallic VO_2 and discuss its rôle in the resolution of the anomolously high specific heat found experimentally.

Secondly, using our one-electron dispersion relations, we calculate the longitudinal dielectric function from whose zero the electron plasma frequency ω_p is obtained. In the absence of any measurements of the energy loss of fast electrons, from which ω_p could be obtained directly, the value of ω_p has to date been obtained *indirectly* via either an oscillator fit or a Kramers-Krönig analysis of the measured frequency-dependent optical reflectivity of metallic VO_2 crystals.

Whilst recent reflectance studies of Fan (1972) using high quality crystals give results (ω_p = 1.3 eV) in close agreement with earlier work of Barker et.al. (1966) (ω_p = 1 eV), the situation in the case of the Hall effect is less definitive (see Rosevear 1972, for a review). Whilst it is probably true to say that a theoretical understanding of the *measured* Hall coefficient R_H is more of immediate interest than that of the quantity ω_p

both quantities do, nevertheless, depend in a detailed way on the features of the electronic band structure and so accordingly may be taken to be of equal utility in assessing the validity of the band structure characterized by those values of the parameters adopted in Chapter 2.

Consistent with our finding in the previous Chapter to the effect that polaron formation is almost entirely suppressed through the screening effect of the degenerate electron gas, we shall in what follows assume the charge carriers in metallic VO_2 to be Bloch electrons.

5.2. Electronic Specific Heat of Metallic VO_2

5.2.1. Introduction

The experimental specific heat at constant pressure, C_p, of metallic VO_2 shows an anomaly above 540^oK. Early measurements by Cook (1947) showed that the equipartition value of the specific heat at constant volume C_v is exceeded by an amount which cannot be explained by the usual correction term relating C_v to C_p. This has been confirmed by more recent measurements of Chandrashekhar et.al. (1973).

The relation between C_p and C_v is given by

$$C_p - C_v = TV \frac{\alpha^2}{\beta} + \Delta C_v(ph) + \Delta C_v(el) \qquad 5.2.1.$$

where V is the molar volume at temperature T. α and β are the volume expansion coefficient and the compressibility, respectively.

Without the last two terms on the R.H.S, which represent, respectively, contributions from phonon-softening and electrons to C_v, equation (5.2.1) is the standard expression for the specific heat differences. Experimentally not C_v but C_p is measured; considering only the harmonic lattice contribution the maximum value of C_v is 9R(= 17.8 cal./mol-deg) from the Debye theory, where the factor 9 comes from the three atoms in a molecule of VO_2, each having three degree of freedom.

The first term on the R.H.S. of equation (5.2.1) has been estimated to be 0.55 cal./mol-deg. (Chandrashekhar et.al. 1973). Simply adding this to the C_v value just quoted is not sufficient to explain the experimentally observed values of C_p. Chandrashekhar et.al. argued that there will be a contribution, $\Delta C_v(ph)$ in equation (5.2.1), from phonon-softening, which from the Raman spectrum of metallic VO_2 (Srivasta and Chase 1971) is estimated to be about 0.7 cal./mol-deg. at $400^{o}K$.

In addition, the contribution made by the electrons in the conduction band should be taken into account and this is represented by the term $\Delta C_v(el)$ in equation (5.2.1). The purpose of the next section is to calculate the electronic specific heat by using the density of states obtained in Chapter 2.

5.2.2. Calculations

If there are N electrons per unit volume then the total energy of the electrons is given by

$$E = N \int E.N(E).f_o(E)dE \qquad 5.2.2.$$

where N(E) is the total density of states and f_o is the Fermi-Dirac distribution function

$$f_o(E) = \frac{1}{1 + \exp\left(\frac{E - \mu}{kT}\right)} \qquad 5.2.3.$$

The chemical potential of the electrons μ is a function of temperature T, and is identified with the Fermi energy E_F.

The specific heat at constant volume C_v is obtained by the derivative of E with respect to T; the result is

$$C_v = \frac{N}{2kT^2} \int N(E) \frac{E(E - \mu + T.\frac{d\mu}{dT})}{1 + \text{Cosh}\left(\frac{E - \mu}{kT}\right)} dE \qquad 5.2.4.$$

The integration is to be taken from the bottom of the d_{11}-band to the top of the Π^*-band. The variation of μ with T which enters equation (5.2.4) can be calculated from the following considerations.

The number of electrons per cation (since N(E) refers to one cation) is, by definition,

$$\bar{n} = \int N(E).f_o(E)dE \qquad 5.2.5.$$

with all quantities defined as in equation (5.2.2). Since there is one electron per cation in the two overlapping d_{11} and Π^*-bands, the condition that $\bar{n}$ remains unity in equation (5.2.5) gives the Fermi energy $E_F(T)$ at a definite temperature T. In this way one is able to calculate numerically the Fermi energies corresponding to different temperatures.

The results show that the Fermi energy is constant within the considered temperature range. This is not unexpected, since the density of states diagram is very flat at E_F = 0.93 eV, having a small slope around this region. We therefore neglect the term $\frac{d\mu}{dT}$ in equation (5.2.4).

It should also be mentioned that the quoted value of the occupancy (n = 0.2) in Chapter 2 has been obtained from equation (5.2.5), where now taking N(E) to be the corresponding values of the Π^*-band.

The calculated specific heat values from equation (5.2.4) are presented in Table 5.1, for the temperature range considered, in units of Nk(=R) and cal/mol-deg.

As pointed out by Brinkman and Rice (1970), these values will be enhanced by correlation effects. Their theory of the correlated electron gas predicts an enhancement (essentially through a mass renormalization) of the specific heat by a factor ξ ,

$$\xi = [1 - (\frac{U}{8\bar{E}})^2]^{-1} \qquad 5.2.6.$$

$\bar{E}$ is the average itinerant energy and U is the intra-atomic Coulomb energy. The value of $\bar{E}$ for each band can be obtained

TABLE 5.1.

T(^{o}K)	Nk	C_v cal/mol-deg.
360	0.16	0.32
400	0.17	0.34
500	0.24	0.48
600	0.28	0.56
700	0.34	0.68
800	0.41	0.81
900	0.49	0.97

easily by using the total energy calculated with the density of states of each band in equation (5.2.2). Comparing these with the energy dispersion relations (equations (2.3.29) and (2.3.32))

$$E_{\ell}(\underset{\sim}{k}) = (E_o - \alpha)_{\ell} - E'_{\ell}(\underset{\sim}{k})$$

where ℓ denotes either the d_{11} or d_{Π^*} band and, where $(E_o - \alpha)$ is the localised electron energy (see Chapter 3), one can extract the average itinerant energy $\overline{E} = \langle E'(\underset{\sim}{k}) \rangle$, where $\langle\ \rangle$ denotes an average taken over the occupied states in the band. The values obtained in this way are 0.84 eV for the d_{11}-band and 1.46 eV for the Π^*-band.

U has been calculated in Chapter 3 and has the value of 1.74 eV. Taking into account the fractional electron occupancy n for each band, the Coulomb interaction in equation (5.2.6) is to be replaced by $(1-n)^2U$ for the d_{11}-band and by n^2U for the Π^*-band, where n has been introduced in Chapter 2.4b. Applying equation (5.2.6) separately to the d_{11} and Π^* bands, it is found that the factor ξ is 1.04 for the d_{11}-band and almost 1 for the Π^*-band. We therefore neglect the correlation effects.

5.2.3. Conclusions

The specific heat measurements made by Cook on powder samples of VO_2 show an increase (from 9R) between 1 and 2 cal/mol-deg. The same amount of increase is observed on the curve given by Chandrashekhar et.al. from the single crystal measurements.

Our calculated values (including correlation enhancement) of the electronic specific heat range from 0.32 cal/mol-deg. at $360^{o}K$ to 0.97 cal/mol-deg. at $900^{o}K$. This alone is insufficient to account for the difference in the results of Cook and Chandrashekhar et.al. from the equipartition of 9R, without taking the contribution from the phonon-softening into account; the latter clearly cannot be neglected, however, being estimated by Chandrashekhar et.al. to be about 0.7 cal/mol-deg. at $400^{o}K$ at which temperature the electronic specific heat is 0.34 cal/mol-deg.

5.3. Plasma Oscillations in metallic VO_2

5.3.1. Introduction

In the previous chapter it was mentioned that the Coulomb interaction can be divided into a short and a long-range part. This latter is frozen out in the plasma mode of longitudinal collective oscillations, thus leaving the electrons to move, to a good approximation, in a screened potential. Therefore only the short range part controls the individual motion of electrons and this explains why the independent particle model is so successful.

Plasmons only exist in the long wavelength limit since above a critical wave vector q_c they are strongly damped and behave like a system of free particles. The plasma oscillation frequency in a uniform background of positive charge is given by the well known expression $\omega_p = (4\pi ne^2/m)^{1/2}$, where n and m are the free electron density and mass, respectively. As an effect of lattice periodicity ω_p will be modified through the introduction of an effective electronic mass and possible interband transitions.

As already mentioned, apart from fast electrons (longitudinal probe) another way of exciting plasmons in solids is by the use of electromagnetic waves. The latter is a transverse probe, the response of the system to which is incorporated in the transverse dielectric function $\epsilon_T(\underset{\sim}{q},\omega)$.

In terms of $\epsilon_T(\omega)$ (neglecting $\underset{\sim}{q}$ dependence) the optical reflectivity $R(\omega)$ is given by

$$R(\omega) = \left| \frac{\sqrt{\epsilon_T(\omega)} - 1}{\sqrt{\epsilon_T(\omega)} + 1} \right|^2 \qquad 5.3.1.$$

In the absence of any knowledge of the electron band structure of the material whose reflectivity is being measured, $\epsilon_T(\omega)$ is usually represented semiclassically in terms of a number of oscillators of strength s_r and linewidth Γ_r, thus

$$\epsilon_T(\omega) = \epsilon_\infty - \frac{\omega_n^2}{\omega^2 + i\omega_c\,\omega} + \sum_{r=1}^{m} \frac{s_r}{1 - \frac{\omega^2}{\omega_r^2} - i\,\frac{\Gamma_r\,\omega}{\omega_r}} \qquad 5.3.2.$$

The parameters appearing in equation (5.3.2) are then obtained by fitting the reflectivity given in terms of ϵ by equation (5.3.1) to the experimental results. Figure 5.1 shows the real part of the dielectric function obtained by Fan (1972) using this method. In consequence of the equality of the longitudinal and transverse dielectric functions in the longwavelength limit the zero of the dielectric function so obtained gives the plasma frequency; it is 1.3 eV.

It may be noted that Fan's experiment uses light incident in the [110] direction in the basal plane of the rutile VO_2 crystal.

Since the one-electron band structure is now known from the results of Chapter 2, there is no need to resort to the above phenomenological procedure since the longitudinal dielectric function can be calculated directly from the one-electron dispersion relations and the plasma frequency is found from the root of the expression

$$\text{Re}\ \epsilon_L(0,\omega) = 0 \qquad 5.3.3.$$

The validity of identifying the value so obtained with that obtained from the above semiclassical analysis of $R(\omega)$ follows from the equality between ϵ_L and ϵ_T which holds in the long wavelength limit (Pines 1963).

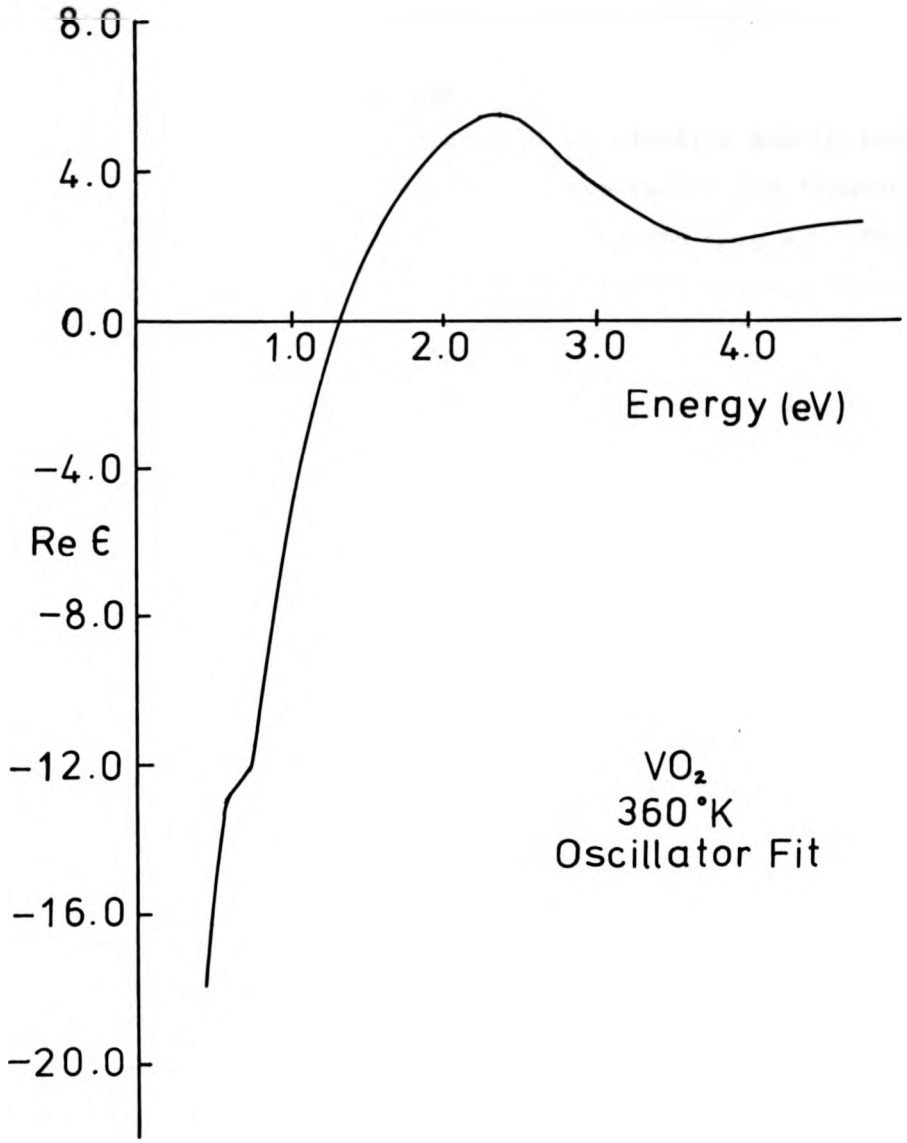

Fig. 5.1. Real part of the dielectric constant obtained by the oscillator fit method, after Fan (1972).

5.3.2. Plasma Oscillations

The linear response of an electron gas in real solids can be expressed in terms of the wave vector and frequency dependent longitudinal dielectric function $\epsilon_L(\underset{\sim}{q},\omega)$. The equation we shall use is the self-consistent field analysis due to Ehrenreich and Cohen (1959),

$$\epsilon_L(\underset{\sim}{q},\omega) = 1 - \frac{4\pi e^2}{q^2 V} \sum_{\underset{\sim}{k},\, l,\, l'} \left| \left\langle \underset{\sim}{k}, l \right| \rho_{\underset{\sim}{q}} \left| \underset{\sim}{k} + \underset{\sim}{q}, l' \right\rangle \right|^2$$

$$\times \frac{f_o(\underset{\sim}{k}+\underset{\sim}{q}, l') - f_o(\underset{\sim}{k}, l)}{(E_{\underset{\sim}{k}+\underset{\sim}{q}, l'} - E_{\underset{\sim}{k}, l}) - \omega - i\eta} \qquad 5.3.4.$$

where $|\underset{\sim}{k}, l\rangle$ is the Bloch state with the band index l and wave vector $\underset{\sim}{k}$, and $E_{\underset{\sim}{k}, l}$ the associated energy. $\rho_{\underset{\sim}{q}}$ is the Fourier component of the electron fluctuation in a volume V of the system and $f_o(\underset{\sim}{k}, l)$ is the equilibrium Fermi-Dirac distribution function. Equation (5.3.4) can be split into an intraband term ($l=l'$) and an interband term ($l \neq l'$) involving vertical ($\underset{\sim}{k}$-conserving) transitions, thus

$$\epsilon_L(q,\omega) = 1 - \frac{4\pi e^2}{q^2 V} \sum_{\underset{\sim}{k}, l} \frac{f_o(\underset{\sim}{k}+\underset{\sim}{q}, l) - f_o(\underset{\sim}{k}, l)}{(E_{\underset{\sim}{k}+\underset{\sim}{q}, l} - E_{\underset{\sim}{k}, l}) - \omega - i\eta}$$

$$- \frac{4\pi e^2}{2m V} \sum_{\underset{\sim}{k},\, l \neq l'} \frac{f_{ll'}(\underset{\sim}{q})}{\omega_{l'l}} \quad \frac{f_o(\underset{\sim}{k}, l) - f_o(\underset{\sim}{k}, l')}{\omega_{ll'} - \omega - i\eta} \qquad 5.3.5.$$

where the Bloch wave oscillator strength $f_{ll'}$ is defined by

$$f_{ll'} = \frac{2m}{q^2} \omega_{l'l} \left| (\rho_{\underset{\sim}{q}})_{ll'} \right|^2$$

with $\omega_{l'l} = E_{\underset{\sim}{k}l'} - E_{\underset{\sim}{k}l'}$

and η is a small positive constant corresponding retarded boundary conditions.

For small $\underset{\sim}{q}$ the real part of equation (5.3.4) becomes

$$\text{Re } \epsilon_L(\underset{\sim}{q},\omega) = 1 - \frac{e^2}{q^2\omega^2\pi^2} \sum_l \int d^3\underset{\sim}{k}\, f_o(\underset{\sim}{k},l) \sum_{\alpha\beta} \frac{\partial^2 E_l}{\partial k_\alpha \partial k_\beta} q_\alpha q_\beta$$

$$- \frac{e^2}{m\pi^2} \sum_{l\neq l'} \int d^3\underset{\sim}{k}\, f_o(\underset{\sim}{k},l)\, f_{\underset{\sim}{k}l,\underset{\sim}{k}l'} \frac{P}{\omega_{ll'}^2 - \omega^2} \qquad 5.3.7.$$

where P denotes principal value. We note that the second term contains q; we therefore express α,β ($\equiv$ x,y,z) in polar coordinates (q,θ,ϕ) which allows the q dependence to be eliminated, to the second order in $\underset{\sim}{q}$. θ and ϕ are the angles measured from the c_r-axis and in the basal plane, respectively.

Hence the sum over (α,β) in equation 5.3.7 can be written as

$$\sum_{\alpha,\beta} \frac{\partial^2 E}{\partial k_\alpha \partial k_\beta} q_\alpha q_\beta = q^2 \frac{\partial^2 E}{\partial k_x^2} \text{Sin}^2\theta + q^2 \frac{\partial^2 E}{\partial k_z^2} \text{Cos}^2\theta$$

$$+ q^2 \frac{\partial^2 E}{\partial k_x \partial k_z} \text{Sin}^2\theta \text{ Sin } 2\phi + q^2 \frac{\partial^2 E}{\partial k_x \partial k_z} \text{Sin } 2\theta \text{Cos}\phi + q^2 \frac{\partial^2 E}{\partial k_y \partial k_z} \times$$

$$\text{Sin } 2\theta \quad \text{Sin}\,\phi \qquad 5.3.8.$$

It should be noted that because of the symmetry the integrals containing the last three terms of equation (5.3.8) become zero in equation (5.3.7); e.g,

$$\int d^3\underset{\sim}{k} \quad f_o(\underset{\sim}{k}, l) \quad \frac{\partial^2 E_l}{\partial k_x \partial k_y} \quad = 0,$$

and similarly for the other two terms.

The last term of equation (5.3.7), which corresponds to interband transitions, can be split further by identifying possible transitions. This can be made by considering the frequency region in which the plasmon energy ω_p lies; from the experimental results quoted above, ω_p is around 1 eV. At the high frequency limit the most likely transitions are between the filled oxygen 2p-band and 3d-bands (d_{11} and Π^*). At the lower limit the only possibility is between the d_{11} and Π^*-bands. Whilst the latter is about 0.5 eV as discussed in Chapter 2, the separation between the p and d bands is 2.5 eV from the optical absorption measurements of Verleur et. al. (1968). Neglecting $\omega_{l,l}$ or ω in the last term of equation (5.3.7) according as whether the transitions are $d_{11} \rightarrow \Pi^*$ or $p \rightarrow d$ respectively, the real part of the dielectric function becomes

$$\text{Re } \epsilon_L(\omega) = \epsilon_\infty - \frac{e^2}{\omega^2\pi^2} \sum_l \int d^3\underset{\sim}{k} f_o(\underset{\sim}{k},l)\left(\frac{\partial^2 E_{\underset{\sim}{k},l}}{\partial k_x^2} \text{Sin}^2\theta + \frac{\partial^2 E_{\underset{\sim}{k},l}}{\partial k_z^2} \text{Cos}^2\theta\right)$$

$$- \frac{e^2}{m\pi^2\omega^2} \sum_{l\neq l'} \int d^3\underset{\sim}{k}\, f_o(\underset{\sim}{k},l)\, f_{l',l} \qquad 5.3.9.$$

where all the p → d and possible higher energy transitions from the deeper levels to the d-bands are incorporated into the high frequency dielectric constant ϵ_∞. Equation (5.3.3) then yields the following plasma dispersion relation

$$\omega_p^2 = \frac{e^2}{\epsilon_\infty \pi^2} \sum_l \int d^3\underset{\sim}{k}\, f_o(\underset{\sim}{k},l) \left(\frac{\partial^2 E_{\underset{\sim}{k},l}}{\partial k_x^2} \text{Sin}^2\theta + \frac{\partial^2 E_{\underset{\sim}{k},l}}{\partial k_z^2} \text{Cos}^2\theta\right)$$

$$+ \frac{e^2}{m\pi^2\epsilon_\infty} \sum_{l\neq l'} \int d^3\underset{\sim}{k}\, f_o(\underset{\sim}{k},l)\, f_{l',l} \qquad 5.3.10.$$

where l refers to the d_{11} and Π^*-bands. It should be pointed out that the high energy transitions reduce the plasma frequency through the dielectric constant ϵ_∞, while the lower frequency transitions ($d_{11} \rightarrow \Pi^*$) give an enhancement.

In the Γ-X direction the interband transitions are from occupied d_{11}-state to unoccupied Π^*-state whilst in the Γ-Z direction they are from occupied Π^* to unoccupied d_{11}, see Fig.2.5.

Finally, since equation (5.3.10) is independent of the angle ϕ, taking $\theta = \frac{\pi}{2}$ we obtain ω_p in the basal plane, which can thus be compared with the experimental measurements made in [110] direction.

To make contact with the experimental works, it is useful to define an optical mass m_{op} at this point (Cohen 1958).

$$\frac{N}{m_{op}} = \sum_{k} \frac{f_o(k)}{m^*(k)} ,$$

hence equation (5.3.10) can be written as, neglecting the interband contribution,

$$\omega_p^2 = \frac{4\pi e^2 N}{\varepsilon_\infty} \left[\frac{1 - n}{m_{op}(d_{11})} + \frac{n}{m_{op}(\Pi^*)} \right] \qquad 5.3.11.$$

where N is the number of conduction electrons per volume and n is the fractional occupancy of the Π^*-band introduced in Chapter 2.

In principle, the coupling of plasmons to the optical phonons in polar materials must be taken into account. This coupling, however, leads to important changes in the plasmon energy only when the latter is comparable to the optical phonon energies (Varga 1965). Considering the phonon frequencies and the experimental value of the plasmon energy this effect can be neglected in metallic VO_2. This can be shown quantitatively as follows. Including the optical phonon contribution in equation (5.3.9), the total dielectric function now becomes

$$\text{Re } \epsilon(\omega) = \varepsilon_\infty + \frac{\varepsilon_s - \varepsilon_\infty}{1 - \frac{\omega^2}{\omega_{TO}^2}} - \frac{\omega_p^2 \varepsilon_\infty}{\omega^2}$$

where ω_{TO} is the frequency of the transverse optical mode (assuming only one is dominant) and where we have neglected the interband

($d_{11} \rightarrow \Pi^*$) term. The solution of this equation for ω^2 gives two roots

$$\omega_{\pm}^2 = \frac{1}{2}(\omega_p^2 + \omega_{LO}^2) \pm \frac{1}{2}\sqrt{(\omega_p^2 + \omega_{LO}^2) - 4\omega_p^2\,\omega_{TO}^2}$$

In the extreme case, i.e. $\omega_p^2 >> \omega_{LO}^2$, one gets

$$\omega_+^2 \rightarrow \omega_p^2 \quad \text{and} \quad \omega_-^2 \rightarrow \omega_{TO}^2 .$$

Physically this implies that the coupled mode associated with the positive root is *mainly* a plasmon and that associated with the negative root is a screened phonon mode. In VO_2 $\omega_{LO}^2/\omega_p^2 \approx 10^{-3}$; we can therefore neglect the phonon contribution to the plasmon energy.

5.3.3. Results

Adopting the values of the high-frequency dielectric constants of TiO_2 in our calculations, equation (5.3.10) gives 1.55 eV along c_r-axis and 0.80 eV in the basal plane for the total plasmon energy. These are due only to the intraband transitions within the d_{11} and Π^*-bands. In our calculations we have not considered the damping and the lifetime of plasmons; we anticipate that the above energies will be slightly decreased by these effects. As mentioned earlier the experimental measurements of Fan are made in the [110] direction and his results for the real part of ϵ are shown in Fig. 5.1, from which the zero is seen to occur at 1.3 eV. This value is to be compared with our calculated one of 0.80 eV and we attribute the discrepancy to the interband transition between the bonding Π^* and antibonding d_{11} bands, which were neglected in our treatment. The possibility of such interband transition is a cause

of the non pure d-nature of the wavefunctions of the Π^*-band (Paul 1970). The same vertical interband transitions are known to be of importance for the interpretation of magnetic spin susceptibility, in particular the temperature independent contribution χ_o (Ford et.al. 1972)(in this case the matrix element of orbital angular momentums are involved in place of the dipole matrix element relevant to plasmons).

Direct calculation of the interband contribution is not possible in the absence of knowing the actual Bloch functions for the two bands involved. The d_{11}-band in the basal plane is completely filled, therefore the intraband contribution to the plasmon energy does not exist. We can thus expect only interband transitions between the Π^* and d_{11} bands; for the c_r-axis direction we do not expect a large contribution from the latter.

It is worth pointing out that the other type of interband transitions, such as $p \rightarrow d_{11}$ or $p \rightarrow \Pi^*$, gives rise to a decrease in the plasmon energy, in contrast to above arguments; these latter transitions are considered to be incorporated in ε_∞.

In view of the above results we conclude that the contribution from the interband transitions to the plasmon energy is by no means negligible, particularly in the basal plane.

Finally another quantity which we can compare with the results of Fan's work is the optical mass, m_{op}; equation (5.3.11) gives a value, in the basal plane, of $m_{op\perp} = 4.3\ m_e$, which is very close to that of Fan's measurements. Our energy dispersion relations give a similar optical mass along the c_r-axis,

which is $m_{op\,||} = 4.6\ m_e$.

On taking directional averages by

$$\frac{3}{m_{op}} = \frac{1}{m_{op\,||}} + \frac{2}{m_{op\,\perp}}$$

we get an optical mass $m_{op} = 4.4\ m_e$ for the metallic state of VO_2.

5.4. The Low Field Hall Effect in Metallic VO_2

5.4.1. Introduction.

The Hall effect measurements, with which our theoretical result will be compared, on metallic VO_2, were made by Rosevear (1972) using a d.c. current and a.c. magnetic field, $\underset{\sim}{H}$, whose frequency was sufficiently high to reduce the noise associated with the current to a level at which the Hall voltage could be detected; in this way the use of an a.c. magnetic field of 3.3 kilogauss r.m.s and a d.c. current of 48 nA produced, at $355^{o}K$, a Hall voltage of 1.5 nV in an apparatus capable of detecting 0.5 nV. The Hall coefficient was found to be nearly temperature independent over the 40^{o} temperature range investigated above T_t and of a sign consistent with conduction by electrons. The number of Hall carriers calculated by Rosevear on the assumption of a single band with spherical Fermi surface indicates that there are 3.3 electrons per cation. As commented by Rosevear this analysis can be improved by considering the two overlapping d_{11} and π^*-bands, (having a non-spherical Fermi surface) which are thought to be operative in metallic VO_2; the purpose of the remainder of this chapter is to carry out such a calculation using again our one-electron dispersion relations.

5.4.2. The Calculation of Hall Constant

Our present approach begins with the Boltzmann equation,

$$\frac{e}{\hbar}\left(\underset{\sim}{\mathcal{E}} + \frac{1}{c_o}\,\underset{\sim}{v} \times H\right).\ \mathrm{grad}_{\underset{\sim}{k}}\, f + \underset{\sim}{v}.\ \mathrm{grad}_{r} f = -\frac{f-f_o}{\tau} \qquad 5.4.1.$$

where f is the distribution function, $\underset{\sim}{\mathcal{E}}$ and $\underset{\sim}{H}$ are the external electric and magnetic fields. $\underset{\sim}{v}$ is the velocity of an electron ($\underset{\sim}{v} = \hbar^{-1}\ \mathrm{grad}_{\underset{\sim}{k}} E$.) and c_o is the speed of light. τ is the relaxation time, which in general depends on $\underset{\sim}{k}$ and must have the same symmetry as crystal. The question of the existence of a relaxation time for the electron-optical phonon scattering of interest will be returned to later.

Noting that the magnitude of the Hall voltage was found to be linearly dependent on $\underset{\sim}{H}$ and on the current density applied to the sample, as expected in the low field regime ($\omega\tau << 1$)* we confine ourselves to the *first order* term in Jones-Zener (1934) perturbative solution for f in ascending powers of $|\underset{\sim}{H}|$, i.e.

$$f = f_o - \Phi\,\frac{\partial f}{\partial E} \qquad 5.4.2.$$

where

$$\Phi = \frac{-e}{\hbar}\left[\tau\,\underset{\sim}{\mathcal{E}}\ \mathrm{grad}_{\underset{\sim}{k}} E + \frac{-e}{\hbar^2 c_o}\ \tau\underset{\sim}{H}.(\mathrm{grad}_{\underset{\sim}{k}} E \times \mathrm{grad}_{\underset{\sim}{k}})(\tau\ \underset{\sim}{\mathcal{E}}.\mathrm{grad}_{\underset{\sim}{k}} E)\right] \qquad 5.4.3.$$

Then, for the diagonal and off-diagonal conductivity tensors in rutile VO_2 one gets

$$\sigma_{xx}^{(o)l} = -\frac{e^2}{\hbar^2}\ \frac{2}{(2\pi)^3}\ \int \tau^{l}(\underset{\sim}{k})\ \ \frac{\partial f_o}{\partial E_l}\ \left(\frac{\partial E_l}{\partial k_x}\right)^2\ \ d^3\underset{\sim}{k} \qquad 5.4.4.$$

---

* For the magnetic field of the strength used this inequality is found to be well justified when expressed in terms of $\underset{\sim}{H}$ and the conductivity mobility whose value is known to be $\sim 1\ cm^2$/volt-sec (Rosevear 1972).

$$\sigma_{zx}^{(1)l} = + \frac{e^3}{\hbar^4} \frac{H}{c_o} \frac{2}{(2\pi)^3} \int d^3\underset{\sim}{k} (\tau^l(\underset{\sim}{k}))^2 \left(\frac{\partial f_o}{\partial E_l}\right) \left[\left(\frac{\partial E_l}{\partial k_x}\right)\left(\frac{\partial^2 E_l}{\partial k_z^2}\right) - \left(\frac{\partial E_l}{\partial k_x}\right)\left(\frac{\partial E_l}{\partial k_z}\right)\left(\frac{\partial^2 E_l}{\partial k_x \partial k_z}\right)\right]$$

$$+ \frac{e^3}{\hbar^4} \frac{H}{c_o} \frac{2}{(2\pi)^3} \int d^3\underset{\sim}{k} (\tau^l(\underset{\sim}{k}))^2 \left(\frac{\partial f_o}{\partial E_l}\right) \left[\left(\frac{\partial E_l}{\partial k_z}\right)\left(\frac{\partial E_l}{\partial k_x}\right)^2 \left(\frac{\partial \tau^l}{\partial k_z}\right) - \left(\frac{\partial E_l}{\partial k_z}\right)^2 \left(\frac{\partial E_l}{\partial k_x}\right)\left(\frac{\partial \tau^l}{\partial k_x}\right)\right] \quad 5.4.5.$$

where l identifies the d_{11} and Π^* bands involved. The superscripts (O) and (1) denote that the associated elements of the conductivity tensors are calculated to zero and first order respectively, in the magnetic field $\underset{\sim}{H}$. Pending later justification we shall in what follows take the relaxation times of the d_{11} and Π^*-bands to be *constants;* the second term of equation (5.4.5) then disappears.

In the experiment of Rosevear, the direction of the primary current is parallel to the c_r-axis of the crystal as grown, and the magnetic field $\underset{\sim}{H}$ is applied along [110] direction, whilst the measurements of the Hall voltage, V_R are made along the perpendicular direction to $\underset{\sim}{H}$. The direction of $\underset{\sim}{H}$ and V_R are at 45^o to the basal plane x and y axes used in the derivation of equations (2.3.34) and (2.3.35). In terms of the foregoing conductivity tensor elements the Hall coefficient for our two-band system may now be written as

$$R_H = \frac{\sqrt{2}}{H} \frac{(\sigma_{zx}^{(1)11} + \sigma_{zx}^{(1)\Pi^*})}{(\sigma_{xx}^{(O)11} + \sigma_{xx}^{(O)\Pi^*})(\sigma_{zz}^{(O)11} + \sigma_{zz}^{(O)\Pi^*})} \quad 5.4.6.$$

where the factor $\sqrt{2}$ takes into account the 45^o rotation mentioned above.

Making use of the equations (2.3.34), (2.3.35), (5.4.4) and (5.4.5) in (5.4.6) we calculate the Hall coefficient for the assumed constant relaxation time.

In our model, however, the d_{11}-band, being completely filled in the basal plane, does not involve any conductivity processes; this reduces the problem to a one-dimensional case.

5.4.3. Results

Our calculations give

$$R_H = - \frac{1.25}{Nec_o} \qquad 5.4.7.$$

Taking N to be the total number of conduction d-electrons per unit volume ($\simeq 3.4 \times 10^{22}$) equation (5.4.7) gives

$$R_H = 23 \times 10^{-5} \ \text{cm}^3 \ \text{C}^{-1} \ .$$

Comparison with the experimental result of Rosevear, namely $R_H^{exp.} = 5.5 \times 10^{-5}$ cm^3 C^{-1}, indicates that the calculated values are about 4 times too large. Considering the assumption made as regards the relaxation time this degree of agreement is not too unsatisfactory.

It is of interest to note the similarity between equations (5.4.7) and the usual expression of a single band with spherical Fermi surface, i.e. $R_H = -r/nec_o$, where r is a constant of order unity, connected with the scattering involved. To explain his experimental results using R_H (with r=1) Rosevear found it necessary to take n = 3.3 per cation (i.e. the effective number of electrons exceeds the number of cations) and suggests that this is symptomatic that more than one band is involved. To extract a meaningful effective number of free electrons from our one-band analysis requires, however, a more realistic treatment of electron-optical phonon scattering; clearly to obtain Rosevear's result from a single band interpretation of such a more sophisticated one-band analysis, requires that the improvement in the treatment of the scattering reduce the numerator in equation (5.4.7) to unity.

5.5. The Relaxtion Time Approximation *

Before considering the validity of the above use of a constant relaxation time it will be appropriate to first consider the origin of the electron scattering and the circumstances under

---

* The considerations of this section are largely due to detailed discussions with Dr. G. J. Hyland.

which a description in terms of a relaxation time is possible. In accordance with the finding of Chapter 4 it will be assumed from the start that polaron formation can, at least to a first approximation, be neglected in metallic VO_2 and the charge carriers taken to be electrons; this results is a great simplification since problematical questions concerning the influence of the structure of the polaron on scattering processes can be neglected.

The scattering of the conduction electrons between different Bloch states is due to the emission and absorption of real (thermal) phonons, the most important of which in metallic VO_2 are undoubtedly those associated with the longitudinal optical modes of vibration of the polar (rutile) VO_2 lattice, in consequence of the associated polarization fields. If ω_{min} is the lowest frequency optical mode when the reduction due to electron screening has been taken into account, then real phonon emission clearly requires

$$E > \hbar \omega_{min} \qquad (I)$$

where E is the electron energy, which for an "active" electron in metallic VO_2 is close to the Fermi energy E_F. Comparison of $E_F \simeq 0.93$ eV with the values of ω given in Table 4.1 of Chapter 4, reveals that the L.H.S. of (I) exceeds the R.H.S. by one order of magnitude; it should be noted that this result *is* conditional on using the screened values of ω.

which a description in terms of a relaxation time is possible. In accordance with the finding of Chapter 4 it will be assumed from the start that polaron formation can, at least to a first approximation, be neglected in metallic VO_2 and the charge carriers taken to be electrons; this results is a great simplification since problematical questions concerning the influence of the structure of the polaron on scattering processes can be neglected.

The scattering of the conduction electrons between different Bloch states is due to the emission and absorption of real (thermal) phonons, the most important of which in metallic VO_2 are undoubtedly those associated with the longitudinal optical modes of vibration of the polar (rutile) VO_2 lattice, in consequence of the associated polarization fields. If ω_{min} is the lowest frequency optical mode when the reduction due to electron screening has been taken into account, then real phonon emission clearly requires

$$E > \hbar \omega_{min} \qquad (I)$$

where E is the electron energy, which for an "active" electron in metallic VO_2 is close to the Fermi energy E_F. Comparison of $E_F \simeq 0.93$ eV with the values of ω given in Table 4.1 of Chapter 4, reveals that the L.H.S. of (I) exceeds the R.H.S. by one order of magnitude; it should be noted that this result *is* conditional on using the screened values of ω.

Condition (I) is, however, not in general sufficient to ensure emission in consequence of restrictions imposed by the Pauli exclusion principle, which must here be respected in consequence of the rather degenerate nature of the conduction electron gas in metallic VO_2 - (recall that $E_F/kT \simeq 31$).

Accordingly, in order that a *vacant* final state exist for an electron after it has emitted a real optical phonon of energy $\hbar\omega_o$ it is necessary that

$$kT \gg \hbar\omega_o \qquad (II)$$

if condition (II) is not satisfied then emission processes are suppressed even though the necessary energy *is* available (condition (I) satisfied); processes in which an electron first *absorbs* an optical phonon are not, of course, subject to these considerations.

From standard transport theory it is known (e.g. Haug 1972) that the possibility of describing electron-phonon scattering in terms of a *relaxation time* τ, follows from a treatment of the collisions as *elastic*, an approximation which can, however only be justified at temperatures T, sufficiently high that

$$\left| E_{initial} - E_{final} \right| = \hbar\omega \ll kT \qquad (III)$$

where $\hbar\omega$ is the energy of the vibrational quantum involved in

the scattering*. In addition to conditions (III) being identical to that obtained above (II) from considerations of the Pauli principle, it also ensures the existence of a sufficient number of optical phonons, with their much stronger† interaction with the electrons, to dominate as the principal scatters over the more numerous but less strongly coupled acoustic phonons.

Before continuing it should be noted that condition (III) arises from consideration of the collision integral in the Boltzmann equation, the very use of which itself requires the fulfillment of certain conditions, additional to those mentioned above." In particular, it is assumed that particles undergo series of collisions which occur independently of each other. This requires that the phases of successive amplitudes associated with the collision processes are uncorrelated, allowing us to sum transition probabilities instead of amplitudes", (Schultz, 1963). This assumption should be valid if the time τ

---

* It might be noted that (III) is a more restrictive condition than that suggested intuitively, namely that the energy of the vibrational quantum can be neglected in comparison with the electron energy provided

$$E \gg \hbar\omega \quad \text{(IV)}$$

whence $E_{initial} \simeq E_{final}$ and the scattering almost elastic.

† Whilst this is certainly so in the case of semiconductors the actual situation in a degenerate system, such as metallic VO_2, can only be ascertained after the screening of the electron-optical phonon matrix element by the conduction electron gas has been taken into account.

between collisions is sufficiently long such that the associated uncertainty in energy is much smaller than the characteristic energies of the electrons in question, namely E_F, i.e.

$$\hbar/\tau < E_F.$$

Turning now specifically to metallic VO_2, it is immediately evident upon taking $E \sim E_F$ (= 0.93 eV) that whilst condition (I) (and IV) is satisfied, condition (III) is not, for taking the minimum possible value of $\hbar\omega$ (namely 0.022 eV, appropriate to the screened A_{2u} mode) and a reasonable maximum value of T, say 440°K (i.e. one hundred degrees above the transition temperature) then the RHS of condition (III) exceeds the LHS by only 0.016 eV; accordingly, the introduction of a relaxation time to describe electron-optical phonon scattering in metallic VO_2 would seem hardly justifiable. However, in view of the identity of conditions (II) and (III), a further implication of course is that emission processes are largely forbidden anyway leaving only the absorption processes. For the case of absorption alone, however, a relaxation time description does again become valid within a treatment which considers subsequent re-emission, after a very short* time interval of an optical phonon with the same energy but in general different momentum. With this second order "resonance" scattering can be associated a relaxation time τ_R, since the scattering processes involved are, overall, elastic, the energies of the initial and final states being equal.

---

* The rapidity of re-emission is a consequence of the phonon emission probabilities being proportional to $(\bar{n}+1)$ whilst absorption is proportional to $\bar{n}$, where $\bar{n}$ is the mean phonon occupation number.

In the case of slow electrons in polar crystals with $E < \hbar\omega$, τ_R is known to be a constant, *independent of E* (Fröhlich 1954). When

$$E \gtrsim \hbar\omega, \qquad 5.5.1.$$

as is the case in metallic VO_2, the L.H.S. of equation (5.5.1) exceeding the R.H.S. by a factor between 15 and 40, the analysis of Fröhlich et.al. (1950) becomes appropriate, provided the emission processes considered by them are suppressed in order to respect the fact that for us $kT \simeq \hbar\omega$, τ_R is then given by

$$\frac{1}{\tau_R} = \frac{e^2}{\hbar}\left(\frac{1}{\varepsilon_\infty} - \frac{1}{\varepsilon_s}\right)\frac{\omega}{v} \qquad 5.5.2.$$

where v is the electron velocity which in our case is close to the *constant*, v_F. To incorporate the presence of a degenerate electron gas in the case of metallic VO_2, the optical-phonon frequency ω in equation (5.5.2) should be taken as the screened value (Table 4.1 of Chapter 4); strictly speaking one might anticipate a further reflection of the screening by an additional factor* in equation (5.5.2) originating from the change in the electron-optical phonon matrix element from $\frac{1}{q}$ to $\frac{q}{q^2+\lambda^2}$ (c.f. equation of Chapter 4). Whilst this remains to be investigated it would appear difficult

---

* A consequence of such a factor could be to reduce the intensity of scattering by optical phonons towards that of the more numerous acoustic phonons; the number of thermally excited optical phonons is not large even at 100 degrees above T_t.

to escape from a relaxation time which is almost constant whatever may be to find v-dependence of τ_R, in consequence of the fact that $v \sim v_F$ = constant. It is gratifying to note that the value of the mean free path ℓ, obtained from equation (5.5.2) using $\ell = v_F \tau_R$, turns out to be several lattice spacings and also to exceed the de Broglie wavelength of electrons at the Fermi surface.

We thus conclude that the assumption of a *constant* relaxation time in the calculations of Chapter 5.4.2 is acceptable at least as a zeroth order description of the electron transport in metallic VO_2. A more sophisticated analysis would start by accepting $\tau \propto v$, and introducing a $\underset{\sim}{k}$-dependence of τ through that of $\underset{\sim}{v}$ via $\underset{\sim}{v} = \frac{1}{\hbar}$ grad E; the terms in the conductivity tensor involving $\frac{\partial \tau}{\partial \underset{\sim}{k}}$ would then, of course, contribute and hopefully lead to an improvement in the degree of agreement with experiment.

CHAPTER 6

SUMMARY OF THE PRESENT INVESTIGATIONS

Considerations of Goodenough, based on the quantum chemistry reveal that the electronic properties of metallic VO_2 are associated with two overlapping bands (d_{11} and π^*). Existing first principle band structure calculations either don't generally support these qualitative conjectures (Caruthers et.al. 1973) or at best attempt to establish possible connection between the two approaches (Mitra et.al. 1973). In Chapter 2 of the present work we have applied the tight-binding approximation to the two bands involved in the metallic conduction; crudely speaking, we have put the k-dependence into the qualitative conjectures of Goodenough. Instead of calculating the tunnel integrals we have treated them as parameters to be determined by comparison with the results of other works and available experimental data. Taking the width of the d_{11}-band to be 2 eV from the calculations of Hearn (1973), the width of the π^*-band is found to be 2.22 eV; at the zone centre, the separation of the bottoms of the two bands is 0.2 eV. Having obtained the one-electron energy dispersion relations it is straightforward to calculate the density of states; the Fermi energy E_F can then be obtained from the density of states diagram and is found to be 0.93 eV above the bottom of the d_{11}-band.

Whilst the majority of experimental and theoretical evidence now tends to support the strong electron-phonon interaction in the high temperature phase, the situation with respect to the electron-electron interaction is less clear. From the point of view of judging the validity of our band structure calculations in metallic VO_2 it is important to consider the Coulomb correlation neglected in the band model. This, however, is not an easy task to achieve; therefore we have approached the problem via a semiclassical consideration. In Chapter 3 we have calculated an upper limit for the Coulomb correlation energy U, by making use of a method originally developed by Hyland (1969), which is based on the calculation of the polarization energies in the lattice, by an adaptation of the Mott-Littleton method originally developed for the alkali halides. The energy of the metallic state thus in this way found to be lower than that of the corresponding Mott-insulating state, thereby justifying the validity of our calculations.

In Chapter 4, we considered the possibility of the polaron formation in the metallic phase of VO_2, as a result of the electron-phonon interaction. As far as the electron-longitudinal polar phonon interactions are concerned, our considerations rule out the formation of conventional polarons; instead we propose that the *electronic polaron* is the more relevant to metallic VO_2. It turns out, however, that the establishment even of this variety of polarons is largely

suppressed through the screening effect of the degenerate conduction electron gas; in the applications considered, therefore, the charge carriers are taken as Bloch electrons.

Having convinced ourselves of the validity of the band model we have in Chapter 5 applied the one-electron dispersion relations of Chapter 2 to the investigation of various electronic properties of metallic VO_2. In particular, we have calculated the electronic specific heat, the plasma frequency and the Hall coefficient. Of these, the first one gave a result in acceptable agreement with the experiment. Whilst the plasma frequency calculation reveals that there are considerable contribution from the interband transitions ($\pi^* \rightarrow d_{11}$), the calculation of the Hall coefficient gave a value four times larger than the experimental value. This last calculation can be improved by the use of a more realistic relaxation time than that assumed in our calculations.

We conclude from our present investigations that the metallic state of VO_2, which consists of two partially overlapping bands, can be explained within the Bloch band model, as commonly agreed, with electrons as charge carriers.

As regards the Hall effect, our result obviously needs improving. Assuming that the discrepancy arises from the assumed constant relaxation times, a detailed investigation of electron-polar optical phonon scattering in the case of a degenerate electron system would be of great interest; hopefully, use of the $\underset{\sim}{k}$-dependent relaxation time so obtained would improve the agreement with experiment. Such an analysis must of course, also form the foundation of the solution of the polaron problem

in metallic VO_2, mentioned above, by reference to which our qualitative conjectures of Chapter 4 could be adjudged.

What appears to be required is a development of existing electronic polaron theory analogous to the achieved by Mahan (1972) for the case of a degenerate gas of conventional (lattice) polarons. This is an interesting problem in its own right, the solution of which has immediate application to metallic VO_2.

Transition metal compounds containing a degenerate conduction electron gas thus pose, in consequence of the coexistence of *many* electrons and a polarizable ionic lattice, many problems the resolution of which requires a fundamental redevelopment of existing text book theory (which deals only with the interaction of a *single* electron with the polar lattice field) to take into account many electron effects. Such materials thus provide fascinating systems, an understanding of whose electronic transport properties will be obtained only from a systematic investigation of the combined effects of electron-electron and electron-optical phonon interactions.

REFERENCES

AUSTIN, I.G., and MOTT, N.F., 1969, Adv. Phys., 19, 41.

BARKER, A.S., VERLEUR, H.W., and GUGGENHEIM, H.J., 1966, Phys. Rev. Letts., 17, 1286.

BLAAUW, C., LENNHOUTS, F., VAN DER WOUDE, F., and SAWATZKY,G.A., 1975, J. Phys. C, 8, 459.

DE BOER, J.H., and VERWEY, E.J.W., 1937, Proc. Phys. Soc., 49, 59.

BOHM,D., and PINES, D., 1951, Phys. Rev., 82 , 625.

BORN, M., and GÖPPERT-MAYER, M., 1933, Handb. d. Phys., 24/2, 623.

BRINKMAN, W.F., and RICE, T.M., 1970, Phys. Rev., B2, 4302.

CARUTHERS, E., KLEINMAN, L. and ZHANG, H.I., 1973, Phys. Rev, B7, 3760.

CHAIKIN, P.M., GARITO, A.F., and HEEGER, A.J., 1972, Phys. Rev., B5, 4966; 1973, J. Chem. Phys., 58, 2366.

CHANDRASHEKHAR, G.V., BARROS, H.L.C, HONIG, J.M., 1973, Mat. Res. Bul., 8, 369.

CHATTERJEE, S., MITRA, T., and HYLAND, G.J., 1972, Phys. Letts., 42A, 56.

COHEN, M.H., 1958, Phil. Mag. [8], 3, 762.

COOK, O.A., 1947, J. Am. Chem. Soc., 69, 331.

COWLEY, R.A., and DOLLING, G., 1965, Phys. Rev. Lett., 14, 549.

EAGLES, D.M., 1964, J. Phys. Chem. Solids, 25, 1243; 1966, Phys. Rev., 145, 645.

EHRENREICH, H., 1959, J. Phys. Chem. Solids, 8, 130.

EHRENREICH, H., and COHEN, M., 1959, Phys. Rev., 115, 786.

FAN, J.C.C., 1972, Techn. Rept. HP-28, Div. Eng. and Apl. Phys. Harvard University, Cambridge, Mass. (unpublished).

FORD, C.J., SEGEL, S.L., SEYMOUR, E.F.W., and HYLAND, G.J., 1972, Phys. kondens. Mater, 13, 111.

FRÖHLICH, H., 1949, Theory of Dielectrics (Oxford Univ. Press); 1954, Advs. in Phys., 3, 325.

FRÖHLICH, H., PELZER, H., ZIENAU, S., 1950, Phil. Mag., 41, 221.

GOODENOUGH, J.B., 1965, Bull. Soc. Chim. Fr., 4, 1200; 1971, J. Solid St. Chem., 3, 490.

HAUG, A., 1972, Theoretical Solid State Physics, (Pergamon Press), Chapter IV.

HEARN, C.J., 1971, Proc. Conf. on Metal-Non Metal Transitions, Aussois (unpublished); 1972, J. Phys. C., 5, 1317; 1973, Solid St. Commun. 12, 53, and 13, 1139.

HEARN, C.J., and HYLAND, G.J., 1973, Phys. Letts., 43A, 87.

HONIG, J.M., DIMMOCK, J.O., and KLEINER, W.H., 1969, J. Chem. Phys., 50, 5232.

HUBBARD, J., 1964, Proc. Roy. Soc. (London) A277, 237.

HULM, J.K., JONES, C.K., MAZELSKY, R., MILLER, R.C., HEIN, R.A., and GIBSON, J.W., 1965 "Proc. 9th Int. Conf. on Low Temperature Physics", (J. G. Daunt et.al. Eds.), p.600, Plenum Press, N.Y.

HYLAND, G.J., 1968, J. Phys. C., 1, 189; 1969, Phil. Mag., 20, 837.

JOHNSON, Q.C., and TEMPLETON, D.H., 1961, J. Chem. Phys. 34, 2004.

JONES, H., and ZENER, C., 1934, Proc. Roy. Soc., A145, 268.

LAZUKOVA, N.I. and GUBANOV, V.A., 1976, Solid St. Commun.,20, 649.

MAHAN, G., 1972, in Polarons in Ionic Crystals and Semiconductors, Ed. by DEVREESE, J.T., (Nort-Holland, Amsterdam), p.553.

MARKHAM, J.J., and SEITZ, F., 1948, Phys. Rev., 74, 1014.

MITRA, T.K., CHATTERJEE, S., and HYLAND, G.J.,
1971, Phys. Letts., 37A, 221;
1973, Can. J. Phys., 51, 352.

MOKEROV, V.G., and RAKOV, A.V., 1969, Sov. Phys. Solid St., 11, 150.

MOKEROV, V.G., and SARAIKEN, V.V., 1976, Sov. Phys. Solid St., 18, 1049.

MOORE, C.E., 1949, Circ. U.S. natn. Bur. Stand., Vol. I, No. 467.

MORIN, F.J., 1959, Phys. Rev. Lett., 3, 34.

MOTT, N.F., 1949, Proc. Phys. Soc., A62, 416;
1969, Phil. Mag., 20, 1.

MOTT, N.F., and FRIEDMAN, L., 1974, Phil. Mag., 30, 389.

MOTT, N.F., and LITTLETON, M. J., 1938, Trans. Faraday Soc.,34, 385.

MOTT, N.F., and ZINAMON, Z., 1970, Rep. Prog. Phys., 33, 881.

PARKER, R.A., 1961, Phys. Rev., 124, 1719.

PAUL, W., 1970, Mater. Res. Bull., 5, 691.

PAULING, L., 1928, Z. Kristallogr., 67, 337;
1960, The Nature of the Chemical Bond (Ithaca: Cornell Univ. Press).

PINES, D., 1963, Elementary Excitations in Solids, (Benjamin, N.Y).

POWELL, R.J., BERGLUNG, C.N., and SPICER, W.E., 1969, Phys. Rev., 178, 1410.

RICE, T.M., McWHAN, D.B., and BRINKMAN, W.F., 1970, Proc. Tenth Int. Conf. on Phys. of Semiconductors, Ed. by KELLER, S.P., HENSEL, J.C., and STERN, F., (U.S. Atomic Energy Commission) p. 293.

ROSEVEAR, W.H., 1972, Techn. Rept. HP-31, Div. Eng. and Appl. Phys., Harvard University, Cambridge, Mass. (unpublished).

SAMARA, G.A., and PEERCY, P.S., 1973, Phys. Rev., B7, 1131.

SCHULTZ, T.D., 1964, in Polarons and Excitons, Ed. by KUPER,C.G., and WHITFIELD, G.D., (Oliver and Boyd), p.111.

SHIMIZU, T., 1967, J. Phys. Soc. Japan, 23, 848.

SOMMERS, C., DE GROOT, R., KAPLAN, D., and ZYLBERSZTEJN, A., 1975, J. de Phys. Letts., 36, L57.

SRIVASTAVA, R., and CHASE, L.L., 1971, Phys. Rev. Lett., 27, 727.

SZIGETI, B., 1949, Trans. Faraday Soc., 45, 155.

TOYOZAWA, Y., 1954, Progr. Theort. Phys. (Kyoto), 12, 421.

TRAYLOR, J.G., SMITH, H.G., NICKLOW, R.M., and WILKINSON, M.K., 1971, Phys. Rev., B3, 3457.

TYABLIKOV, S.V., 1952, Zh. Eksperim. i Teor. Fiz., 23, 381.

VALIEV, K.A., MOKEROV, V.G., and GALIEV, G.B., 1975, Sov. Phys. Solid St., 16, 1535.

VARGA, B.B., 1965, Phys. Rev., 137, A1896.

VERLEUR, H.W., BARKER, A.S., and BERGLUNG, C.N., 1968, Phys. Rev, 172, 788.

WESTMAN, S., 1961, Acta Chem. Scand., 15, 217.

ZIMAN, J.M., 1964, Principles of the Theory of Solids, (Cambridge Univ. Press) Chapter 5.

ZYLBERSZTEJN, A., and MOTT, N.F., 1975, Phys. Rev., B11, 4383.

APPENDIX I

The electrostatic and repulsive forces F_e and F_r respectively of Chapter 3, are given by (where now $x_1 = x$, $x_2 = y$, $x_3 = z$):

$$F_e(1) = 2(e^*)^2 \left\{ \frac{3.48}{(1.9 + x)^2} - \frac{2}{(3.8 + x)^2} - 0.019 \right.$$

$$+ 6 \frac{(1.9 + x)(1.95 + y)}{[(1.9 + x)^2 + (1.95 + y)^2]^{5/2}} \cdot \left(\frac{\mu_2}{e^*}\right) + \frac{1.33}{(1.9 + x)^3} \left(\frac{\mu_1}{e^*}\right)$$

$$- 1.51 \frac{(2.87-z)^2 + (1.9 + x)^2 - 2.36(2.87-z)(1.9 + x)}{[(1.9 + x)^2 + (2.87 - z)^2 - 1.51(2.87-z)(1.9 + x)]^{5/2}} \left(\frac{\mu_3}{e^*}\right)$$

$$+ 1.51 \frac{(2.87-z)^2 + (1.9 + x)^2 + 2.36(2.87-z)(1.9 + x)}{[(1.9 + x)^2 + (2.87-z)^2 + 1.51(2.87-z)(1.9 + x)]^{5/2}} \left(\frac{\mu_3}{e^*}\right)$$

$$-2 \frac{(x + 2.17)}{(x^2 + 4.33x + 8.24)^{3/2}} - 2 \frac{(x + 1.63)}{(x^2 + 3.26x + 6.2)^{3/2}}$$

$$+ 4 \frac{y}{x} (1.95 + y) \left[\frac{1}{[(1.95+y)^2 + (1.9+x)^2]^{3/2}} - \frac{1}{[(1.95+y)^2+3.61]^{3/2}} \right]$$

$$+4 \frac{z}{x} \left[\frac{0.76x - z + 4.31}{[(2.87-z)^2 + (1.9+x)^2 + 1.51(2.87-z)(1.9+x)]^{3/2}} \right.$$

$$- \frac{4.31 - z}{[(2.87-z)^2 + 2.87(2.87-z) + 3.61]^{3/2}}$$

$$+ \frac{1.44 - 0.76x - z}{[(2.87-z)^2 + (1.9+x)^2 - 1.51(2.87-z)(1.9+x)]^{3/2}}$$

$$- \frac{1.44 - z}{[(2.87-z)^2 - 2.87.(2.87-z) + 3.61]^{3/2}} \Bigg] \Bigg\}$$

$$F_e(2) = 2(e^*)^2 \left\{ \frac{2.06}{(1.95 + y)^2} - 0.009 \right.$$

$$+ 12 \frac{(1.95 + y)(1.9 + x)}{[(1.95 + y)^2 + (1.9 + x)^2]^{5/2}} \left(\frac{\mu_1}{e^*}\right) + \frac{0.25}{(1.95 + y)^3} \left(\frac{\mu_2}{e^*}\right)$$

$$+6 \frac{(2.87-z)(1.95+y)}{[(2.87-z)^2 + (1.95+y)^2]^{5/2}} \left(\frac{\mu_3}{e^*}\right) - \frac{2}{(3.9 + y)^2}$$

$$+8 \frac{x}{y} (1.9+x) \left[\frac{1}{[(1.9+x)^2 + (1.95+y)^2]^{3/2}} - \frac{1}{[(1.9+x)^2 + 3.8]^{3/2}} \right]$$

$$+8 \frac{z}{y} (2.87-z) \left[\frac{1}{[(2.87-z)^2 + (1.95+y)^2]^{3/2}} - \frac{1}{[(2.87-z)^2 + 3.8]^{3/2}} \right] \Bigg\}$$

$$F_e(3) = 4(e^*)^2 \left\{ \frac{0.56}{(2.87-z)^2} - 0.044 + \frac{0.25}{(2.87-z)^3} \left(\frac{\mu_3}{e^*}\right) \right.$$

$$+6 \frac{(1.95+y)\,(2.87-z)}{[(1.95+y)^2 + (2.87-z)^2]^{5/2}} \left(\frac{\mu_2}{e^*}\right) + \frac{4}{(5.74-z)^2}$$

$$-3.02 \frac{(2.87-z)^2 + (1.9+x)^2 - 2.36\,(2.87-z)(1.9+x)}{[(1.9+x)^2 + (2.87-z)^2 - 1.51(2.87-z)(1.9+x)]^{5/2}} \left(\frac{\mu_1}{e^*}\right)$$

$$+3.02 \frac{(2.87-z)^2 + (1.9+x)^2 + 2.36(2.87-z)(1.9+x)}{[(1.9+x)^2 + (2.87-z)^2 + 1.51(2.87-z)(1.9+x)]^{5/2}}$$

$$-4 \frac{y}{z} (1.95+y) \left[\frac{1}{[(1.95+y)^2 + (2.87-z)^2]^{3/2}} - \frac{1}{[(1.95+y)^2 + 8.24]^{3/2}} \right]$$

$$-4 \frac{x}{z} \left[\frac{x - 0.76z + 4.07}{[(2.87-z)^2 + (1.9+x)^2 + 1.51(1.9+x)(2.87-z)]^{3/2}} \right.$$

$$- \frac{x + 4.07}{[8.24 + (1.9 + x)^2 + 4.33\,(1.9 + x)]^{3/2}}$$

$$+ \frac{x + 0.76z - 0.27}{[(2.87-z)^2 + (1.9+x)^2 - 1.51\,(1.9+x)(2.87-z)]^{3/2}}$$

$$\left. - \frac{x - 0.27}{[8.24 + (1.9+x)^2 - 4.33\,(1.9+x)]^{3/2}} \right] \Bigg\}$$

$$F_r(1) = 9B_o\, e^2\, \beta_{+-}\, (r_+ + r_-)^8 \left[\frac{1}{(1.9 + x)^{10}} \right.$$

$$+ \frac{x + 0.76z - 0.27}{[(1.9+x)^2 + (2.87-z)^2 - 1.51(1.9+x)(2.87-z)]^{11/2}}$$

$$\left. + \frac{x - 1.28}{[(1.9+x)^2 - 6.35\,(1.9+x) + 12.21]^{11/2}} \right]$$

$$+ 18\, B_o\, e^2\, (2r_-)^8\, \beta_{--} \left[\frac{1.9 + x}{[(1.95+y)^2 + (1.9+x)^2]^{11/2}} \right.$$

$$+ \frac{x - 0.27}{[(1.9+x)^2 - 4.34(1.9+x) + 12.07]^{11/2}}$$

$$+ \frac{x - 0.21}{[(1.9+x)^2 - 4.23(1.9+x) + 11.86]^{11/2}}$$

$$+ \frac{x - 2.38}{[(1.9+x)^2 - 8.56(1.9+x) + 20.08]^{11/2}}$$

$$\left. + \frac{0.05}{(1.9+x)^{10}} + 0.5 \frac{x - 2.17}{[(1.9+x)^2 - 8.15(1.9+x) + 20.11]^{11/2}} \right]$$

$$F_r(2) = 9\, B_o\, \beta_{+-}\, e^2\, (r_+ + r_-)^8 \left[\frac{1}{(1.95+y)^{10}} \right.$$

$$\left. + 2 \frac{y - 1.24}{[(1.95+y)^2 - 6.38(1.95+y) + 12.21]^{11/2}} \right]$$

$$+ 9B_o\, \beta_{--}\, e^2 (2r_-)^8 \left[4 \frac{1.95 + y}{[(1.95+y)^2 + (1.9+x)^2]^{11/2}} \right.$$

$$+ 4 \frac{y - 1.26}{[(1.95+y)^2 - 6.42(y+1.95) + 16.15]^{11/2}}$$

$$- \frac{1}{(2.503 - x)^{10}}$$

$$\left. -2 \frac{y - 0.003}{[(1.95+y)^2 - 3.9(1.95+y) + 12.07]^{11/2}} \right]$$

$$F_r(3) = 18\, B_o\, \beta_{+-}\, e^2 (r_+ + r_-)^8 \times$$

$$\left[\frac{z + 0.76x - 1.435}{[(2.87-z)^2 + (1.9+x)^2 - 1.51\,(1.9+x)(2.87-z)]^{11/2}} \right.$$

$$+ \frac{z + 0.004}{[(2.87-z)^2 - 5.75(2.87-z) + 12.07]^{11/2}}$$

$$\left. + \frac{z + 1.44}{[(2.87-z)^2 - 8.62(2.87-z) + 20.12]^{11/2}} \right]$$